

See discussions, stats, and author profiles for this publication at: <https://www.researchgate.net/publication/319679731>

Non-local growth of Penrose tilings

Thesis · September 2005

DOI: 10.13140/RG.2.2.34775.16805

CITATIONS

2

READS

98

1 author:



Elissa Ross

MESH Consultants Inc.

17 PUBLICATIONS 110 CITATIONS

SEE PROFILE

Some of the authors of this publication are also working on these related projects:



Tilings [View project](#)

NON-LOCAL GROWTH OF PENROSE TILINGS

by

ELISSA JOANNE ROSS

B.Sc. University of Guelph, 2003

A THESIS SUBMITTED IN PARTIAL FULFILLMENT OF
THE REQUIREMENTS FOR THE DEGREE OF

MASTERS OF SCIENCE

in

THE FACULTY OF GRADUATE STUDIES

Department of Mathematics

We accept this thesis as conforming
to the required standard

.....
.....
.....
.....
.....
.....

THE UNIVERSITY OF BRITISH COLUMBIA

September 2005

© Elissa Joanne Ross, 2005

In presenting this thesis in partial fulfillment of the requirements for an advanced degree at the University of British Columbia, I agree that the Library shall make it freely available for reference and study. I further agree that permission for extensive copying of this thesis for scholarly purposes may be granted by the head of my department or by his or her representatives. It is understood that copying or publication of this thesis for financial gain shall not be allowed without my written permission.

(Signature) _____

Department of Mathematics
The University of British Columbia
Vancouver, Canada

Date _____

Abstract

The problem of mistakes in Penrose tilings will be investigated. Specifically, we will consider the non-locality of any growth process that attempts to avoid errors in the construction of a tiling of the plane by Penrose rhombs. This discussion will be framed by considering the one dimensional version of this problem for Fibonacci Tilings, the aperiodic tilings of the line. These considerations lead to the conclusion that local growth algorithms for correct Penrose tilings of the plane do not exist.

Table of Contents

| | |
|---|------------|
| Abstract | ii |
| Table of Contents | iii |
| List of Figures | v |
| Acknowledgement | ix |
| Chapter 1. Introduction | 1 |
| 1.1 Introduction | 1 |
| 1.2 Outline | 2 |
| Chapter 2. Fibonacci tilings | 3 |
| 2.1 Introduction to Fibonacci tilings | 3 |
| 2.2 Fibonacci tilings using the Projection Method | 3 |
| 2.2.1 Definitions and Background | 5 |
| 2.2.2 The general projection method | 5 |
| 2.2.3 Using the Projection method to create Fibonacci tilings | 7 |
| 2.2.4 Properties of the Fibonacci tiling | 9 |
| 2.3 Updown generation of Fibonacci tilings | 13 |
| 2.3.1 Decomposition and Composition of Fibonacci Strings | 13 |
| 2.3.2 Definition of Fibonacci Strings and Fibonacci tilings | 15 |
| 2.3.3 Decomposition and Composition of Fibonacci tilings | 17 |
| 2.3.4 More Properties of Fibonacci tilings | 19 |
| 2.3.5 Updown Generation of Fibonacci tilings | 23 |
| 2.4 Summary | 25 |
| Chapter 3. Penrose Tilings | 27 |
| 3.1 Introduction to Penrose Tilings | 27 |
| 3.1.1 Background: Introduction to Tiling | 28 |
| 3.1.2 Background: The Penrose Tiles | 28 |
| 3.1.3 Composition and Decomposition of Penrose Tiles | 29 |
| 3.1.4 Properties of the Penrose tilings | 32 |
| 3.2 Penrose Tilings using the projection method | 33 |
| 3.3 Penrose Tilings using de Bruijn's Pentagrid Method | 34 |

| | |
|---|------------|
| 3.3.1 The Pentagrid method is the projection method | 48 |
| 3.4 Penrose Tilings using Updown Generation | 49 |
| 3.4.1 Relationship between path and tessellation | 53 |
| 3.5 Summary | 56 |
| Chapter 4. Non-locality of Fibonacci Tilings | 57 |
| 4.1 Introduction | 57 |
| 4.2 Local rules for building Fibonacci tilings | 57 |
| 4.3 Algorithm for correct placements | 60 |
| 4.4 Non-Locality of Fibonacci Sequences | 60 |
| 4.4.1 Forcing in Fibonacci Sequences | 60 |
| 4.4.2 Mistakes | 63 |
| 4.5 Summary | 68 |
| Chapter 5. Non-locality of Penrose Tilings | 69 |
| 5.1 Introduction | 69 |
| 5.2 Local matching rules for Penrose tilings | 69 |
| 5.3 An algorithm for correct placements | 79 |
| 5.4 Non-locality of Penrose tilings | 84 |
| 5.4.1 Worms | 94 |
| 5.4.2 Mistakes | 97 |
| 5.4.3 Worms and Fibonacci Strings | 119 |
| 5.5 Summary | 120 |
| Chapter 6. Conclusions | 121 |
| Bibliography | 123 |
| Appendix A. Colophon | 124 |

List of Figures

| | | |
|------|---|----|
| 2.1 | The Integer lattice and the line $y = x/\tau$ | 4 |
| 2.2 | The “staircase” corresponding to the line $y = x/\tau$ | 4 |
| 2.3 | The Fibonacci staircase | 7 |
| 2.4 | The orthogonal projection of X onto ℓ | 8 |
| 2.5 | The delone set $\Lambda = \Pi(X)$ | 9 |
| 2.6 | The Voronoï cell of the origin | 10 |
| 2.7 | The resulting Fibonacci tiling | 10 |
| 2.8 | The window of acceptance of the projection | 11 |
| 2.9 | The divided window of acceptance | 12 |
| 2.10 | Proof of Theorem 2.9 | 16 |
| 2.11 | Proof of Theorem 2.9 | 17 |
| 2.12 | Decomposition of Fibonacci tiles | 18 |
| 2.13 | Composition of Fibonacci tiles | 19 |
| 2.14 | Proof of Theorem 2.10 | 20 |
| 2.15 | Proof of Theorem 2.10 | 20 |
| 2.16 | Proof of Theorem 2.10 | 20 |
| 2.17 | Proof of Theorem 2.10 | 21 |
| 2.18 | The three vertex neighborhoods | 21 |
| 2.19 | Proof of Theorem 2.11 | 22 |
| 2.20 | Proof of Theorem 2.11 | 22 |
| 2.21 | Proof of Theorem 2.11 | 23 |
| 2.22 | The FSA for Updown Generation of Fibonacci tilings | 24 |
| 2.23 | Visual representation of the FSA | 25 |
| 2.24 | Updown generation of Fibonacci tilings | 26 |
| 3.1 | A tiling of the plane by Penrose rhombs | 27 |
| 3.2 | The Penrose rhombs | 29 |
| 3.3 | A tiling of the plane by arrowed rhombs | 29 |
| 3.4 | Decomposition of Penrose rhombs | 30 |
| 3.5 | Decomposition of a patch of tiles | 31 |
| 3.6 | A ‘ribbon’ of tiles | 35 |
| 3.7 | A regular pentagrid | 36 |
| 3.8 | The two types of intersections of grid lines | 38 |
| 3.9 | The intersections of grid lines with normal vectors | 39 |
| 3.10 | The rhombs resulting from the intersections of Figure 3.8 | 39 |

| | | |
|------|---|----|
| 3.11 | The tiling corresponding to the pentagrid of Figure 3.7 | 40 |
| 3.12 | The tiling from the pentagrid, coloured. | 40 |
| 3.13 | Two possible indexings of the thick rhomb | 42 |
| 3.14 | Two possible indexings of the thin rhomb | 42 |
| 3.15 | Double arrows associated with the indexed thick rhombs | 42 |
| 3.16 | Double arrows associated with the indexed thin rhombs | 42 |
| 3.17 | Orientation of the single arrows of the thick rhomb | 43 |
| 3.18 | Orientation of the single arrows of the thin rhomb | 43 |
| 3.19 | Proof of Lemma 3.5 | 44 |
| 3.20 | Proof of Lemma 3.5 | 45 |
| 3.21 | Intersections of the lines of the pentagrid | 46 |
| 3.22 | A pentagrid example | 47 |
| 3.23 | A pentagrid example | 47 |
| 3.24 | A pentagrid example | 47 |
| 3.25 | A pentagrid example | 48 |
| 3.26 | The divided rhombs | 50 |
| 3.27 | Decomposition of the elementary triangles | 50 |
| 3.28 | Decomposition of the elementary triangles in colour | 51 |
| 3.29 | A visual representation of the maps of the FSA | 53 |
| 3.30 | The directed graph of Updown generation | 54 |
| 3.31 | Updown generation of Penrose tilings | 55 |
| 3.32 | Patch of tiles produced by Updown generation | 56 |
| 4.1 | Disallowed sequences of Fibonacci tiles | 58 |
| 4.2 | A fragment of a Fibonacci tiling | 60 |
| 4.3 | Using the Updown procedure to determine tile placement | 61 |
| 4.4 | Decomposing the large tile determines tile placement | 61 |
| 4.5 | Example: growing a Fibonacci tiling | 62 |
| 4.6 | Example: growing a Fibonacci tiling | 62 |
| 4.7 | Example: growing a Fibonacci tiling | 62 |
| 4.8 | Example: growing a Fibonacci tiling | 63 |
| 4.9 | Example: growing a Fibonacci tiling | 63 |
| 4.10 | Example: growing a Fibonacci tiling | 63 |
| 4.11 | Example: growing a Fibonacci tiling | 63 |
| 4.12 | Example: growing a Fibonacci tiling | 64 |
| 4.13 | Example: growing a Fibonacci tiling | 64 |
| 4.14 | Example: growing a Fibonacci tiling | 64 |
| 4.15 | Example: growing a Fibonacci tiling | 64 |

| | | |
|------|--|----|
| 4.16 | Eight-tile Fibonacci tilings beginning with a long tile | 65 |
| 4.17 | Eight-tile Fibonacci tilings beginning with a short tile | 65 |
| 5.1 | Forced tiles | 70 |
| 5.2 | A hole in the tiling | 70 |
| 5.3 | A gap in the tiling that cannot be filled | 71 |
| 5.4 | Choice of tiles | 71 |
| 5.5 | A growing patch of tiles | 72 |
| 5.6 | Example of a simple mistake | 72 |
| 5.7 | Example of a simple mistake | 73 |
| 5.8 | Example of a simple mistake | 74 |
| 5.9 | Example of a simple mistake | 74 |
| 5.10 | Two thick rhombs joined along a single arrow edge | 75 |
| 5.11 | The arrangement of Figure 5.7, composed | 75 |
| 5.12 | A simple mistake | 76 |
| 5.13 | The simple mistake, decomposed | 77 |
| 5.14 | Example of a deception | 78 |
| 5.15 | A growing patch of tiles | 79 |
| 5.16 | Two possibilities for tile placement | 80 |
| 5.17 | An algorithm for correct placement of tiles | 80 |
| 5.18 | An algorithm for correct placement of tiles | 81 |
| 5.19 | An algorithm for correct placement of tiles | 82 |
| 5.20 | An algorithm for correct placement of tiles | 83 |
| 5.21 | An algorithm for correct placement of tiles | 85 |
| 5.22 | An algorithm for correct placement of tiles | 86 |
| 5.23 | An algorithm for correct placement of tiles | 87 |
| 5.24 | Growing patches of tiles | 88 |
| 5.25 | Adding a thin or thick rhomb | 89 |
| 5.26 | Overlapped possibilities | 90 |
| 5.27 | We proceed unambiguously until this point | 91 |
| 5.28 | Two correct arrangements | 92 |
| 5.29 | The configurations of Figure 5.28 overlapped | 92 |
| 5.30 | Decomposed version of Figure 5.29 | 93 |
| 5.31 | The tiles that distinguish the arrangements | 93 |
| 5.32 | Separating the overlapped arrangements of Figure 5.31 | 94 |
| 5.33 | The thick and thin units that make up a worm | 94 |
| 5.34 | Decomposed worms | 95 |
| 5.35 | A worm oriented up | 96 |

| | | |
|------|---|-----|
| 5.36 | A downward oriented worm | 96 |
| 5.37 | Overlapped worm orientations | 96 |
| 5.38 | Worms intersecting in two ways | 97 |
| 5.39 | Decomposed worm intersections | 98 |
| 5.40 | An incompatible worm arrangement | 99 |
| 5.41 | Our original mistake | 99 |
| 5.42 | Decomposed error | 100 |
| 5.43 | Changing one tile resolves the error | 101 |
| 5.44 | Three legal arrangements of tiles surrounding a thick rhomb | 102 |
| 5.45 | The patches of Figure 5.44 overlapped. | 103 |
| 5.46 | The arrangements of Figure 5.44 decomposed | 103 |
| 5.47 | Overlapping the arrangements of Figure 5.46 | 104 |
| 5.48 | The patterns of worms in Figure 5.47 | 105 |
| 5.49 | The arrangement of Figure 5.46 with worms coloured | 105 |
| 5.50 | All three arrangements share all of the tiles in this diagram. | 106 |
| 5.51 | The seven possible worm arrangements around a thick rhomb | 107 |
| 5.52 | The seven possible worm arrangements around a thick rhomb | 108 |
| 5.53 | The thick rhomb can be surrounded by four worms | 109 |
| 5.54 | There must be four worms in the coloured areas | 110 |
| 5.55 | One possible arrangement of worms around a thick worm | 110 |
| 5.56 | The worm quadrilateral obtained by decomposing Figure 5.55 ... | 111 |
| 5.57 | The quadrilateral associated with the thick rhomb | 111 |
| 5.58 | Decomposing the central rhomb | 112 |
| 5.59 | Adding forced tiles to the decomposed patch | 112 |
| 5.60 | Decomposing the new patch | 113 |
| 5.61 | Repeating the process | 113 |
| 5.62 | The quadrilateral surrounding a thin rhomb | 114 |
| 5.63 | The five arrangements of worms that can surround a thin rhomb . | 115 |
| 5.64 | This blank space needs to be filled with a worm | 116 |
| 5.65 | One tile determines the orientation of the worm | 116 |
| 5.66 | The worm orientation is determined by the first tile placed. | 116 |
| 5.67 | The quadrilateral of forced tiles surrounding a thin rhomb | 117 |
| 5.68 | Worms are the difference between thin and thick rhombs | 118 |
| 5.69 | The simple mistake | 119 |
| 5.70 | The erroneous <i>LLL</i> sequence | 120 |
| 6.1 | Growing a quasicrystal | 121 |

Acknowledgement

I would like to acknowledge the guidance and support of a number of people who helped me in various ways over the course of the last two years. First and foremost, my supervisor, Bill Casselman for encouraging me to pursue this direction. I am thankful for his support, and I am constantly inspired by his firm belief that pictures are an integral part of mathematical exposition.

I would also like to thank Michael Monagan for helping me clarify what I didn't want to study, and Julie Tolmie for reinvigorating my interest in the visual side of math.

Personally, I wish to thank my parents and friends for providing a vital network of support. In particular, I need to thank Jeff Weir for his patience and stability.

Chapter 1

Introduction

1.1 Introduction

The topic of non-periodic tilings has been of great interest to both mathematicians and those outside the discipline who seek to use tilings as a model for natural processes. Specifically, tilings are an important area of research for scientists studying crystal growth. The discovery of non-periodic tilings of the plane by Roger Penrose in the seventies raised many questions within the areas of crystal research. Previous to this important discovery, it was assumed that crystals could be broken down into unit cells: finite groupings of atoms that packed together to fill space and create a crystal [Sen95]. For this reason, tilings of the plane have been used as elementary models of crystals, with hexagons, triangles, and rhombs (among others) serving to model the unit cells. Then, in 1984, several materials scientists claimed to have found a crystals exhibiting fivefold rotational symmetry – something previously thought to be impossible in a crystal [SBC84]. Suddenly, Penrose's tilings didn't seem like merely a mathematical recreation.

Although the fivefold symmetry exhibited by Penrose tilings seemed to provide a good 2D model for quasicrystals, there is one significant problem with this association. That is, the Penrose tiles fail to provide a good model for the growth of quasicrystals. We have numerous methods to construct Penrose tilings, but none of them seem to have plausible extensions to the way that 'nature' would construct a crystal. More importantly, any attempt to create a tiling of the plane by adding tiles one at a time will yield mistakes: gaps in the tiling that cannot be filled with tiles.

This paper will investigate the problem of growth for Penrose tilings.

1.2 Outline

Chapter Two is an introduction to the one-dimensional analogue of Penrose tilings, Fibonacci tilings. These non-periodic structures share many characteristics of Penrose tilings, and provide a good framework in which to situate the discussion of Penrose tilings. Their basic structures and properties will be discussed, and three methods for their generation will be presented. The chapter concludes with a discussion of forcing and the impossibility of local rules for their construction.

Chapter Three will follow the format of Chapter Two, with an added dimension. The properties of Penrose tiles and several methods for their construction will be discussed.

The fourth Chapter is an analysis of the growth of Fibonacci tilings. Specifically, we will consider the problem of attempting to avoid errors in the tiling, which involves a non-local decision making procedure.

Chapter Five will be a consideration of these concerns for Penrose tilings. We will see that there is no local growth algorithm for these tilings, and that the process of avoiding mistakes is inherently nonlocal.

Chapter 2

Fibonacci tilings

2.1 Introduction to Fibonacci tilings

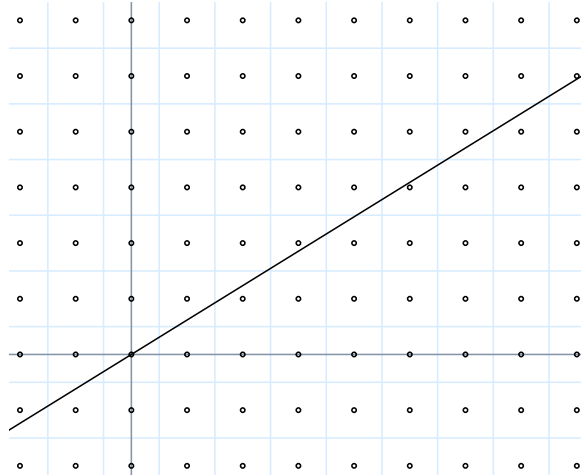
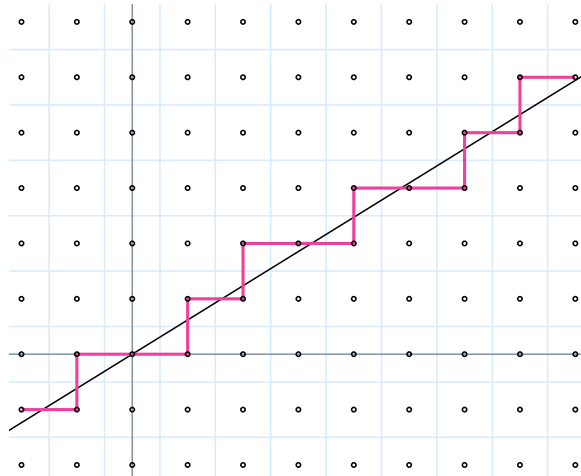
A **Fibonacci tiling** is a one dimensional non-periodic structure. In a general sense, this means that it is a tiling of the line that does not admit any translations. The tiles are intervals of two lengths, with the ratio of the lengths of the short and long intervals being $1 : \tau$, where τ is the golden mean, or $\frac{1+\sqrt{5}}{2}$. Note that Fibonacci tilings of the line are alternately known as **Musical Sequences** [GS87], or **Fibonacci Sequences** [Pen89].

We will begin by defining Fibonacci tilings using the projection method, and investigating their properties. The central concern of this chapter thereafter will be describing alternative characterizations of these tilings. All of the methods that I will discuss have two dimensional versions that will be useful later. Notationally, we will refer to Fibonacci tilings as actual tilings of the Real line by intervals. Fibonacci strings will be symbolic versions of the tilings.

2.2 Fibonacci tilings using the Projection Method

In this section we will explore sequences created using the projection method. In short, this method uses the projection of an integer lattice on to the line of slope $1/\tau$ to obtain a sequence of short and long intervals.

Begin with the integer lattice given by $\{(x, y) \mid x, y \in \mathbb{Z}\}$, and take the line through the origin given by $y = x/\tau$, as shown in Figure 2.1. Now draw a “staircase” with vertical steps of 1 unit length, and horizontal steps of 1 or 2 unit lengths, such that every step (horizontal or vertical) will cut the line exactly once (Figure 2.2). From this staircase, we can record a string of S 's and

Figure 2.1: The Integer lattice and the line $y = x/\tau$ Figure 2.2: The “staircase” corresponding to the line $y = x/\tau$

L 's, such that each vertical step corresponds to S , each horizontal step of one unit corresponds to L , and each horizontal step of two units corresponds to LL . The staircase above yields the string $LSLLSLSLLSLLSLSL$. An infinite sequence generated in this way is called a **Fibonacci string**. This method is

called the **projection method**. Let us consider this process in more detail. First we need some definitions and background on the general projection method.

2.2.1 Definitions and Background

A point set $\Lambda \in \mathbb{R}^n$ is said to be **discrete** if there exists $r > 0 \in \mathbb{R}$ such that for every $x, y \in \Lambda$, $|x - y| \geq 2r$. Λ is **relatively dense** in \mathbb{R}^n if there exists $R > 0 \in \mathbb{R}$ such that every sphere of radius greater than R contains at least one point of Λ in its interior. A point set that is both relatively dense and discrete is called a **Delone set**.

Let $\Lambda \in \mathbb{R}^n$ be any Delone set. The **Voronoi cell** of a point $x \in \Lambda$ is defined as:

$$V(x) = \{u \in \mathbb{R}^n : |x - u| \leq |y - u|, \forall y \in \Lambda\}$$

That is, $V(x)$ is the set of points of \mathbb{R}^n that lie at least as close to x as to any other point of Λ .

A **\mathbb{Z} -module** is the countably infinite group generated by any set of vectors, $\mathbf{b}_1, \mathbf{b}_2, \dots, \mathbf{b}_k \in \mathbb{R}^n$ under addition. It has elements $m_1\mathbf{b}_1 + \dots + m_k\mathbf{b}_k$, where $m_i \in \mathbb{Z}$. A \mathbb{Z} -module in \mathbb{R}^n is called a **lattice** if it is generated by n linearly independent vectors. A lattice will be denoted \mathcal{L} , and its orbit will be given by \mathcal{L}^p .

Let \mathcal{L} be a lattice and \mathcal{E} any k -dimensional subspace of \mathbb{R}^n where $0 < k < n$. If $\mathcal{E} \cap \mathcal{L} = \{0\}$, then \mathcal{E} is said to be **totally irrational** [Sen95]. A Delone set will be called **non-periodic** if it admits no translations except the identity.

2.2.2 The general projection method

Let \mathcal{E} be a totally irrational d -dimensional subspace of \mathbb{R}^n , and let \mathcal{E}^\perp be its orthogonal complement (\mathcal{E}^\perp will not necessarily be totally irrational). Let Π be the orthogonal projector onto \mathcal{E} and Π^\perp be the orthogonal projector onto \mathcal{E}^\perp . Then Π and Π^\perp are linear maps. Furthermore, $\Pi(\mathcal{L}^p)$ and $\Pi^\perp(\mathcal{L}^p)$ are orbits of \mathbb{Z} -modules in \mathcal{E} and \mathcal{E}^\perp respectively, generated by the projections of any given basis of \mathcal{L}^p .

Proposition 2.1 [Sen95] When \mathcal{L} is an integral lattice, the following are equivalent:

- i) $\Pi(\mathcal{L})$ is everywhere dense in \mathcal{E} .
- ii) $\mathcal{L} \cap \mathcal{E} = \{0\}$.

iii) $\Pi^\perp|_{\mathcal{L}}$ is one-to-one.

Since $\Pi(\mathcal{L}^p)$ is dense in \mathcal{E} , it is not a Delone set. So we need to select a subset of the points of \mathcal{L}^p for projection. To do this, fix a compact subset with nonempty interior, $K \subset \mathcal{E}^\perp$, and call K the **window** or acceptance domain. We will now project onto \mathcal{E} those points $x \in \mathcal{L}^p$ such that $\Pi^\perp(x) \in K$. These will be the points that lie in the cylinder $C = K \oplus \mathcal{E}$.

Proposition 2.2 [Sen95] $\Pi(X)$ is a Delone set.

Proof. To prove this, we need to show two things: that $\Pi(X)$ is discrete, and that $\Pi(X)$ is relatively dense in \mathcal{E} .

To show that $\Pi(X)$ is discrete, we will show that there is a neighborhood of the origin in \mathcal{E} that contains no other points of $\Pi(X)$. Let x be a point in the integer lattice \mathcal{L}^p , and take $c > 0$ such that $\Pi(x)$ lies in the ball of radius c centered at 0, $B_0(c)$. Now x has the property that

$$|x|^2 = |\Pi(x)|^2 + |\Pi^\perp(x)|^2$$

and since the set $\Pi^\perp(X)$ is bounded by assumption, x must lie in a sphere about 0 of some finite radius $m > 0$. Let $U = \mathcal{L}^p \cap B_0(m)$, and notice that U must be a finite subset of \mathcal{L}^p since \mathcal{L}^p is discrete. Then $\Pi(U)$ must also be finite, and for $r > 0$ sufficiently small, we will have that $\Pi(u) \cap B_0(r) = \{0\}$, hence $\Pi(X)$ is discrete.

Relative density follows immediately from the fact that \mathcal{L}^p is relatively dense in \mathbb{R}^n and hence in the cylinder C . \square

Proposition 2.3 [Sen95] If \mathcal{E} is totally irrational, then the Delone set $\Pi(X)$ is non-periodic.

This will be shown for the specific case of Fibonacci tilings later in this chapter (see Theorem 2.10).

Proposition 2.4 [Sen95] For the canonical projection given by the window $K = \Pi^\perp(V(0))$ (where $V(0)$ is the Voronoï cell of the origin), the following are equivalent:

- i) $x \in X$
- ii) $\Pi^\perp(x) \in \Pi^\perp(V(0))$
- iii) $\mathcal{E} \cap V(x) \neq \emptyset$

The projection method as described above will be used to create what we will call Fibonacci tilings.

2.2.3 Using the Projection method to create Fibonacci tilings

Consider the integer point lattice I_2^p , where the Voronoï cell of any point is a square (Figure 2.1). Let ℓ be the line through the origin, with slope $1/\tau$. Then ℓ is a totally irrational subspace of E^2 , as it contains NO other lattice points of E^2 , and hence does not pass through the vertex of the Voronoï cell of any lattice point.

Now, let X be the subset of I_2^p whose Voronoï cells are cut by ℓ . These points will be unambiguously ordered by ℓ . These will be the vertices of the “staircase” of Figure 2.2. The m th point is given by the vector

$$\mathbf{p}_m = (m_1, m_2), \text{ with } m_1, m_2 \in \mathbb{Z}, \text{ and } m_1 + m_2 = m$$

and the $(m + 1)$ th point will be:

$$\mathbf{p}_{m+1} = (m_1 + 1, m_2) \text{ or}$$

$= (m_1, m_2 + 1)$. So the points in X can be seen as the nodes of a unique staircase, with the sequence $\{\mathbf{p}_m\}$ keeping track of the number of horizontal and vertical steps.

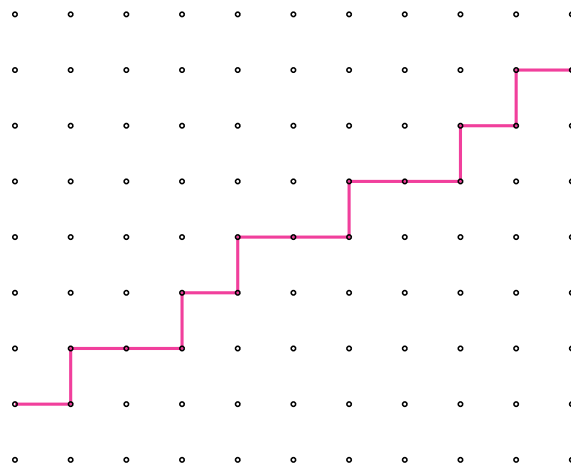


Figure 2.3: The Fibonacci staircase

Consider the staircase generated by this procedure. Record a 'S' for every vertical step, and an 'L' for every horizontal step by one interval. As we have seen, the staircase shown will generate the sequence $LSLLSLSLLSLLSLSL$.

This will be called a Fibonacci string. To obtain what we will call a Fibonacci tiling, we need to do a little more work.

Let Π be the orthogonal projector onto ℓ , as shown in Figure 2.4. Then

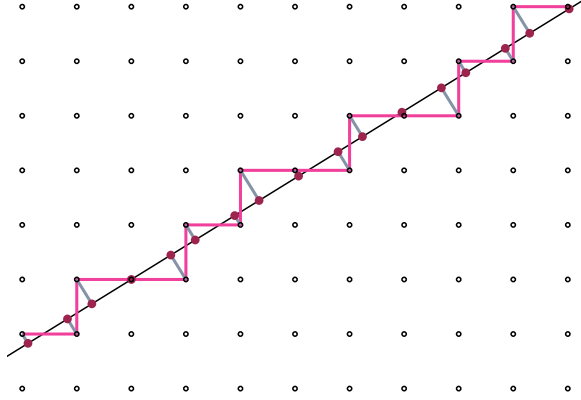


Figure 2.4: The orthogonal projection of X onto ℓ

$\Pi(X)$ is a Delone set Λ with steps of lengths

$$|\Pi(\mathbf{e}_1)| = \tau/\nu, \quad |\Pi(\mathbf{e}_2)| = 1/\nu$$

where $\nu^2 = \tau^2 + 1^2$, and \mathbf{e}_1 and \mathbf{e}_2 are the eigenvectors corresponding to the matrix $P = \begin{pmatrix} 1 & 1 \\ 1 & 0 \end{pmatrix}$. The vectors $\mathbf{e}_1 = \frac{1}{\nu}(\tau, 1)$ and $\mathbf{e}_2 = \frac{1}{\nu}(-1, \tau)$ form an orthonormal basis for E^2 .

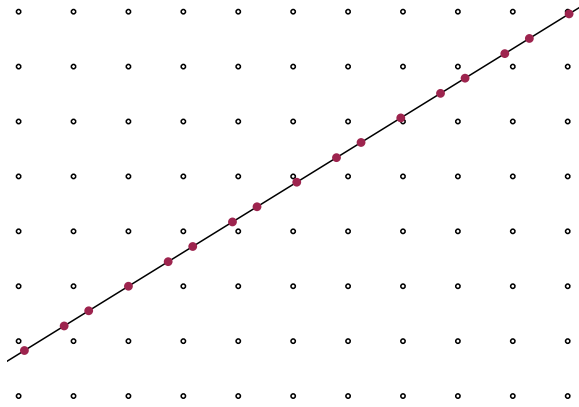
The line ℓ cuts the Voronoi cell of the lattice point (u, v) if and only if it intersects the principal diagonal of the cell. The lines of the diagonals are $x + y = m$ for $m \in \mathbb{Z}$, and ℓ is the line $y = x/\tau$. They intersect at the point $(m/\tau, m/\tau^2)$. In other words, ℓ cuts the Voronoi cell of (u, v) iff

$$u - 1/2 < \frac{m}{\tau} < u + 1/2$$

$$v - 1/2 < \frac{m}{\tau^2} < v + 1/2$$

with $v = m - u$. Then $u = \left\| \frac{m}{\tau} \right\|$, where $\|x\|$ represents the nearest integer function. So the coordinates of the m th node are

$$\mathbf{p}_m = \left(\left\| \frac{m}{\tau} \right\|, m - \left\| \frac{m}{\tau} \right\| \right)$$

Figure 2.5: The delone set $\Lambda = \Pi(X)$ (in pink)

Projecting on to ℓ , the m th point of $\Lambda = \Pi(X)$ has coordinates

$$x_m = \frac{m}{\nu} + \frac{1}{\tau\nu} \left\| \frac{m}{\tau} \right\|$$

where x_m is just $|(a, b)|$, when (a, b) is the projection of the point (u, v) onto the line ℓ (Figure 2.5). Then by proposition 2.4, $X = \{x \in I_2^p \mid \Pi^\perp(x) \in K\}$, where Π^\perp is the orthogonal projector onto the line perpendicular to ℓ , ℓ^\perp ; $K = \Pi^\perp(V(0))$ is the window of the projections, and $V(0)$ is the Voronoï cell of the origin. In this case, $K = [-\tau^2/2\nu, \tau^2/2\nu]$ on ℓ^\perp . We will call the projection of X , $\Lambda = \Pi(X)$, a **Fibonacci tiling**. By Proposition 2.3 this is a non-periodic Delone set.

To obtain other Fibonacci tilings, we may simply translate the line ℓ vertically so that it cuts the Voronoï cells of the Integer lattice in a different way. This will yeild uncountably many different Fibonacci tilings.

2.2.4 Properties of the Fibonacci tiling

We can gain much information about a Fibonacci tiling generated by projection by examining the window of acceptance. First: a few definitions.

Let $r > 0$. The **r-star** at $x \in \Lambda$ is the finite point set $\bar{B}_x(r) \cap \Lambda$, where $\bar{B}_x(r)$ is the closed ball of radius r centred at x . The set of all r-stars, up to M -equivalence, where M is a group of motions, is called its **r-atlas**.

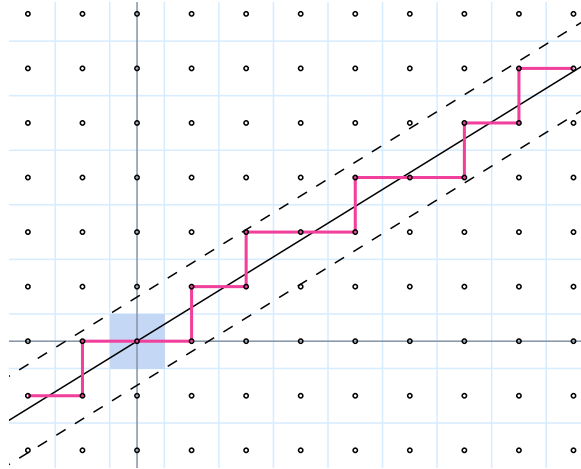


Figure 2.6: The Voronoi cell of the origin

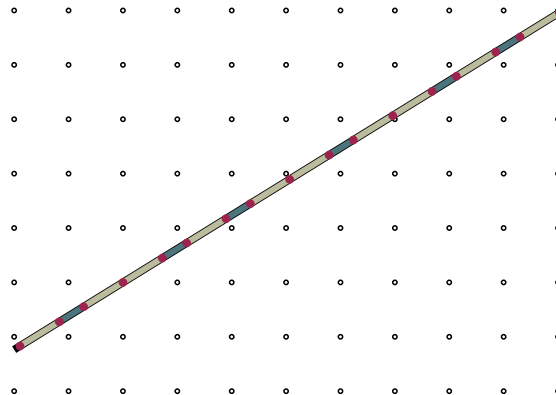


Figure 2.7: The resulting Fibonacci tiling

We are interested in determining the (τ/ν) -atlas of the Fibonacci tilings. Consider the three valid words of length 2 in a Fibonacci tiling: LL , LS , and SL . Recall that L has length τ/ν and S has length $1/\nu$. To determine the frequencies of these three words of length two in the atlas, consider K , the window of acceptance of the projection. Note that the four edges of $V(0)$ project to

four subintervals of K , which in turn partition K into 3 distinct subintervals with disjoint interiors (Figure 2.8).

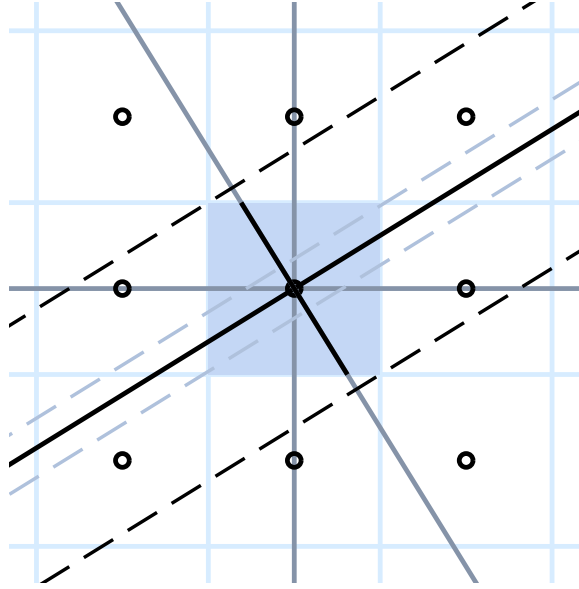


Figure 2.8: The window of acceptance of the projection

These are:

$$\begin{aligned} U_1 &= \frac{1}{\nu}[-\tau^2/2, (1-\tau)/2] \\ U_2 &= \frac{1}{\nu}[(1-\tau)/2, (\tau-1)/2] \\ U_3 &= \frac{1}{\nu}[(\tau-1)/2, \tau^2/2] \end{aligned}$$

$|U_1| = |U_3| = 1/\nu$, and $|U_2| = \frac{\tau-1}{\nu}$. Moreover, $|U_2 \cup U_3| : |U_1| = \tau : 1$. We have the following:

Proposition 2.5 [Sen95] *The point x_k is of adjacency type LL iff $\Pi^\perp(x_k) \in U_2$.*

Proof. We know that a lattice point $(u, v) \in X$ projects to a point of type LL if and only if $\{\Pi^\perp(u-1, v), \Pi^\perp(u, v), \Pi^\perp(u+1, v)\}$ all lie in the acceptance interval $K = [-\tau^2/2\nu, \tau^2/2\nu]$. So u and v must satisfy:

$$\frac{-\tau^2}{2\nu} \leq \frac{-u + \tau v}{\nu} \leq \frac{\tau^2}{2\nu}$$

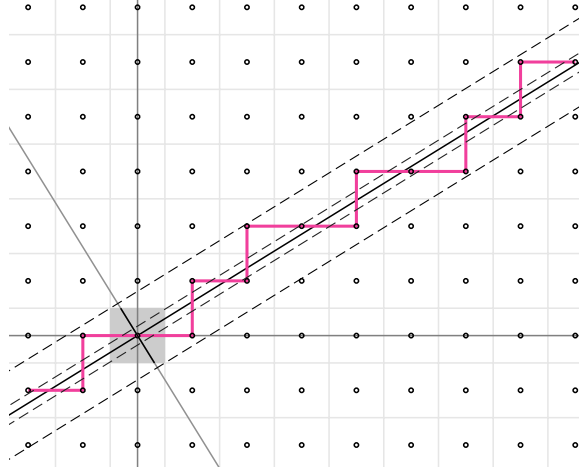


Figure 2.9: The Fibonacci staircase with the divided window of acceptance

$$\begin{aligned} \frac{-\tau^2}{2\nu} - 1 &\leq \frac{-u + \tau v}{v} \leq \frac{\tau^2}{2\nu} - 1 \\ \frac{-\tau^2}{2\nu} + 1 &\leq \frac{-u + \tau v}{v} \leq \frac{\tau^2}{2\nu} + 1 \end{aligned}$$

which means that the projection of x_k , $\frac{-u+\tau v}{2\nu}$ must be in the interval $[(1 - \tau)/2\nu, (\tau - 1)/2\nu] = U_2$ \square

Using this method, we can also show that the point x_k is of adjacency type LS iff $\Pi^\perp(x_k) \in U_3$, or is of the adjacency type SL iff $\Pi^\perp(x_k) \in U_1$. We can also show the following important fact:

Proposition 2.6 [Sen95] *The relative numbers of short and long intervals in $\Pi(X)$ is $\tau : 1$.*

Proof. Let $x_n = \Pi(\mathbf{p}_n)$, and let $y_{n+1} = x_{n+1} - x_n$. We want to show that $y_{n+1} = \tau$ iff $\Pi^\perp(\mathbf{p}_n) \in U_2 \cup U_3$, otherwise, $y_{n+1} = 1$.

Now $\Pi(\mathbf{p}_{n+1} - \mathbf{p}_n) = \tau$ iff ℓ cuts the Voronoï cells of both (u, v) and $(u + 1, v)$. We need both points to project into K , and this means that $\frac{-u+\tau v}{v} \in U_2 \cup U_3$, using the same argument as in the previous proposition. Recall that $|U_2 \cup U_3| : |U_1| = \tau : 1$. \square This result will be shown again later, using different techniques.

2.3 Updown generation of Fibonacci tilings

Now that we have seen Fibonacci tilings, it seems natural to ask if these sequences can be created in any other way. The answer is that there is a very elegant symbolic way in which to generate Fibonacci tilings. To understand this technique, we need to outline some background concepts.

2.3.1 Decomposition and Composition of Fibonacci Strings

Suppose we are trying to recreate the Fibonacci sequences as described by the projection method. We know that the relative numbers of short to long intervals is $1 : \tau$. Consider the following example.

Let $\mathbf{p}_0 = (0, 1)$ represents an initial string of one L , and $\mathbf{p}_1 = (1, 0)$ represents a string of one S , and consider the linear transformation given by the matrix

$$P = \begin{pmatrix} 1 & 1 \\ 1 & 0 \end{pmatrix}$$

In other words, P performs the transformation given by

$$\begin{aligned} S &\longrightarrow S + L \\ L &\longrightarrow S \end{aligned}$$

Since

$$\mathbf{p}_0 P = (0, 1) \begin{pmatrix} 1 & 1 \\ 1 & 0 \end{pmatrix} = (1, 0) = \mathbf{p}_1$$

and

$$\mathbf{p}_1 P = (1, 0) \begin{pmatrix} 1 & 1 \\ 1 & 0 \end{pmatrix} = (0, 1) \begin{pmatrix} 1 & 1 \\ 1 & 0 \end{pmatrix}^2 = (1, 1) = (1, 0) + (0, 1) = \mathbf{p}_1 + \mathbf{p}_0$$

Let \mathbf{p}_i represent the number of S 's and L 's after the i^{th} application of P to \mathbf{p}_i . Note that

$$\mathbf{p}_{m+1} = \mathbf{p}_0 P^{m+1} = (0, 1) \begin{pmatrix} 1 & 1 \\ 1 & 0 \end{pmatrix}^{m+1}$$

$$= (0, 1) \begin{pmatrix} F_{m+1} & F_m \\ F_m & F_{m-1} \end{pmatrix} = (F_m, F_{m-1})$$

where F_m are the Fibonacci numbers, given by $F_{n+1} = F_n + F_{n-1}$, with $F_0 = 0, F_1 = 1$. This means that there will be F_m S's and F_{m-1} L's in the $(m + 1)$ th iteration. It is a well known fact that the ratio of the Fibonacci numbers $F_m : F_{m-1}$ approaches $\tau : 1$ as m approaches ∞ . So keeping this in mind, suppose we view the transformation multiplicatively instead of additively, and we perform the following:

$$\begin{aligned} S &\longrightarrow SL \\ L &\longrightarrow S \end{aligned}$$

These substitution rules are the basis of the **decomposition** procedure. For example, beginning with the simple string consisting of one L, and applying the decomposition rules yields the following:

$$\begin{aligned} &L \\ &S \\ &SL \\ &SLSS \\ &SLSSL \\ &SLSSLSLSSL \\ &SLSSLSLSSLSSL \\ &\vdots \end{aligned}$$

Note that the string at each stage of this process is simply the concatenation of the previous two strings. Continuing in this way, decomposition produces strings that are infinite in one dimension.

After the i^{th} application of this decomposition procedure, there will be F_{i-1} S's and F_i L's. This means that these strings will be non-periodic. That is, they admit no translations. This result follows from the well known fact¹ that the ratio of the Fibonacci numbers, F_m/F_{m-1} approaches τ , the golden mean, as m increases. We have seen that the ratio of S's to L's in the $(m + 1)$ th

¹The proof of this fact is an elementary argument using the eigenvectors of the matrix P

iteration of the substitution process is $F_m : F_{m+1}$. Hence the ratio of S 's to L 's will approach an irrational number, and will never be periodic as a result.

Composition is the opposite procedure to decomposition and is used to reduce strings of S 's and L 's to shorter such strings. Composition uses the following transformation:

$$\begin{aligned} SS &\longrightarrow L \\ L &\longrightarrow S \\ S &\longrightarrow e \end{aligned}$$

For example:

$$\begin{aligned} &SLSSLSLSSLSSLSLSSLSS \\ &SLSSLSLSSLSSL \\ &SLSSLSLS \\ &SLSS \\ &SL \\ &S \end{aligned}$$

2.3.2 Definition of Fibonacci Strings and Fibonacci tilings

Consider any two way infinite string of S 's and L 's in which neither SSS nor LL appear. Compose it according to the composition rules above, to yield another infinite string of S 's and L 's, called the *predecessor*. If this string does not contain either of the substrings SSS or LL , we can compose it to obtain another predecessor, and so on. We have the following definitions: [Sen95]

Definition 2.7 A **Fibonacci string** \mathcal{F} is a two way infinite string of S 's and L 's that has predecessors in all levels with respect to the composition rules.

Now associate with S and L line segments of two lengths, with $L/S = \tau$. Define the Fibonacci Delone set to be the end points of the sequence of line segments associated to the letters.

Definition 2.8 A **Fibonacci tiling** is a two way infinite sequence

$$\dots, -x_2, -x_1, x_0, x_1, x_2, \dots$$

of points on the Real line such that

- i) $x_{n+1} - x_n \in c\{1, \tau\}$ for $c > 0$
- ii) the difference sequence $x_{n-1} - x_n$ has predecessors of all levels under composition

Now we need to make sure that this definition agrees with our original Fibonacci tilings generated using the projection method. We have the following:

Theorem 2.9 [Sen95] $\Lambda = \Pi(X)$ is a Fibonacci tiling.

Proof. We need to show that the sequence $\Pi(\mathbf{p}_{m+1} - \mathbf{p}_m)$ has predecessors at all levels. That is, we need to show that there exists a rescaled copy of the integer lattice I_2^p that is to the predecessor of Λ as I_2^p is to Λ itself. This argument can then be repeated to find a predecessor of the predecessor, etc.

Consider the lattice generated by the vectors $\tau\mathbf{e}_1$ and $\tau\mathbf{e}_2$. Not surprisingly, this yields the lattice τI_2^p , and its Voronoi cell projects to τK on ℓ^\perp . That is, it projects to the interval $\tau k = [-\tau^3/2\nu, \tau^3/2\nu]$ on ℓ^\perp . We have the lattices and projections shown in figure 2.10 below.

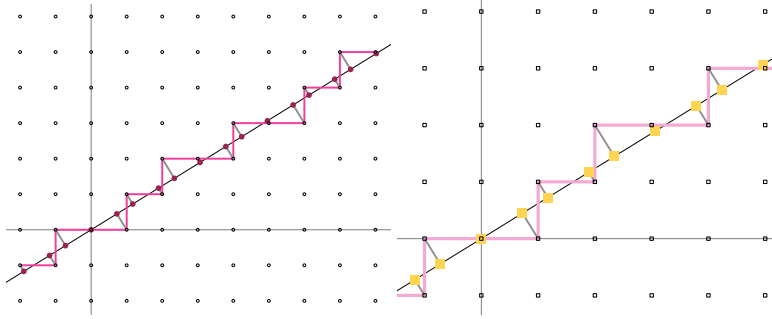


Figure 2.10: Proof of Theorem 2.9: the integer lattice I_2^p and the scaled integer lattice τI_2^p with projections onto the line ℓ

We need to ensure that this new construction does not introduce any new points. That is, we need to show that all points projected from τI_2^p are also projected from I_2^p . Overlapping the projections, we have the situation depicted in Figure 2.11 (points of the scaled lattice, τI_2^p are squares).

A point of τI_2^p has coordinates $(\tau u, \tau v)$, where (u, v) is in the standard integer lattice, I_2^p . The projection of $(\tau u, \tau v)$ onto ℓ is $\frac{\tau^2 u + \tau v}{\nu}$. We now need to show that this is also a point of $\Pi(X)$. Recalling the identity $\tau^2 = \tau + 1$, note that

$$\tau^2 u + \tau v = \tau(u + v) + u = (u + v, u) \cdot (\tau, 1)$$

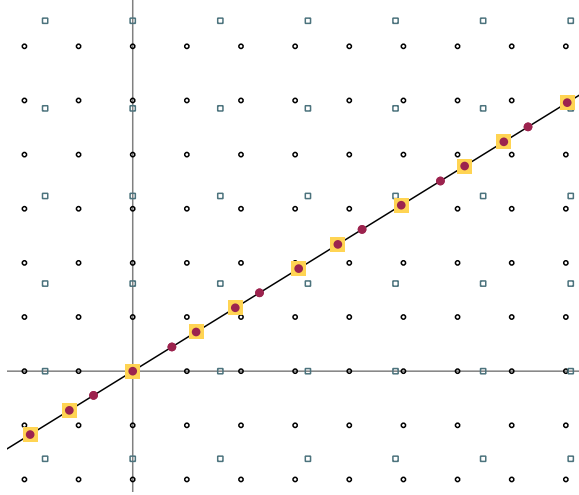


Figure 2.11: Proof of Theorem 2.9: the overlapped projections of the Integer lattice and the scaled lattice (τI_2^p) onto the line ℓ

which means that we must show: $\Pi^\perp(u + v, u) \in [-\tau^2/2\nu, \tau^2/2\nu]$, or that $\nu\Pi^\perp(u + v, u) \in [-\tau^2/2, \tau^2/2]$. But this must be true since we know that $\nu\Pi^\perp(u, v)$ is in the interval, and

$$\nu\Pi^\perp(u + v, u) = -(u + v) + \tau u = \frac{1}{\tau}(u - \tau v)$$

□ Note that for every Fibonacci tiling there is an

associated Fibonacci string, and vice versa. In the remainder of this work we will use Fibonacci tiling to mean either the string or the tiling.

2.3.3 Decomposition and Composition of Fibonacci tilings

Decomposition of Fibonacci tilings works on the same premise as decomposition of the Fibonacci strings. The only difference is that instead of generating longer and longer strings, decomposition *cuts up* the existing tiles of a Fibonacci tiling into smaller tiles that resemble the original tiles. We are still

performing the same transformation:

$$\begin{aligned} S &\longrightarrow L \\ L &\longrightarrow LS \end{aligned}$$

and this transformation is performed simultaneously to each interval in the sequence. In Figure 2.12 the decomposition process cuts up existing tiles into smaller tiles.

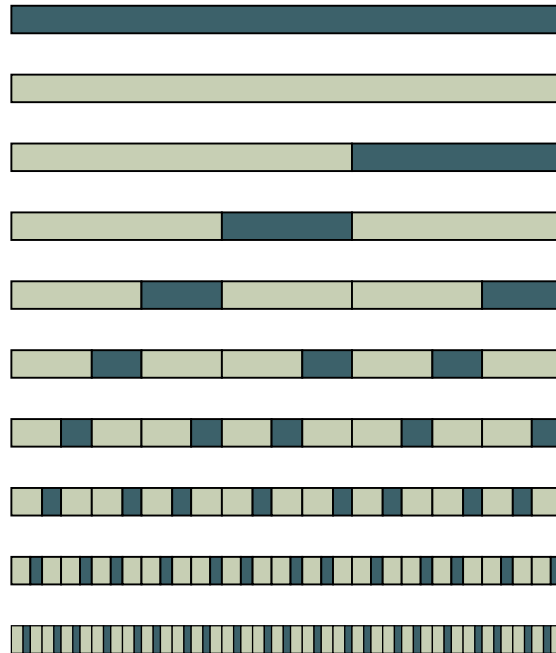


Figure 2.12: Decomposition of Fibonacci tiles

Similarly, composition of Fibonacci tilings involves taking the unions of tiles to build up larger tiles. To compose a Fibonacci sequence, we perform the following transformation:

$$\begin{aligned} LL &\longrightarrow S \\ S &\longrightarrow L \\ L &\longrightarrow e \end{aligned}$$

The composition process is shown in Figure 2.13

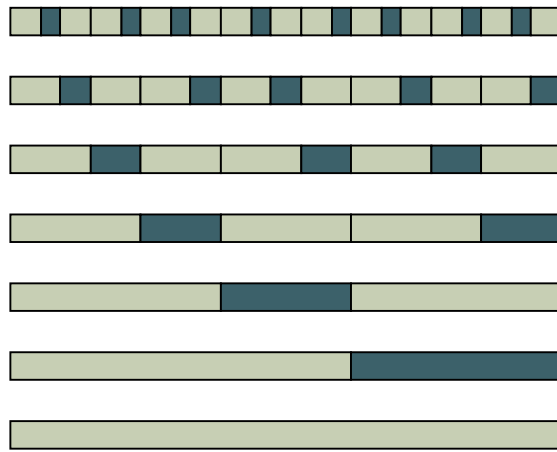


Figure 2.13: Composition of Fibonacci tiles

In summary, composition (decomposition) of Fibonacci *strings* makes the strings shorter (longer). In contrast, composition (decomposition) of a Fibonacci *tiling* yeilds a tiling of the same length with fewer (more) tiles. That is, decomposition subdivides the \mathbb{R} line into more intervals, while maintaining the ratio of interval lengths.

We can also preserve the length of the original tile in the decomposition procedure by applying an **inflation** at each stage of decomposition. That is, after each subdivision of intervals into shorter intervals, multiply the endpoints of our intervals, $\dots, -x_2, -x_1, x_0, x_1, x_2, \dots$ by a factor of τ , to yield tiles on the same scale as the original tile. Similarly, composition can be accompanied by **deflation** to achieve a similar effect.

2.3.4 More Properties of Fibonacci tilings

Fibonacci tilings may, at first glace, seem random, but are in fact governed by a few rules. Specifically, it is easy to see that a Fibonacci tiling will not contain three adjacent Long intervals, nor will it contain two adjacent Short intervals.



Figure 2.14: Proof of Theorem 2.10: A fragment of a Fibonacci tiling



Figure 2.15: Proof of Theorem 2.10: F has a translation symmetry of length d

The decomposition rules preclude such arrangements, and it is easy to see so. From the definitions we can show a few more interesting results.

Theorem 2.10 *Every Fibonacci sequence is non-periodic. That is, it cannot be written as a finite block of terms that is repeated infinitely often.*

Proof. We wish to show that every Fibonacci sequence is non-periodic, that is, does not exhibit any translational symmetry. Notice that a symmetry of a Fibonacci tiling must also be a symmetry of the composed Fibonacci tiling.

Begin with an infinite Fibonacci tiling of the line, \mathcal{F} . A fragment is shown in Figure 2.14. Suppose that \mathcal{F} has a translation symmetry through the length d , as indicated by the yellow bar in Figure 2.15. Compose \mathcal{F} according to the composition rules to obtain $\tau^2\mathcal{F}$ (Figure 2.16). Iterate this process to obtain longer and longer intervals (in the same proportions). We obtain a sequence $\tau^{2n}\mathcal{F}$ with arbitrarily long intervals (Figure 2.17). Then a translation through some distance d cannot be a symmetry of $\tau^{2n}\mathcal{F}$ if n is chosen to be sufficiently large so that each interval in $\tau^{2n}\mathcal{F}$ is longer than d . Therefore no translation is a symmetry of \mathcal{F} , and hence \mathcal{F} is non-periodic. \square

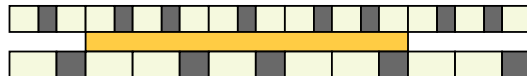


Figure 2.16: Proof of Theorem 2.10: The fragment composed to obtain $\tau^2\mathcal{F}$

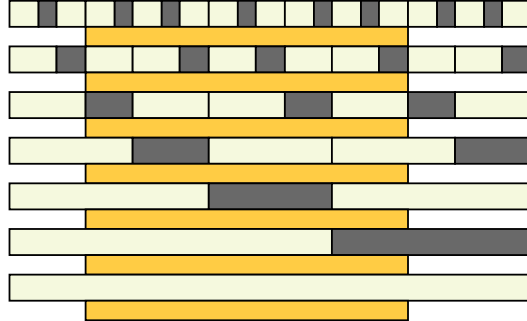


Figure 2.17: Proof of Theorem 2.10: The composed fragment

Theorem 2.11 [GS87] Fibonacci tilings exhibit local isomorphism. That is, every finite block of consecutive terms in any Fibonacci tiling occurs infinitely often in every other Fibonacci tiling.

Proof. For the purpose of this discussion, the meeting point of two tiles in a 1-dimensional Fibonacci tiling will be called a vertex. The two tiles adjacent to this vertex will be called the vertex neighborhood. Note that there are exactly 3 possible kinds of vertex neighborhoods in a Fibonacci tiling. They are $\{SL, LS, LL\}$ (Figure 2.18). We have the following lemma:



Figure 2.18: The three vertex neighborhoods

Lemma 2.12 Each of the 3 vertex neighborhoods occurs in every Fibonacci tiling of the line, and does so infinitely often.

This fact is easy to see, and almost as easy to prove! Since we can't have two adjacent short intervals, it is clear that we must have SL appearing infinitely often in every Fibonacci tiling of the line. Recall that the decomposition of a Fibonacci tiling is also a Fibonacci tiling by definition. Hence we must have the sequence LLS appearing infinitely often in every Fibonacci tiling, since it is the decomposition of SL .

Continuing with the proof of theorem 2.11, take \mathcal{F} to be some infinite Fibonacci tiling of the line, and let $\mathcal{F}^{(n)}$ be the Fibonacci tiling obtained by composing \mathcal{F} n times. Let \mathcal{A} be some fragment of \mathcal{F} and suppose that \mathcal{A} has length $d(\mathcal{A})$ (Figure 2.19). Take n large enough so that it exceeds the minimal distance



Figure 2.19: Proof of Theorem 2.11: \mathcal{F} with the fragment \mathcal{A} shown in orange and pink

between two vertices of $\mathcal{F}^{(n)}$. (It is clear that we must have $n \geq S^{(n)}$, where $S^{(n)}$ is the length of the S interval at the n th stage of composition.) Now \mathcal{A} will have at most 1 vertex of $\mathcal{F}^{(n)}$, and by extending \mathcal{A} if necessary, we can assume without loss of generality that \mathcal{A} contains precisely one vertex of $\mathcal{F}^{(n)}$, say V . It is clear now that the vertex neighborhood of this vertex, $N(V)$, will contain two tiles that together will cover all of \mathcal{A} (Figure 2.20). Now suppose that we

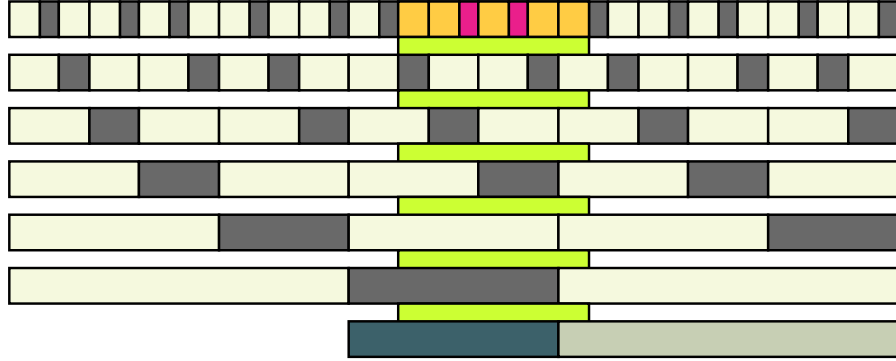


Figure 2.20: Proof of Theorem 2.11: Composing the fragment of \mathcal{F} to obtain $\mathcal{F}^{(n)}$

have some other infinite Fibonacci tiling of the line, \mathcal{F}_1 , and again let $\mathcal{F}_1^{(n)}$ denote the n th composition of \mathcal{F}_1 . Let V_1 be some vertex in $\mathcal{F}_1^{(n)}$, with its vertex neighborhood, $N(V_1)$ congruent to the vertex neighborhood of V , $N(V)$. Decomposing $N(V_1)$ n times yeilds a patch of short and long intervals that is

congruent to the patch \mathcal{A} . We know that V_1 can be chosen in infinitely many

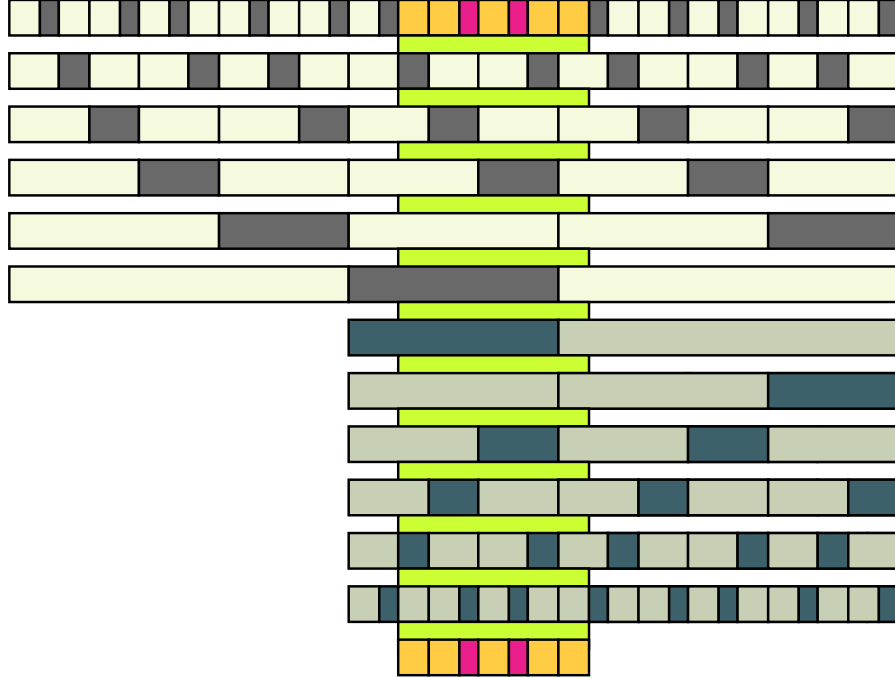


Figure 2.21: Proof of Theorem 2.11: the topmost fragment is \mathcal{F}_1 . This composes to yield $\mathcal{F}_1^{(n)}$, which shares the same vertex neighborhood as $\mathcal{F}^{(n)}$. The orange and pink tiles appear in both \mathcal{F} and \mathcal{F}_1

ways from $\mathcal{F}_1^{(n)}$ by our lemma, which means that \mathcal{F}_1 must contain infinitely many fragments congruent to \mathcal{A} . \square

In summary, the two most important characteristics of Fibonacci tilings are the fact that they are non-periodic and exhibit local isomorphism.

2.3.5 Updown Generation of Fibonacci tilings

So far we have constructed Fibonacci tilings using the projection method, and explored their properties. We have also seen the composition and decomposition rules for these tilings. Note that the decomposition technique used as

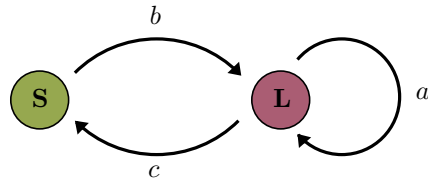


Figure 2.22: The finite state automaton for the Updown generation procedure for Fibonacci tilings

in the example above, only generates tilings that are infinite *in one dimension*. By definition, a Fibonacci tiling is a two way infinite sequence of points. This means that decomposition alone is not enough to generate a Fibonacci tiling. The question becomes how can we generate arbitrarily large segments of an Fibonacci tiling, that is, a two way infinite tiling of the line.

Updown Generation is one method that can be used to generate Fibonacci tilings. It uses the a variation on the decomposition procedure to produce infinite tilings. What is so striking about this method is that Updown generation uses a finite state automaton to prescribe the growth of the tiling.

Define three maps as follows:

$$a : L \longrightarrow L$$

$$b : S \longrightarrow L$$

$$c : L \longrightarrow S$$

We can place these into a simple finite state automaton as shown in Figure 2.22. These maps are represented visually in Figure 2.23 It is somewhat easier to think of these maps as representing embeddings of a small tile into a larger tile.

The updown generation process begins with a single tile, either a S or a L , and choosing a path through the directed graph. This path will be represented by a sequence of composed embeddings, say $a \circ c \circ b \circ a \circ a \circ c \dots$. Performing these embeddings on a tile, we get progressively larger and larger tiles (always a single tile at any stage). When we have a tile of a desired size,

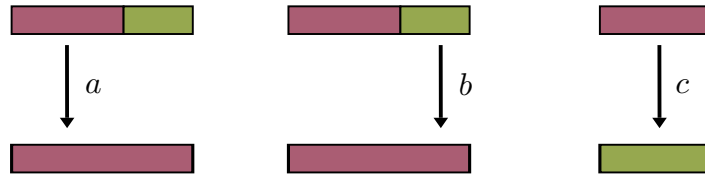


Figure 2.23: Visual representation of the FSA

we can then perform the regular decomposition procedure n times, where n is the number of maps in our path through the directed graph, to yield a tiling which contains our starting tile. In this way, an infinite path through the automaton will yield an infinite tiling. We can use this method to produce arbitrarily long fragments of Fibonacci tilings.

In Figure 2.24, we start with a long tile, and perform the sequence of embeddings given by $a \circ c \circ b \circ a$. We then apply the decomposition rules as usual four times, to obtain a tiling on the scale of our original tile.

2.4 Summary

In conclusion, we have seen two different ways of constructing Fibonacci tilings. These are the projection method and the method of updown generation. We have considered several properties of Fibonacci tilings, namely that they are non-periodic and exhibit local isomorphism. We know that all Fibonacci tilings by definition must accord with the composition and decomposition rules.

In the following chapter we will consider these techniques again, this time for the Penrose tilings.

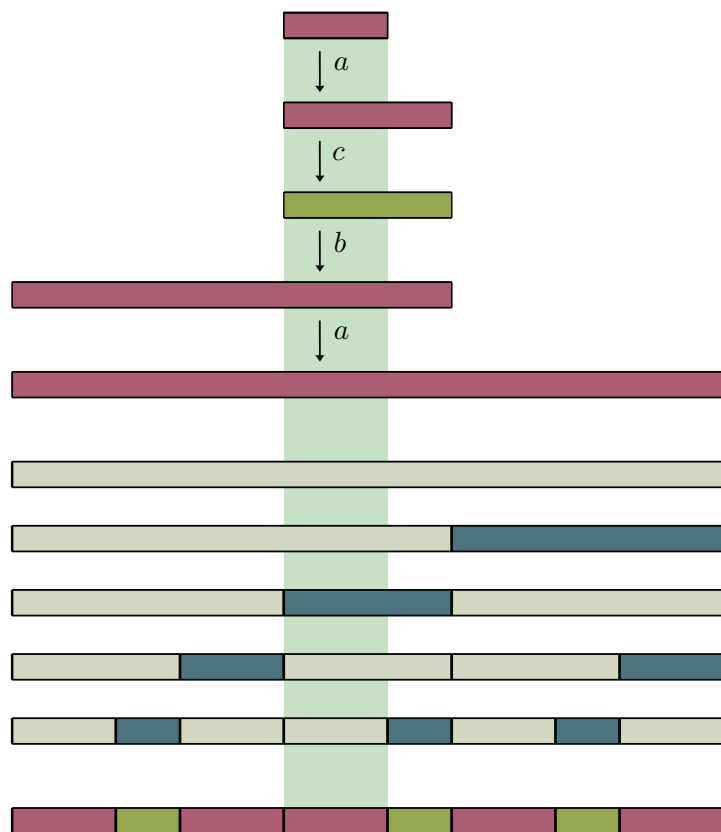


Figure 2.24: Updown generation of Fibonacci tilings

Chapter 3

Penrose Tilings

3.1 Introduction to Penrose Tilings

In the mid-seventies, Roger Penrose experimented with tilings, attempting to find a single shape that could tile the plane nonperiodically. Although he did not succeed in finding a single tile, he found two shapes that together could accomplish this goal [Gar77]. There have been many subsequent variations on these shapes, but the ones that we will consider here are the rhombs (Figure 3.1).

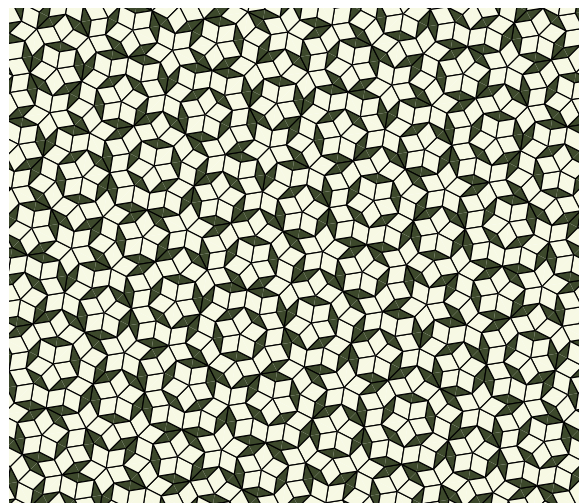


Figure 3.1: A portion of a tiling of the plane by Penrose rhombs

In this chapter we will consider tilings of the plane by Penrose rhombs. These tilings can be viewed as a two dimensional version of the Fibonacci tilings, and we will consider similar methods for their construction. In particular, we will look at a two dimensional version of Updown generation, and a variation on the projection method for tilings of the plane.

3.1.1 Background: Introduction to Tiling

We need a few definitions [Sen95]. A **tiling** \mathcal{T} of the space \mathbb{R}^n is a countable family of closed sets called tiles: $\mathcal{T} = \{T_1, T_2, \dots\}$ such that $\text{int}(T_i) \cap \text{int}(T_j) = \emptyset$ if $i \neq j$, and $\bigcup_{i=1}^{\infty} T_i = \mathbb{R}^n$, where $\text{int}(T)$ is the interior of T .

Let $\{T_1, T_2, \dots\}$ be the tiles of a tiling \mathcal{T} , partitioned into a set of equivalence classes by some criterion M . A set P of representatives of these classes is called the **proto-set** for \mathcal{T} with respect to M .

A tiling of \mathbb{R}^n is **periodic** if it admits translations in n linearly independent directions. A tiling is **nonperiodic** if it admits no translations. Tilings that admit translations in k linearly independent directions with $1 < k < n$ are called **subperiodic**. A proto-set is called **aperiodic** if it admits only nonperiodic tilings.

Using this terminology, the S and L tiles form a non-periodic proto-set of the Fibonacci tilings.

3.1.2 Background: The Penrose Tiles

Consider the Penrose Rhombs as shown in Figure 3.2, which have interior angles of $2\pi/5$ radians (72°) and $\pi/10$ radians (36°) respectively. The ratio of the long diagonal of the ‘thick’ rhomb to the short diagonal of the ‘thin’ one is $\tau : 1/\tau$, where $\tau = (1 + \sqrt{5})/2$, the golden mean.

Penrose found that one can play a kind of game with these shapes. Placing the tiles together matching the markings given by the arrows will yield an increasingly larger surface covered by tiles (Figure 3.3). In fact, we will soon show Theorem 3.1.

Theorem 3.1 [GS87] *The Penrose rhombs, together with the matching rules, admit a tiling of the plane.*

There are many variations on these matching rules to produce a variety of visual results. In Figure 3.1 the tiles are coloured according to type.

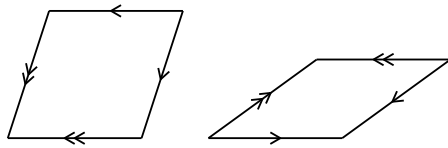


Figure 3.2: The Penrose rhombs

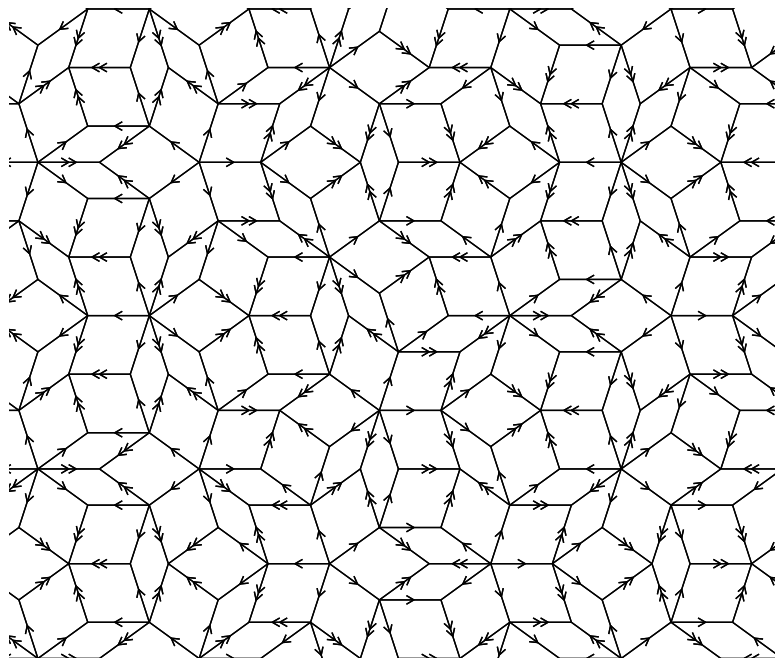


Figure 3.3: A tiling of the plane by arrowed rhombs

3.1.3 Composition and Decomposition of Penrose Tiles

Penrose tilings can be viewed as a two dimensional analogue of the Fibonacci tilings of the line. There are corresponding composition and decomposition rules that play a crucial role in Penrose's work. Here **decomposition** involves

substituting several tiles in the place of one tile, according to the divisions indicated in Figure 3.4.

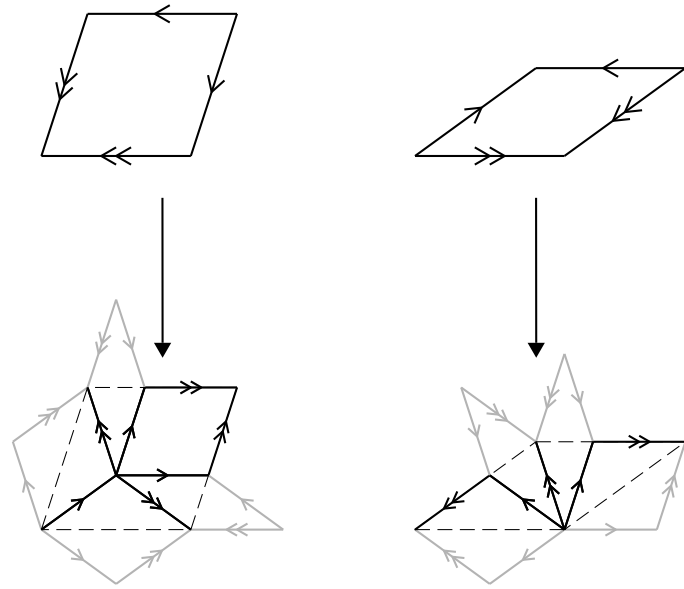


Figure 3.4: Decomposition of Penrose rhombs

This decomposition can be repeated as many times as desired. In short, decomposition transforms a finite patch of tiles into a finite patch with a greater number of tiles, as shown in Figure 3.5.

The finite patch may be resized to accommodate this substitution. This secondary step is often referred to as *inflation*, and can also be used to produce very large sections of tiles (not shown).

Composition is the reverse procedure to decomposition, and involves grouping tiles together to form bigger tiles. These groupings are exactly the same as the decomposed tiles shown in the previous figures.

We now have the necessary tools to prove theorem 3.1.

Proof. Using the decomposition rules, we can begin with a single tile, and divide into smaller tiles. To cover a large area with tiles, simply scale the tiling by a factor of τ at every decomposition step. This will yield an arbitrarily

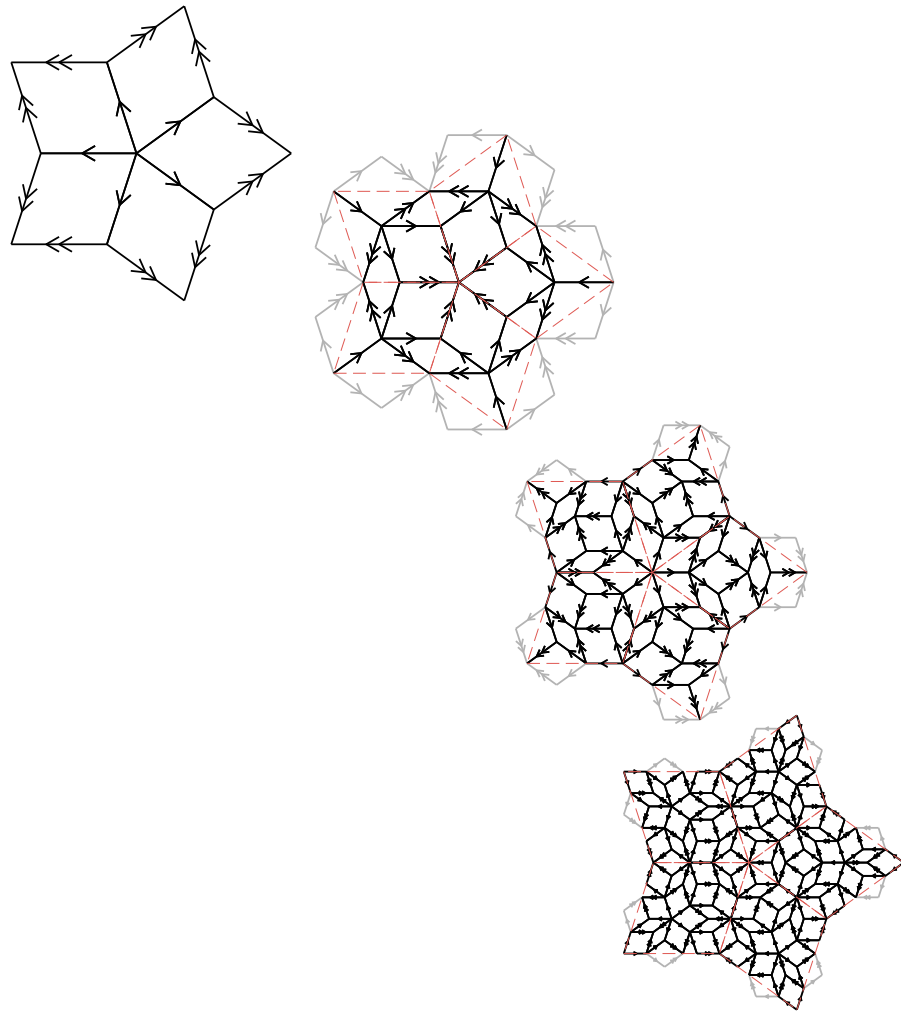


Figure 3.5: Decomposition of a patch of tiles

large patch of tiles. Recall the **Extension Theorem**: [GS87] *Let \mathcal{F} be a finite set of prototiles, each of which is a topologically closed disk. If \mathcal{F} tiles over arbitrarily large circular disks D , then \mathcal{F} admits a tiling of the plane.* So by the extension theorem, the Penrose rhombs admit a tiling of the plane. \square

We can also define the Penrose tilings analogously to our definition of Fibonacci tilings:

Definition 3.2 *A Penrose tiling of the plane is an infinite tiling of the plane by Penrose rhombs that has predecessors in all levels with respect to the composition rules.*

3.1.4 Properties of the Penrose tilings

As illustrated by the previous figures, the resulting tessellation has an undeniable aesthetic appeal. It also has numerous mathematical properties of interest, most importantly that it is a *nonperiodic* tiling. This means that the tessellation can never be broken down into a *unit cell*: some finite patch of tiles which is then repeated as a whole to cover the plane. In other words, the Penrose rhombs form an *aperiodic* protoset. The other property of relevance here is that Penrose tilings exhibit local isomorphism. That is, every patch in a tiling of Penrose tiles is congruent to infinitely many patches in every other Penrose tiling by the same tiles. These properties of Penrose tilings - that they are nonperiodic and exhibit local isomorphism - are properties we proved for Fibonacci Tilings in section 2.3.4, and the methods used here are similar. See [GS87] and [Sen95] for details.

In addition to these unique attributes, the Penrose tilings can exhibit five-fold rotational symmetry, a property which was previously thought to be impossible in a plane tiling. Penrose tilings only exhibit this symmetry in exceptional cases, however, and I will not discuss these here.

The aspect of Penrose tiles that we will be concerned with pertains to their construction. What is particularly interesting about these tilings is the fact that according to the matching rules, it is possible to create a tiling of the rhombs that **cannot** be extended to a tiling of the entire plane. That is, in constructing the tessellation according to the matching rules, we may encounter a problem: a section of the tiling in which neither a thin rhomb nor a thick rhomb would be appropriate. Note that these impossibilities will also occur in Penrose tilings constructed from other shapes, for instance the kite and dart. This problem will be discussed at length in Chapter 5. What we are primarily concerned with here is a desire to answer the following question: how can generate a tiling of the plane by Penrose rhombs, and not encounter any

impossibilities? We know that it is possible to construct a tiling of the plane by Theorem 3.1. But the question is how?

There have been several different methods developed to generate Penrose tilings. There is a three dimensional analogue to the projection method used to create the Fibonacci Tilings of Chapter 2. As this method involves projecting from five dimensional hyperspace, I will not discuss it in too much detail here. In the following sections however, I will outline two other methods for the construction of Penrose tilings, both developed by de Bruijn. The first is called the pentagrid method, and involves creating a grid of intersecting lines which is then translated into a tiling. That is, the grid is the dual of the tiling. The second method is called Updown generation, which is a two dimensional version of the method presented for Fibonacci tilings in 2.3.5.

3.2 Penrose Tilings using the projection method

The projection method for Penrose tilings is a direct analogue of the projection method for Fibonacci Tilings, as discussed in 2.2. I have not included illustrations of this method for the Penrose tilings, however, as we will be projecting from five dimensional space, and this is hard to depict in a mere two dimensions.

Consider the integer point lattice I_5 of the five dimensional space \mathbb{R}^5 , where the Voronoï cell of any point is a five dimensional hypercube. Let the point $\vec{k} = (k_0, \dots, k_4)$ where $k_i \in \mathbb{Z}$ be the location vector of any point in I_5 . Suppose also that we are given a shift vector, $\vec{\gamma} = (\gamma_0, \dots, \gamma_4)$ which is a translation in \mathbb{R}^5 . We will call this hypercube tessellation the Voronoï tessellation $V(I_5) + \vec{\gamma}$. We are now ready to construct Penrose tilings by projection.

In short we want to find a plane, \mathcal{E} that intersects the shifted hypercube tessellation (the Voronoï tessellation) in such a way that \mathcal{E} does not meet any vertex, edge or 2-face of this tiling.

We know that I_5 is invariant under rotation through $2\pi/5$ about $\vec{w} = (1, 1, 1, 1, 1)$, which is the body diagonal of the unit hypercube. This rotation has 2 invariant *totally irrational* planes that are orthogonal to one another, and to the fixed axis given by $\langle \vec{w} \rangle$, which is the one-dimensional subspace generated by \vec{w} . Pick, for \mathcal{E} , the plane rotated through $2\pi/5$. Now the orthogonal complement of \mathcal{E} , \mathcal{E}^\perp , will be 3-dimensional, and will be given by $\mathcal{E}' \oplus \langle \vec{w} \rangle$,

where \mathcal{E}' is the second totally irrational plane rotated through an angle of $4\pi/5$.

Let X be the set of lattice points of I_5 corresponding to the points of the Voronoï tessellation $V(I_5) + \vec{\gamma}$ whose facets are cut by \mathcal{E} . We know that \mathcal{E} will only meet faces of $V(I_5) + \vec{\gamma}$ of dimensions 3, 4, or 5. As a result, projecting the points of X orthogonally onto (E) will yeild a Delone set with dimensions 2, 1 or 0. This Delone set will be a Penrose tiling [Sen95]. Indeed the set X of lattice points that we project onto \mathcal{E} are equivalent to the set of lattice points that project under Π^\perp into the acceptance window $K = \Pi^\perp(V(0) + \vec{\gamma})$.

Similar to the Fibonacci Tilings, we can gain an understanding of the types of vertices in a Penrose tiling by examining the points in the acceptance window, K . See [Sen95] for details.

3.3 Penrose Tilings using de Bruijn's Pentagrid Method

In his paper *Algebraic theory of Penrose's non-periodic tilings of the plane* [dB81], de Bruijn presents some remarkable results pertaining to the construction of Penrose tilings. In particular, he develops an underlying structure for all Penrose Tilings which he calls the **pentagrid**.

In short, this method makes use of one key observation: that a Penrose tiling of the plane can be viewed as a ‘weave of ribbons’ [Sen95]. Let us examine this idea in more detail. Every rhomb has two sets of parallel edges. So placing two rhombs side by side will yield three parallel lines. Continuing to add tiles according to the matching rules, we will get a series of rhombs with parallel edges which make up a kind of ‘ribbon’ (figure 3.6).

Now replacing the ribbons of tiles by lines that are perpendicular to the edges that determine them, we obtain a sequence of parallel lines. In the case of Penrose tiles, there are only five possible orientations an edge in the tiling can have, and as a result we obtain a kind of grid structure that has five families of infinite parallel. This construction will be dual to the tiling in some way, and we can reconstruct the tiling from it. In addition we can construct grid structures independently and use them as a blueprint to create a tesselation.

A pentagrid is constructed from five superimposed grids. These ordinary grids are simply sets of parallel lines, that is, the set of points whose distance

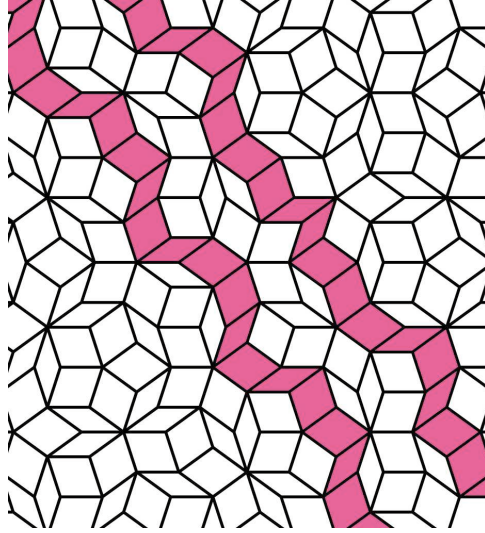


Figure 3.6: A ‘ribbon’ of tiles

to a fixed line is an integral multiple of a certain positive number. The five grids are obtained by rotating one grid through angles of $2k\pi/5$, $k = 0, \dots, 4$. In addition, each grid is shifted by a certain amount, described by the real numbers $\gamma_0, \dots, \gamma_4$, and satisfying $\gamma_0 + \dots + \gamma_4 = 0$, and $0 < \gamma_j < 1$, $j = 0, \dots, 4$. Two quintuples of Real numbers, $(\gamma_0, \dots, \gamma_4)$ and $(\gamma'_0, \dots, \gamma'_4)$ define the same pentagrid if and only if $\gamma_j - \gamma'_j \in \mathbb{Z}$ for $j = 0, \dots, 4$.

Take ζ to be the fifth root of unity, $\zeta = e^{2\pi i/5}$. Now we can define the j th grid to be

$$\{z \in \mathbb{C} \mid \operatorname{Re}(z\zeta^{-j}) + \gamma_j \in \mathbb{Z}\}$$

which is equivalent to

$$\{z \in \mathbb{C}, z = x + iy \mid x \cos(-j(2\pi/5)) - y \sin(-j(2\pi/5)) + \gamma_j \in \mathbb{Z}\}$$

The Pentagrid will be defined as the union of the above for $j = 0, \dots, 4$.

A pentagrid is called **regular** if no more than two grid lines intersect at any point in the plane, otherwise it is called **singular** [dB81]. In other words, a regular grid will have no point in \mathbb{C} belonging to more than two grids. The shifts given by $\gamma_0, \dots, \gamma_4$ are established to force regularity. A regular pentagrid is shown in Figure 3.7.

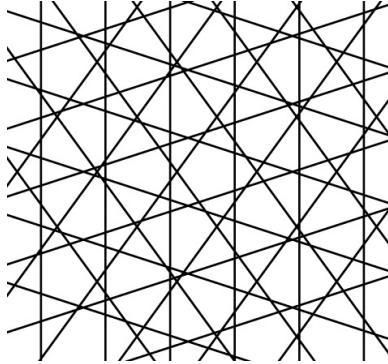


Figure 3.7: A regular pentagrid

Note that the Pentagrid is, itself a tiling of the Complex plane. To distinguish between the pentagrid tiling and the Penrose tiling, we will call a tile of the pentagrid a **mesh**. De Bruijn proves the astonishing fact that a regular pentagrid will determine a tiling of the plane by Penrose rhombs. Let us outline this construction.

With every point $z \in \mathbb{C}$ associate five integers $K_0(z), \dots, K_4(z)$ where

$$K_j(z) = \lceil \operatorname{Re}(z\zeta^{-j}) + \gamma_j \rceil$$

Now let $r, s \in \mathbb{Z}$ with $0 \leq r \leq s \leq 4$, and let $k_r, k_s \in \mathbb{Z}$ as well. Then the point z_0 determined by the two equations

$$\operatorname{Re}(z\zeta^{-r}) + \gamma_r = k_r$$

$$\operatorname{Re}(z\zeta^{-s}) + \gamma_s = k_s$$

will be the intersection point of a line of the r th grid with a line of the s th grid. In a small neighborhood of z_0 , the quintuple $(K_0(z), \dots, K_4(z))$ will take on four values given by

$$(K_0(z_0), \dots, K_4(z_0)) + \epsilon_1(\delta_{0r}, \dots, \delta_{4r}) + \epsilon_2(\delta_{0s}, \dots, \delta_{4s})$$

where $(\epsilon_1, \epsilon_2) = (0, 0), (0, 1), (1, 0), (1, 1)$ respectively, and δ_{ij} is the standard Kronecker-delta symbol, with

$$\delta_{ij} = \begin{cases} 0 & i \neq j \\ 1 & i = j \end{cases}$$

These four points will form the vertices of a rhombus. If the pentagrid is indeed regular, we can attach such a rhombus to every intersection point of the pentagrid.

Alternatively, we can describe the set of all vertices of the rhombs as the set of all points $f(z)$, with

$$f(z) = \sum_{j=0}^4 K_j(z) \zeta^j$$

as z runs through \mathbb{C} . Note that $f(z)$ will be constant in every mesh of the Pentagrid.

Proposition 3.3 [dB81] *Attaching a rhombus to each intersection point of the pentagrid as described above yields a tiling of the plane by rhombs.*

Proof. Every mesh of the pentagrid has an associated point $f(z)$. The four meshes surrounding a point of intersection of 2 grid lines (the only kind of intersection point in a regular pentagrid) form the vertices of a rhombus. Locally, these rhombs do not overlap and this is clear by construction. It remains to show that every point in \mathbb{C} is covered by a rhombus. Consider the pentagrid tiling, and suppose z runs clockwise around a large circle. We know

$$f(z) = \sum_{j=0}^4 K_j(z) \zeta^j$$

and recall

$$K_j(z) = \lceil \operatorname{Re}(z\zeta^{-j}) + \gamma_j \rceil$$

now let

$$\lambda_j(z) = K_j(z) - (\operatorname{Re}(z\zeta^{-j}) + \gamma_j)$$

and we see that $0 \leq \lambda_j(z) < 1$. So $f(z)$ becomes

$$f(z) = \sum_{j=0}^4 (\lambda_j(z) + \operatorname{Re}(z\zeta^{-j}) + \gamma_j) \zeta^j$$

$$f(z) = \sum_{j=0}^4 (\lambda_j(z) + \gamma_j) \zeta^j + \sum_{j=0}^4 \operatorname{Re}(z\zeta^{-j}) \zeta^j$$

$$f(z) = \sum_{j=0}^4 (\lambda_j(z) + \gamma_j) \zeta^j + \frac{5}{2}(z)$$

So we see that $f(z) - \frac{5}{2}(z)$ is bounded, and hence as z runs clockwise around a large circle in \mathbb{C} , $f(z)$ describes a closed curve that runs clockwise around w . \square

In effect, this construction is equivalent to associating with each intersection of two grid lines, the two unit vectors perpendicular to the lines of intersection. These will, in turn, determine the rhombs.

Recall that we have arranged the pentagrid so that no more than two lines of the grids will intersect at any point of \mathbb{C} . This means that there will only be $\binom{5}{2} = 10$ possible configurations of intersections. In addition, the grid vectors will determine the prototiles of the tiling. Consider the intersections shown in Figure 3.8: To convert a pentagrid into a tiling of the plane by rhombs, sim-

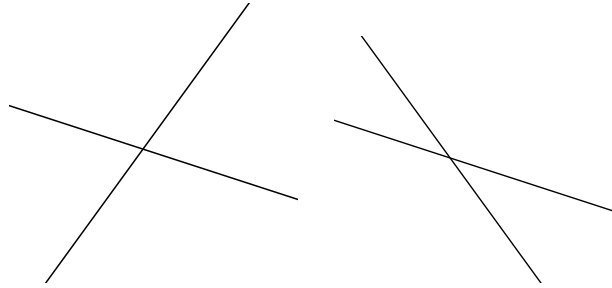


Figure 3.8: The two types of intersections of grid lines

ply associate with each intersection point of the pentagrid the rhomb whose edges are the unit vectors orthogonal to the lines of the grid (Figures 3.9 and 3.10).

In this way, we obtain the ‘thin’ and ‘thick’ rhomb shapes. It is easy to see that these are the only shapes that can be obtained through the intersection of the grid lines. Associating each intersection of two lines with a rhomb will yield a tiling of the plane. Figures 3.11 and 3.12 were generated using the regular pentagrid shown above. [Sen95]

In this way, every intersection of two grid lines corresponds to a tile in the

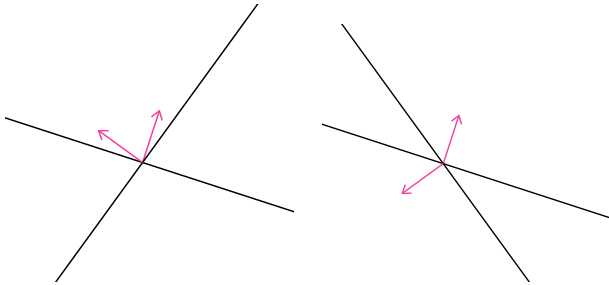


Figure 3.9: The intersections of grid lines of Figure 3.8 with associated orthogonal unit vectors



Figure 3.10: The rhombs associated with the intersections of Figure 3.8. The edges of these rhombs are the unit vectors orthogonal to the lines of the grid.

dual tiling, and every mesh in the pentagrid will correspond to a vertex in the dual tiling.

Note that the pentagrid only acts as a blueprint for the tiling. That is, the lines of the pentagrid cannot be superimposed over the tiling because the associations mentioned above will not match up in a scaled way.

Once we have generated a tiling of the plane by rhombs using information gathered from the pentagrid, it remains to pick orientations of the rhombs (interpreted in matching rules) so that they obey Penrose's matching conditions, and hence are Penrose tilings of the plane.

Theorem 3.4 [dB81] *We can orient the rhombs in the tiling generated by the pentagrid so that the tiling is a Penrose tiling.*

Proof.

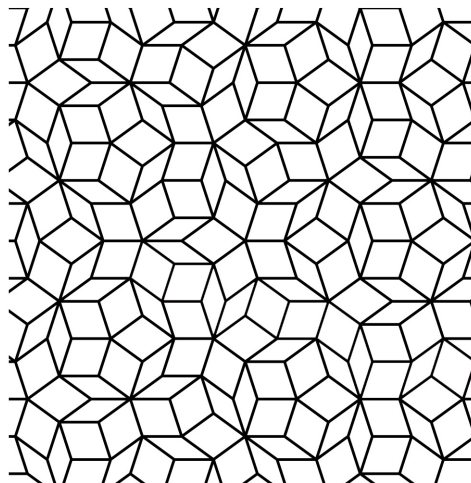


Figure 3.11: The tiling corresponding to the pentagrid of Figure 3.7

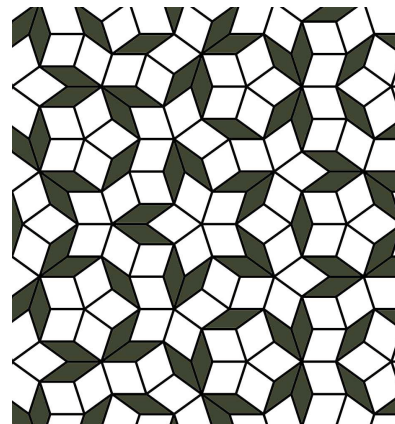


Figure 3.12: The tiling from the pentagrid, coloured.

First we need a few definitions. In a regular pentagrid, only two lines will intersect at any point. Hence for any point $z \in \mathbb{C}$, at most two of the numbers

$\lambda_0(z), \dots, \lambda_4(z)$ will be zero. So we will have $0 < \sum_{j=0}^4 \lambda_j < 5$. Recall $\lambda_j(z) = K_j(z) - (Re(z\zeta^{-j}) + \gamma_j)$. So

$$\sum_{j=0}^4 \lambda_j(z) = \sum_{j=0}^4 (K_j(z) - (Re(z\zeta^{-j}) + \gamma_j))$$

Now we have $\gamma_0 + \dots + \gamma_4 = 0$, and similarly, $\sum_{j=0}^4 Re(z\zeta^{-j}) = 0$, as shown below.

$$\sum_{j=0}^4 Re(z\zeta^{-j}) = \sum_{j=0}^4 \left\{ x \cos(-j\frac{2}{5}\pi) - y \sin(-j\frac{2}{5}\pi) \right\}$$

$$= x \cos(0) - y \sin(0) + x \cos(-2\pi/5) - y \sin(-2\pi/5) + x \cos(-4\pi/5) \\ - y \sin(-4\pi/5) + x \cos(2\pi/5) - y \sin(2\pi/5) + x \cos(4\pi/5) - y \sin(4\pi/5)$$

but this reduces to

$$= x + 2x \cos(2\pi/5) + 2x \cos(4\pi/5) \\ = x(1 + 2(\frac{1}{2\tau}) + 2(\frac{\tau}{2})) \\ = x(1 + \frac{1}{\tau} - \tau) \\ = 0$$

since $\tau = \tau^{-1} + 1$ (from the fact that $\tau^2 = \tau + 1$).

Now, combining these facts we find that

$$\sum_{j=0}^4 \lambda_j(z) = \sum_{j=0}^4 K_j(z)$$

and since $\sum_{j=0}^4 K_j(z)$ must be an integer, it must take one of the four values, 1, 2, 3 or 4. In this way, every vertex in the rhombus pattern can be represented by $k_0 + k_1\zeta + \dots + k_4\zeta^4$ where $k_0 + \dots + k_4 \in \{1, 2, 3, 4\}$. This integer value given by $k_0 + \dots + k_4$ will be called the **index** of the vertex.

De Bruijn notes that moving a point along the edges of the rhombs, one will note that the index increases by 1 in the directions $1, \zeta, \zeta^2, \zeta^3, \zeta^4$, and decreases by 1 in the directions $1, \zeta^{-1}, \zeta^{-2}, \zeta^{-3}, \zeta^{-4}$. It follows that the thick

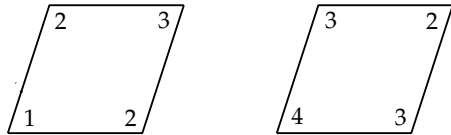


Figure 3.13: Two possible indexings of the thick rhomb

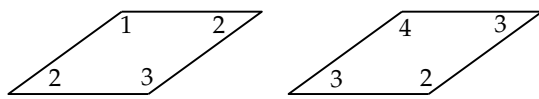


Figure 3.14: Two possible indexings of the thin rhomb

rhombs have one of the two indexings shown in Figure 3.13. Similarly, the thin rhombs will be indexed as in Figure 3.14.

The arrows are assigned as follows: Edges connecting a vertex of index 1 to a vertex of index 2, and edges connecting vertices of index 3 and 4 will have double arrows. These arrows will point from 2 to 1, or from 3 to 4 (Figures 3.15 and 3.16).

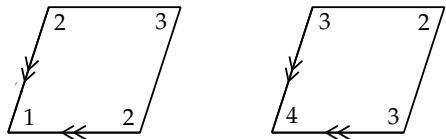


Figure 3.15: Double arrows associated with the indexed thick rhombs

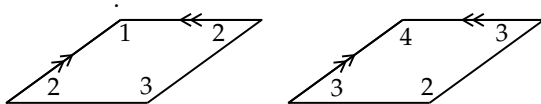


Figure 3.16: Double arrows associated with the indexed thin rhombs

Edges that connect a vertex of index 2 to a vertex of index 3 will have single arrows. We need to orient these edges, and this will be more complicated than the orientation of the double-arrow edges. Of course, the orientation of the single arrows follows directly from the placement of the double arrows.

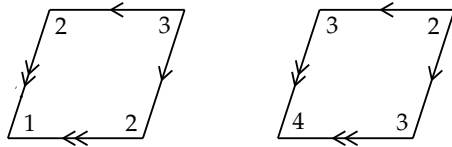


Figure 3.17: Orientation of the single arrows of the thick rhomb

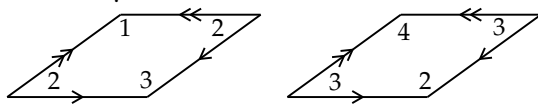


Figure 3.18: Orientation of the single arrows of the thin rhomb

The question is whether adjacent rhombs in a tiling will share the same orientation of the edges. Assuming that we have marked the rhombs with the arrows as shown above, we need to convince ourselves that we will not have adjacent tiles with conflicting arrow orientations. To show this, we need to prove the following:

Lemma 3.5 *Let PQ be a edge with a single arrow. Let the two rhombs that share the edge PQ have angles α and β respectively at P . Then α and β are either both $< \pi/2$ or they are both $> \pi/2$.*

It is easy to see why this will mean that we will not have conflicts. The two arrangements shown in Figure 3.19 are the cases described in the lemma. The arrangement in Figure 3.20 is what we wish to avoid.

To prove the lemma, let us consider it in terms of the pentagrid. Figure 3.21 shows a line l of the 0th grid and its intersections with the other lines of the pentagrid. Now take this line l of the 0th grid (the lines of the other

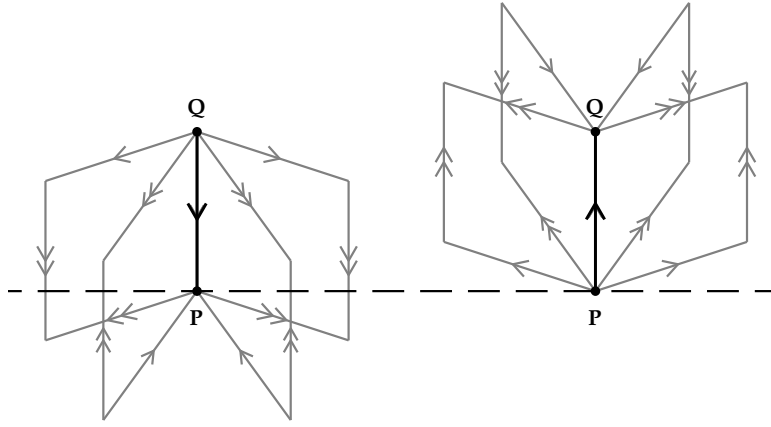


Figure 3.19: The two rhombs sharing the edge PQ have angles α and β respectively at P . On the left, both α and β are $> \pi/2$. On the right, α and β are $< \pi/2$.

grids may be obtained by cyclic permutation), and consider two consecutive intersection points of this line with lines from the p th and q th grids.

Call A the intersection of l with a line of the p th grid, and B the intersection of l with the q th grid. Note that we do not assume here the $p \neq q$, although it will be clear that this is true later. Of course p and q are in $\{1, 2, 3, 4\}$. Our lemma becomes the following: If the segment AB has a single arrow, then $p+q$ is odd. The segment AB will have a single arrow if and only if $\sum_j K_j(z)$ is 2 in the mesh on one side of AB and 3 on the mesh on the other side.

Performing a translation we can reduce the problem to the case when $\gamma_0 = 0$ and l is the imaginary axis of the Complex plane, given by iy where $y \in \mathbb{R}$. We have the following values of $K_j(z)$ on this line:

$$K_1(iy) = \lceil y \sin(2\pi/5) + \gamma_1 \rceil$$

$$K_2(iy) = \lceil y \sin(4\pi/5) + \gamma_2 \rceil$$

$$K_3(iy) = \lceil -y \sin(4\pi/5) + \gamma_3 \rceil$$

$$K_4(iy) = \lceil -y \sin(2\pi/5) + \gamma_4 \rceil$$

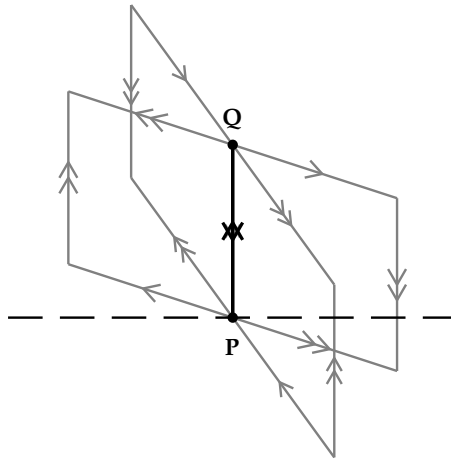


Figure 3.20: In this arrangement, $\alpha < \pi/2$ but $\beta > \pi/2$. This violates the matching rules.

Note that because the pentagrid is regular, and $\gamma_0 = 0$, we must have that neither $\gamma_1 + \gamma_4$ nor $\gamma_2 + \gamma_3$ is equal to zero. Allowing y to run from $-\infty$ to ∞ we find that $K_1(iy) + K_4(iy) - [\gamma_1 + \gamma_4]$ will jump from 0 to 1 when $([\gamma_1 + \gamma_4] - \gamma_1)/\sin(2\pi/5)$ is in \mathbb{Z} , and it will jump from 1 to 0 when $\gamma_1/\sin(2\pi/5)$ is in \mathbb{Z} .

Similarly, $K_2(iy) + K_3(iy) - [\gamma_2 + \gamma_3]$ will jump from 0 to 1 when $([\gamma_2 + \gamma_3] - \gamma_2)/\sin(4\pi/5)$ is in \mathbb{Z} , and it will jump from 1 to 0 when $\gamma_2/\sin(4\pi/5)$ is in \mathbb{Z} .

Now l will intersect lines of the 2nd and 3rd grids alternately, and similarly it will intersect the 1st and 4th grid lines alternately, so we see that $p \neq q$. Toward a proof of the contrapositive, assume that $p+q$ is even. Hence $\{p, q\} = \{1, 3\}$ or $\{p, q\} = \{2, 4\}$. In addition, since $\gamma_0 = 0$, we have that $\gamma_1 + \dots + \gamma_4 = 0$ and as a consequence we must also have that $[\gamma_1 + \gamma_4] + [\gamma_2 + \gamma_3] = 1$.

Using these facts, we can check that the sum $K_1(iy) + K_2(iy) + K_3(iy) + K_4(iy)$ is either 1 or 3 between the points A and B . It follows that $K_0(iy) + \dots + K_4(iy)$ is either 1 on one side and 2 on the other, or it is 3 on one side and

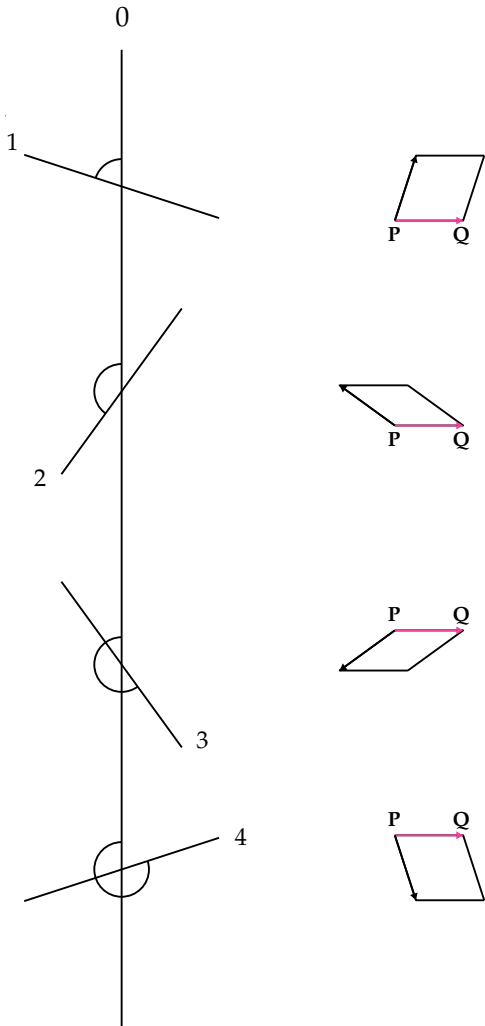


Figure 3.21: A line of the 0th grid and its intersections with the other lines of the pentagrid

4 on the other. In either case the edge corresponding to the segment AB will have a double arrow, and we are done.

\square [dB81]

To sum up, De Bruijn has shown that there is a Penrose tiling of the plane

corresponding to every regular pentagrid. More remarkably, he goes on to show that ALL Penrose tilings of the plane by rhombs have a corresponding regular pentagrid.

Figures 3.22 - 3.25 show an example of a tiling and its corresponding pentagrid. In this example, tiles are added one by one to a growing region, and the corresponding grid lines are shown.

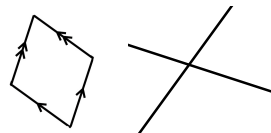


Figure 3.22: A single rhomb and the corresponding intersection of the pentagrid

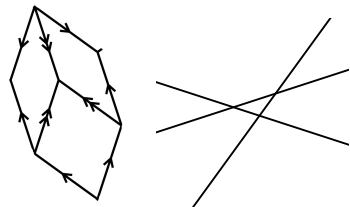


Figure 3.23: Adding two rhombs to the tiling adds a grid line.

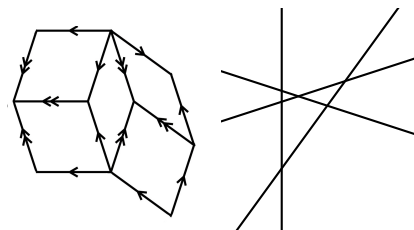


Figure 3.24: Adding two more rhombs adds another grid line.

Note that a generalization of this pentagrid method exists and can be used to generate non-periodic tilings of the plane in \mathbb{R}^n . It is known as the multi-grid method.

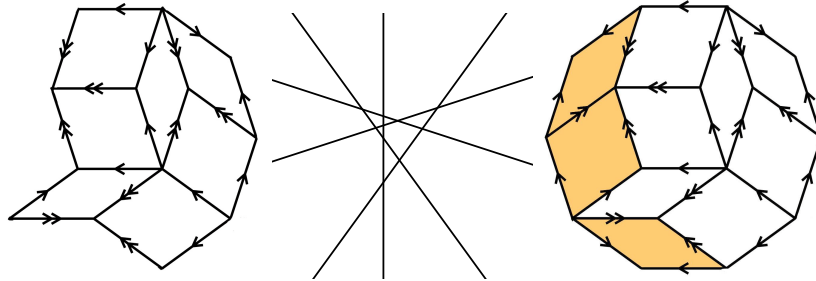


Figure 3.25: Adding the bottom rhombs adds the fifth grid line. There are now 10 intersections of grid lines, but we have only added seven tiles. The final three intersections correspond to the three orange rhombs.

3.3.1 The Pentagrid method is the projection method

De Bruijn's pentagrid is intrinsically related to the projection method. In fact, the projection method can be seen as simply a geometric interpretation of the pentagrid method.

Recall that the Voronoï tessellation is the hypercube tessellation of \mathbb{R}^5 translated by the shift vector γ . An intersection of a plane with the Voronoï tessellation will yeild a pentagrid. A regular pentagrid will be obtained when we have a plane \mathcal{E} that intersects the hypercube tessellation in such a way that \mathcal{E} does not meet any vertex, edge or 2-face of the Voronoï tessellation. This is, in fact, equivalent to the case where our shift vector is that required for a regular pentagrid. That is, when $\gamma = (\gamma_0, \dots, \gamma_4)$, with $\gamma_0 + \dots + \gamma_4 = 0$.

Now if \mathcal{E} intersects $V(k) + \vec{\gamma}$, which is the interior of the translate by $(\gamma_0, \dots, \gamma_4)$ of the Voronoï cell of k , $V(k)$, then $k \in I^5$ is the location vector of a mesh in the pentagrid. This is equivalent to the requirement that

$$\Pi^\perp(\vec{k}) \in \Pi^\perp(V(0) - \vec{\gamma})$$

Drawing on De Bruijn's work, we can show

Theorem 3.6 *The vertices of a Penrose Tiling produced by a regular pentagrid given by $\vec{\gamma} = (\gamma_0, \dots, \gamma_4)$ are the points*

$$k_0 + k_1\zeta + k_2\zeta^2 + k_3\zeta^3 + k_4\zeta^4$$

where (k_0, \dots, k_4) runs through the points of the integer lattice I_5 whose Voronoï cell has a non-empty intersection with the plane given by:

$$\begin{aligned} \sum_{j=0}^4 x_j &= 0 \\ \sum_{j=0}^4 (x_j - \gamma_j) Re\zeta^{2j} &= 0 \\ \sum_{j=0}^4 (x_j - \gamma_j) Im\zeta^{2j} &= 0 \end{aligned}$$

See [dB81] for an outline of the proof.

3.4 Penrose Tilings using Updown Generation

In [dB90], de Bruijn formalizes a technique due to John Conway called **up-down generation** that provides an algorithmic technique that generates Penrose tilings of the plane. Not surprisingly, this method involves two phases: *up* and *down*. In short, the *up* part of the process associates the assembly of a Penrose tiling with a path through a directed graph. Any infinite path through this graph will produce a tiling of the plane which extends infinitely in any direction. The *down* part of the process is simply Penrose's decomposition technique, repeated a suitable number of times. In other words, any path in the directed graph is a "recipe" for a portion of a Penrose tiling, and an infinite path in the graph can determine a tiling of the whole plane.

In this procedure, the rhombs are divided into triangles, the thick rhombs along the long diagonal and the thin rhombs along the short diagonal (Figure 3.26). Senechal calls the resulting triangles, **elementary triangles** [Sen95]. The triangles are labeled T for the triangles resulting from the 'thick' rhombs, and t for those from the 'thin' rhombs. The T and t triangles are then divided into L for left and R for right, to distinguish the two sides. The resulting tiles are labeled T_R , T_L , t_R , and t_L , and are shown in the top row of Figure 3.27.

Similar to the decomposition method, each tile is associated with a grouping of smaller tiles as seen in the second row of the same figure. Letting T'_R ,

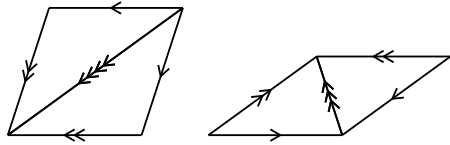


Figure 3.26: The divided rhombs

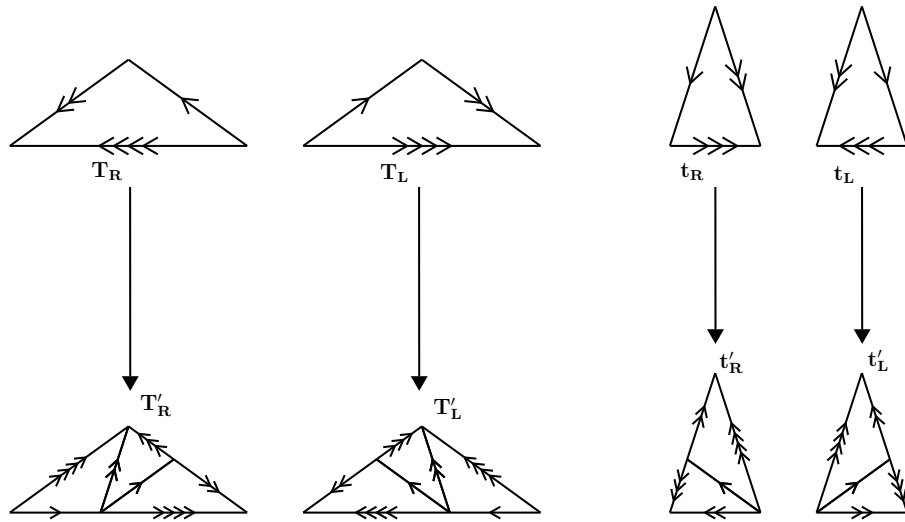


Figure 3.27: Decomposition of the elementary triangles

T'_R , t'_R , and t'_L represent the composed triangles, that is, those triangles that are composed of smaller triangles, we have the following substitution rules:

$$T'_R = T_R + t_R + T_L$$

$$T'_L = T_R + t_L + T_L$$

$$t'_R = T_L + t_R$$

$$t'_L = T_R + t_L$$

Note that these substitution rules are *unique*, meaning that given the type (T or t) and direction (L or R) of some elementary tile, we know the exact ways that it can be subdivided into smaller shapes. These relationships are shown

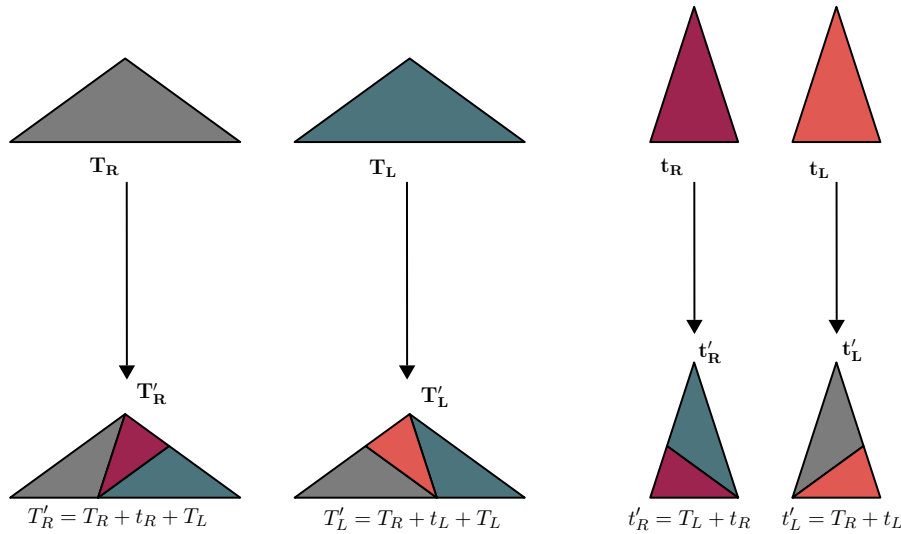


Figure 3.28: Decomposition of the elementary triangles in colour

in colour in Figure 3.28 to provide an intuition of the elementary triangles and their subdivision rules. This representation cannot be used in practice, however, because it does not contain information embedded in the matching rules of the arrowed rhombs.

These composition rules are the cornerstone of updown generation, and their purpose is dual. They provide the basis for the subdivision of the *down* process similar to the decomposition process seen in section 3.1.2. In addition, unlike the deflation process, the composition rules also provide the basis for the *up* process. That is, the *up* stage of updown generation involves mapping a small tile into the larger tile that it is a part of.

We have ten embeddings which map the tiles into their composed tiles. That is, these embeddings map a small tile into the larger tile that they are a

part of according to the substitution rules given above. For instance, t_R is a part of T'_R . So we say that $\epsilon : t_R \rightarrow T'_R$, where it is understood that the small tile t_R is a part of a larger T'_R . The ten maps of this kind are as follows:

$$\begin{aligned}\alpha : T_R &\rightarrow T_R & \alpha' : T_L \rightarrow T_L \\ \beta : T_R &\rightarrow T_L & \beta' : T_L \rightarrow T_R \\ \gamma : T_R &\rightarrow t_L & \gamma' : T_L \rightarrow t_R \\ \delta : t_R &\rightarrow T_R & \delta' : t_L \rightarrow T_L \\ \epsilon : t_R &\rightarrow t_R & \epsilon' : t_L \rightarrow t_L\end{aligned}$$

These ten maps are presented visually in Figure 3.29. These maps correspond to the edges of the directed graph (or finite state automaton) seen in Figure 3.30.

Figure 3.31 illustrates the process of updown generation. The **up** part of Updown generation involves mapping a small elementary tile into a much larger elementary tile, through the sequence of maps given by a path in the FSA. Starting with t_R (bottom left) we map by δ' to T_R , by α to t_L , by δ to T_L , by α' to t_R and finally by δ' back to T_R . This is the **up** part of the process, which results in one large scale elementary triangle seen at the top of the previous picture.

Here begins the **down** stage. This is really just Penrose's decomposition process, repeated as many times as we have stages in the up process. That is, the down process simply subdivides the elementary triangle resulting from the up stage until all of the elementary tiles making up our big tile are at the same scale as our starting triangle. The elementary triangles are then coloured with two colours, one for type T triangles, and one for type t triangles. The result is a tiling of rhombs, as shown in Figure 3.32. In this way, updown generation begins with one small tile, and creates a tessellation of the plane. In fact, not all infinite paths through the graph determine a tiling of the whole plane. Restricted paths through the graph can be chosen to produce partial tilings of the plane. These will be either tilings of the half plane, or tilings of a 36° wedge. These partial tilings can be reflected and/or rotated to obtain full tilings of the plane. It is also these singular cases that exhibit the remarkable fivefold symmetry that have made Penrose tilings so widely known. These

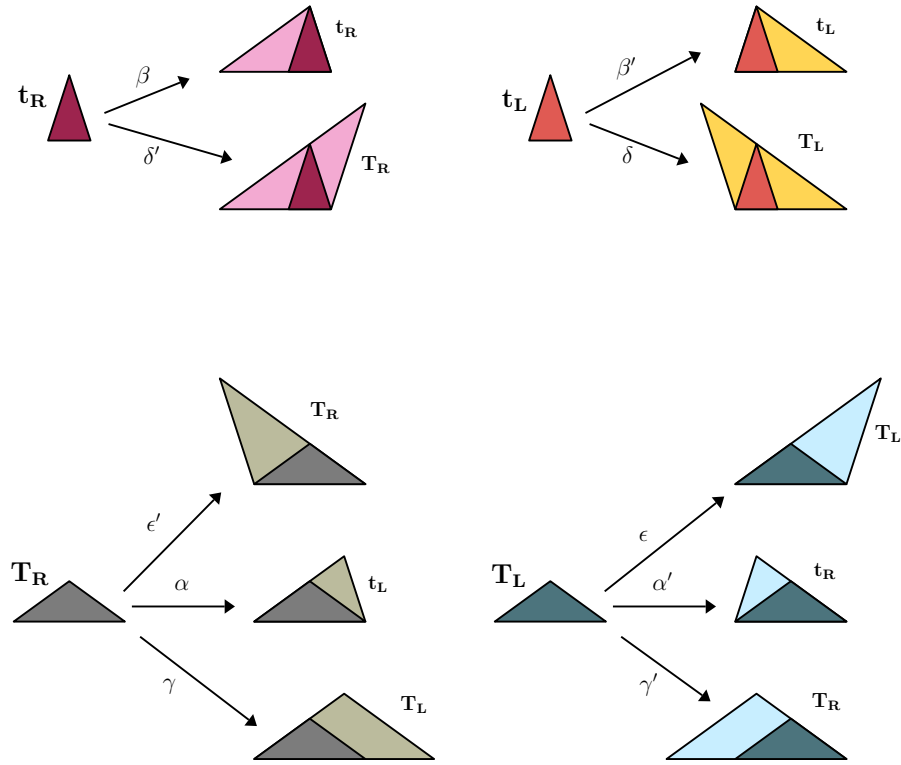


Figure 3.29: A visual representation of the maps of the FSA

are not the cases we are concerned with here, however. See [dB90] for a treatment of these tilings.

3.4.1 Relationship between path and tessellation

Through the process of updown generation, every infinite path through the directed graph yields a tiling of the plane (or some portion thereof). However, every Penrose tiling can be associated with many sequences of maps through the directed graph, because for every elementary triangle there is a unique composition sequence which maps it into the full tiling. We say that two se-

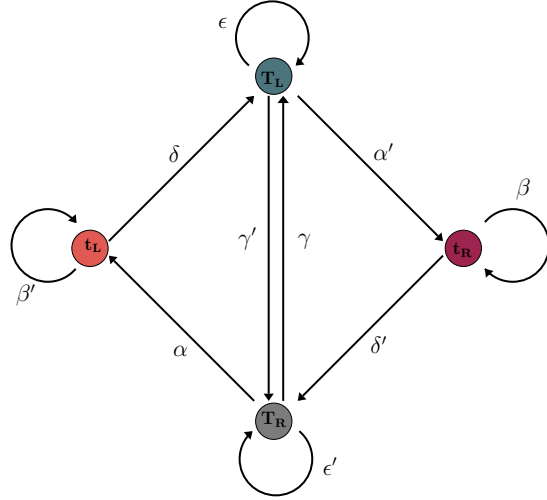


Figure 3.30: The directed graph of Updown generation

quences of maps in the directed graph are **cofinal** if their sequences agree after a finite number of terms [Sen95]. We say that an infinite path p in the automaton *matches* a given elementary tile t if the starting state of p corresponds to the type of tile t . Let (p, t) describe the tiling with starting tile t and path p . The following theorem says that if two paths generate the same tiling, then the paths differ in at most a finite number of places.

Theorem 3.7 [Sen95] *A tiling is generated by both (p_1, t_1) and (p_2, t_2) if and only if the paths p_1 and p_2 are cofinal.*

Proof. Assuming that the tiling has no line of symmetry, we know by the process of updown generation that the tiling covers the whole plane. Now the distance between t_1 and t_2 must be finite, which means that after some k steps, we have a big triangle T that contains both elementary tiles, t_1 and t_2 in its interior. From this big triangle onward, the composition sequences must be the same. Conversely, suppose that p_1 and p_2 are cofinal. Then they must describe the same tiling, beginning at some level, say the tiling T^* . But composition is unique, so T^* can be decomposed into elementary tiles in only one way, which means that $(t_1, p_1) = (t_2, p_2)$. \square

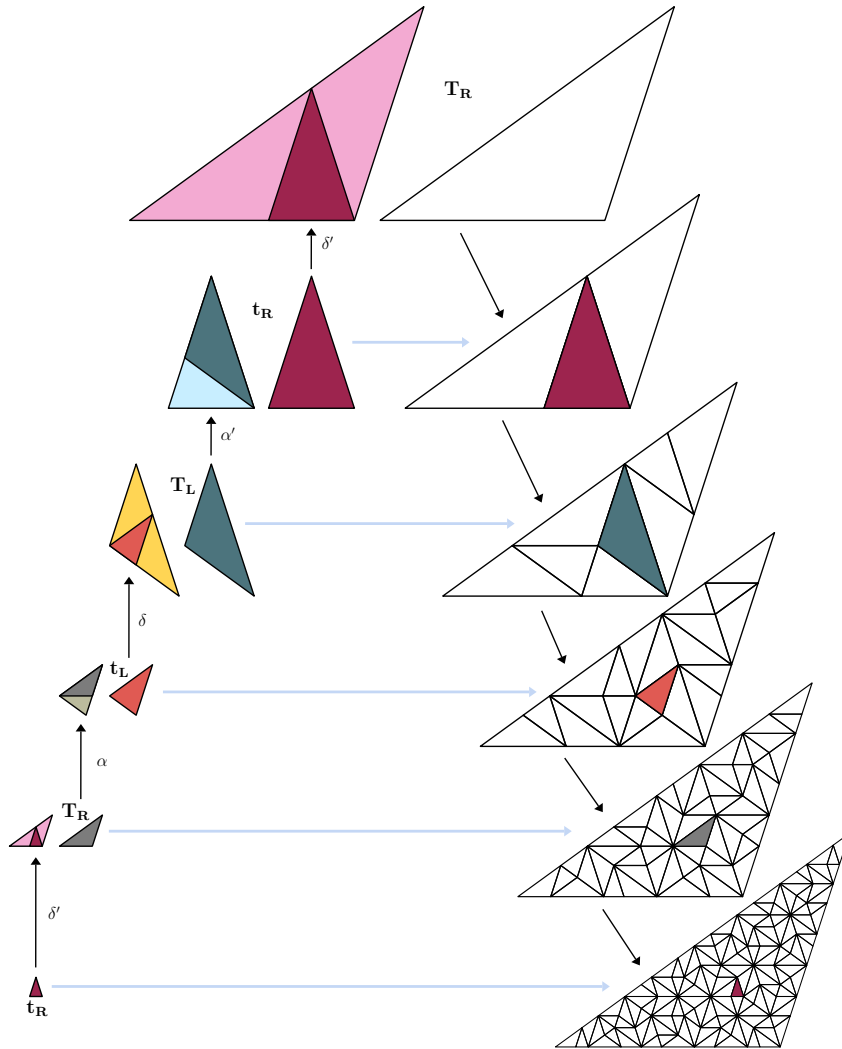


Figure 3.31: Updown generation of Penrose tilings: the map $\delta' \circ \alpha \circ \delta \circ \alpha' \circ \delta'$

Cofinality is an equivalence relation on the set of paths through the directed graph. It partitions these paths in groups we will call **families**. Note that composition preserves families. That is, if we let $C(p)$ represent the composed path p , then we say that two sequences p and p' are cofinal if and only

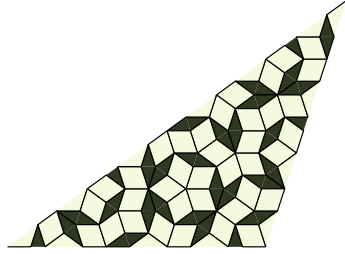


Figure 3.32: The patch of tiles produced by the Updown generation procedure seen in Figure 3.31

if $C(p)$ and $C(p')$ are also cofinal. Using these facts we have the remarkable corollary:

Corollary 3.8 [Sen95] *There are uncountably many distinct Penrose tilings of the plane.*

Proof. If there were only countably many families of sequences, then we could pick a representative of each family to create a list of family representatives. However, using the directed graph, we can always find a sequence that is not on that list. \square

3.5 Summary

In summary, Penrose tilings are a two dimensional version of the Fibonacci tilings that exhibit many of the same properties, including nonperiodicity and local isomorphism. We have several algorithmic methods for generating Penrose tilings of the plane, specifically the projection method, the pentagrid method and updown generation. In the next chapter we will consider the problem of attempting to grow Penrose Tilings by adding tiles one by one.

Chapter 4

Non-locality of Fibonacci Tilings

4.1 Introduction

So far we have seen two types of tilings, the Fibonacci tilings of the line, and Penrose tilings of the plane. We are aware of two procedures to generate these tilings, the projection method (which, in the case of Penrose tiles, is de Bruijn's pentagrid method) and Updown generation. The question to which we now turn our attention is whether it is possible to create these tilings in a different way. Specifically, we want to examine whether or not it is possible to generate these tilings simply by adding one tile at a time to a growing patch of tiles. In this chapter, we will consider this problem for Fibonacci tilings.

4.2 Local rules for building Fibonacci tilings

Suppose we want to build up a fragment of a Fibonacci tiling by adding tiles one at a time to some starting tile. Recall that there are precisely three valid words of length 2 in a Fibonacci string: LL , LS , and SL . For Fibonacci tilings, this means that these are the only kinds of vertex neighborhoods. In addition, we know that there are only four valid words of length 3: LSL , SLS , LLS and SLL . So suppose we add short and long tiles to our starting tile, without too much regard for their placement, except to avoid the invalid vertex arrangements of SS , or LLL .

We know that by definition, a Fibonacci tiling must have predecessors of all levels with respect to the decomposition rules. It follows that any fragment of a Fibonacci tiling will also accord by the composition and decomposition rules. So the fragment that we have built up must have some predecessor that

is also a fragment of a Fibonacci tiling.

This means that we must never have either of the invalid vertex arrangements SS or LLL appearing in any predecessor of our tiling. To avoid these configurations at all levels of the hierarchy, we must avoid any strings that will compose to yield LLL . In other words, we must avoid the following fragments:

$$\begin{aligned} & SS \\ & LLL \\ & SLSLS \\ & LLSLLSLL \\ & SLSLLSLSLLSLS \\ & \vdots \end{aligned}$$

These fragments are shown visually in Figure 4.1.

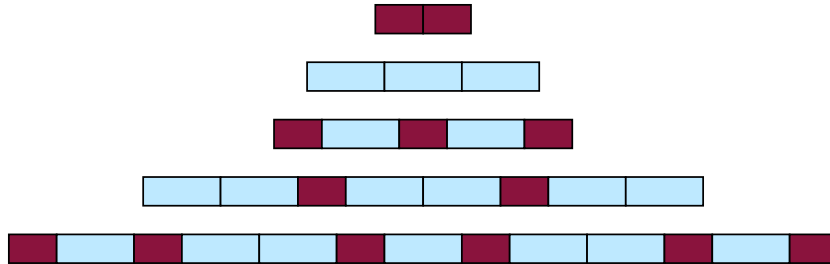


Figure 4.1: Disallowed sequences of Fibonacci tiles

Continuing to decompose these sequences yields longer and longer sequences of short and long intervals that are NOT permitted in a Fibonacci Tiling or any fragment thereof. These sequences are deceptive, however, because they are not immediately recognizable as problematic. It is only after composing them that we see that they cannot be part of a valid Fibonacci

tiling. Let a **fragment** of **order d** be a finite, non-overlapping set of tiles in \mathbb{R} that covers some line of length d . We have the following definition:

Definition 4.1 [DS95] A fragment F of order d will be a **deception of order d** if every connected subfragment of F of cardinality less than d is a subset of some Fibonacci tiling of the line but F is NOT a subset of any Fibonacci tiling of the line.

The fragments pictured in Figure 4.1 are examples of deceptions in Fibonacci tilings. Note that we have deceptions of lengths 2, 3, 5, 8, 13, . . . , the Fibonacci numbers. We can continue to decompose these deceptions indefinitely, to obtain arbitrarily long strings of short and long intervals that cannot appear in Fibonacci tilings.

Theorem 4.2 The Fibonacci tiles admit deceptions in the orders of the Fibonacci numbers.

Proof. Simply decompose the fragment LLL to obtain them. The decomposition rules will force the number of tiles in each deception to be a Fibonacci number. \square

Corollary 4.3 When attempting to construct an infinite Fibonacci tiling of the line, there is no limit on the size of regions that must be examined around the tile being placed to ensure a correct tiling.

Proof. As the Fibonacci numbers are not bounded, we can obtain arbitrarily long deceptions. As a direct consequence, we may have to examine an arbitrarily large number of tiles around the tile being placed to ensure that it is not part of some deception. \square

In addition, we have the following:

Corollary 4.4 There is no local algorithm for the growth of Fibonacci tilings.

In other words, no amount of local information is enough to ensure that the tiles we are placing are not in error. In constructing a Fibonacci tiling, we need to consider arbitrarily long fragments of the existing tiling in order to decide how to proceed. So how can we possibly decide how to place a tile?

4.3 Algorithm for correct placements

Composition can always be used to determine whether or not a certain string of S 's and L 's is indeed a Fibonacci string. Simply compose the existing fragment repeatedly, until all the original tiles are contained in one large scale tile. Then we may decompose this back down, to find out what tile we should place next.

Alternatively, we can use the updown generation procedure to do this. Suppose we have the fragment shown in Figure 4.2. and we want to decide



Figure 4.2: A fragment of a Fibonacci tiling: what tile should come next?

what tile comes next in the tiling. Of course we *know* that the next tile must be short, otherwise we will have the forbidden LLL arrangement. But suppose we are nevertheless uncertain about what tile to place next.

Pick one tile, and compose it according to a path through the FSA. Here we have chosen the tile next to the site of the tile to be placed, but this is not necessary. Follow a map through the FSA until we have all of the tiles of our original fragment contained in one large tile (Figure 4.3). Here we have used the map $a \circ c \circ b \circ a$. Now decompose this large tile, until its constituent tiles are the size of the tiles of our fragment (Figure 4.16). According to this algorithm, the tile to be placed is indeed short.

However, this is NOT a local algorithm.

4.4 Non-Locality of Fibonacci Sequences

In the remainder of the chapter we will consider the idea of non-locality in the growth of Fibonacci tilings.

4.4.1 Forcing in Fibonacci Sequences

Let us consider an example to illustrate the difficulty inherent in building up a Fibonacci tiling.

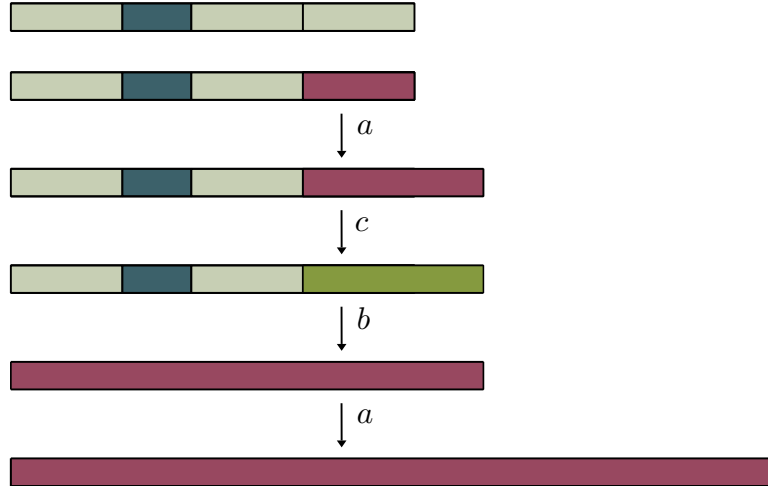


Figure 4.3: Using the Updown procedure to determine tile placement: the map $a \circ c \circ b \circ a$

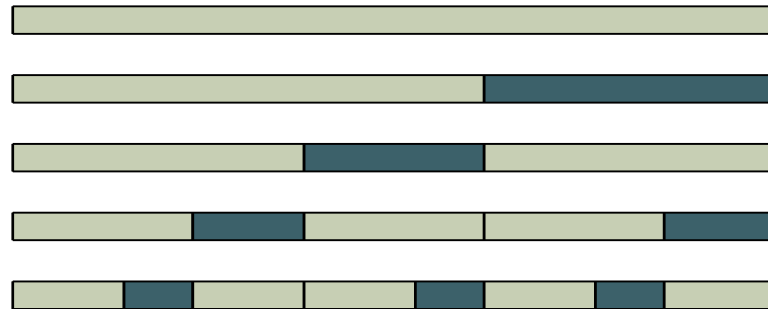


Figure 4.4: Decomposing the large tile determines tile placement

Suppose we begin with a Long interval (Figure 4.5, and we wish to create a Fibonacci Tiling that is eight tiles long. It is clear that at this point, we can add either a long or a short interval. Suppose we add a Short interval (Figure 4.6. Then the next tile, which will be the third tile in the sequence, must be a long tile, otherwise we will have the prohibited *SS* sequence, as shown in pink (Figure 4.7). In other words, the long tile in the third position is *forced* by the adjacent short tile, as indicated in Figure 4.8. So far we have *LSL*.

Now again we have a choice of whether to place a short or long tile. Suppose we pick the short tile (Figure 4.9). Then again avoiding the SS error forces the next tile to be long (Figure 4.10). Hence we have $LSLSL$. But now the problem becomes more interesting. At a local level, it would seem that we can again choose either the short or long tile to continue this Fibonacci Tiling. However, a closer study of the entire sequence reveals that this is not the case! If we place a Short tile in the sixth position, we will have created one of the deceptions, $SLSLS$, as shown in Figure 4.11. Hence the sixth tile must be a Long one, giving us $LSLSLL$. Note that to make this decision, we had to consider tiles that were four tiles away from the site of growth (Figure 4.12). We now have two adjacent Long tiles, and we need to avoid the error LLL shown in blue in Figure 4.13. Hence the seventh tile must be short (Figure 4.14). This in turn forces the eighth tile to be long, and we have the eight-tile sequence: $LSLSLLSL$ (Figure 4.15).



Figure 4.5: A long interval: we can add either another long tile, or a short tile



Figure 4.6: We add the short tile



Figure 4.7: The prohibited sequence LSS

If we use the technique of this example but consider the other options where we had choices, we find that there are five different eight-tile Fibonacci tilings beginning with a long tile (Figure ??). Similarly, there are four eight-



Figure 4.8: The third tile in the sequence must be long, to avoid the arrangement in Figure 4.7



Figure 4.9: The sequence *LSSL*



Figure 4.10: Avoiding the *SS* error forces the next tile to be long.



Figure 4.11: The prohibited sequence *SLSLS*, shown in red and blue

tile Fibonacci tilings beginning with a short tile (Figure 4.17). Hence, there are only nine different possible eight-tile fibonacci tilings.

4.4.2 Mistakes

As we have seen, when constructing a Fibonacci tiling by adding tiles one at time, one needs to consider tiles adjacent to the tile to be placed AND tiles that are much farther away.

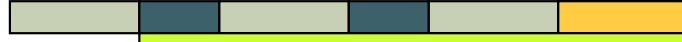


Figure 4.12: To obtain this fragment of a tiling, we had to consider tiles that are four tiles away from the site of growth



Figure 4.13: We need to avoid the *LLL* arrangement, shown in blue

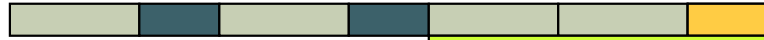


Figure 4.14: Avoiding the *LLL* error forces the next tile to be short

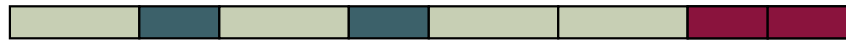


Figure 4.15: Our final eight tile sequence *LSLSLLSL*

Suppose now that we abandon the idea of an error-free tiling, and decide to avoid mistakes of a certain length. Then this means that the number of possible tilings of a given length is determined by the restrictions placed on mistakes.

We can construct some recurrence relations that will illuminate this idea.

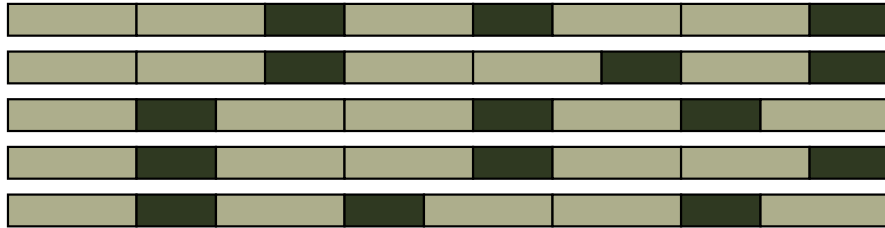


Figure 4.16: Five different eight-tile Fibonacci tilings beginning with a long tile

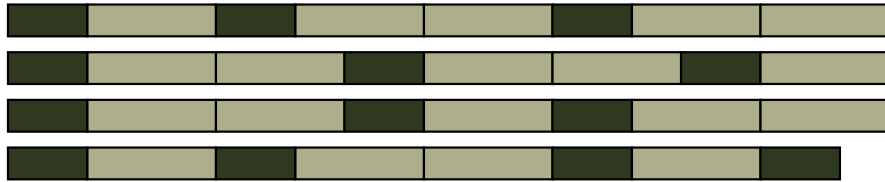


Figure 4.17: The four eight-tile Fibonacci tilings beginning with a short tile

Consider the number, $n_{r,k}$ of tilings of length r compatible with constraints of length k . For instance, $n_{9,3}$ is the number of different tilings of length 9 that can be constructed avoiding mistakes of length 3 or less. That is, these tilings cannot contain the mistake 'SS' or 'LLL'.

When $k = 1$ there are no constraints on tilings of any length. Therefore, the number of tilings of length r is just $n_{r,1} = 2^r$. It is easy to see that the following is true:

$$n_{r,k} + n_{r,k} = n_{r+1,k} \quad (k = 1; r \geq 0)$$

Consider the case when $k = 2$. In this instance, we are building tilings that do not contain the error SS. Suppose that we are trying to build a sequence of length $r + 2$. Since we are not concerned with anything other than the SS

error, we can add a 1 to any sequence to obtain a longer sequence. So we will have $n_{2,r+1}$ tilings of length $r + 2$ ending in 1. We now need to determine how many tilings of length $r + 2$ will end in 0. Because we are avoiding the error SS , we can't simply add a 0 to every sequence of length $r + 1$. We can, however, add a 1 to every sequence of length r , followed by a 0, to yield $n_{2,r}$ tilings of length $r + 2$ ending in 0. That is we have the following recurrence relation:

$$n_{r,k} + n_{r+1,k} = n_{r+2,k} \quad (k = 2; r \geq 0)$$

We can use similar reasoning for the case $k = 3, 4$. Recall that errors are created by decomposing the original error SS , and therefore appear in lengths given by the Fibonacci numbers. So avoiding errors of length 4 will be the same as avoiding errors of length 3, because there are no errors of length 4. In this case we are not allowing the strings SS or LLL to appear in our tilings. Suppose we are trying to construct a tilings of length $r + 3$. Consider the following table of possibilities:

| ... | r | $r + 1$ | $r + 2$ | $r + 3$ |
|-----|-----|---------|---------|---------|
| ... | S | L | S | L |
| ... | L | L | S | L |
| ... | L | S | L | S |
| ... | L | S | L | L |
| ... | S | L | L | S |

To enumerate the number of possible tilings, notice that in the first three lines of the table, we add a SL to every sequence of length $r + 1$ ending in L , and we add LS to every sequence of length $r + 1$ ending in S . Hence the first three lines of the table represent $n_{3,r+1}$ correct tilings of length $r + 3$. In the last two lines of the table, note that we add SLL to every sequence of length r ending in L , and LLS to every sequence of length r ending in S . So the last two lines of the table represent $n_{3,r}$ additional tilings of length $r + 3$. We have established:

$$n_{r,k} + n_{r+1,k} = n_{r+3,k} \quad (k = 3, 4; r \geq 1)$$

Continuing in this manner, we find the following:

$$n_{r,k} + n_{r,k} = n_{r+1,k} \quad (k = 1; r + 1 \geq 1)$$

$$n_{r,k} + n_{r+1,k} = n_{r+2,k} \quad (k = 2; r + 1 \geq 1)$$

$$n_{r,k} + n_{r+1,k} = n_{r+3,k} \quad (k = 3, 4; r + 1 \geq 2)$$

$$n_{r,k} + n_{r+2,k} = n_{r+5,k} \quad (k = 5, 6, 7; r + 1 \geq 3)$$

$$n_{r,k} + n_{r+3,k} = n_{r+8,k} \quad (k = 8, 9, 10, 11, 12; r + 1 \geq 5)$$

$$n_{r,k} + n_{r+5,k} = n_{r+13,k} \quad (k = 13, 14, \dots, 20; r + 1 \geq 8)$$

⋮

In general we have

$$n_{r,k} + n_{r+f_i-2,k} = n_{r+f_i,k} \quad (k = f_i, \dots, f_{i+1}-1; r + 1 \geq f_{i-1})$$

where the f_i 's are the Fibonacci numbers given by

$$f_i = f_{i-1} + f_{i-2}; \quad i = 2, 3, 4, \dots \quad f_0 = 0, f_1 = 1$$

These recurrence relations generate the following table of the number of tilings of length r compatible with constraints of length r .

| r | $k = 1$ | 2 | 3, 4 | 5, 6, 7 | 8, ..., 12 | ... |
|-----------------------|----------|----------|----------|----------|------------|-----|
| 0 | 1 | 1 | 1 | 1 | 1 | ... |
| 1 | 2 | 2 | 2 | 2 | 2 | ... |
| 2 | 4 | 3 | 3 | 3 | 3 | ... |
| 3 | 8 | 5 | 4 | 4 | 4 | ... |
| 4 | 16 | 8 | 5 | 5 | 5 | ... |
| 5 | 32 | 13 | 7 | 6 | 6 | ... |
| 6 | 64 | 21 | 9 | 7 | 7 | ... |
| 7 | 128 | 34 | 12 | 8 | 8 | ... |
| 8 | 256 | 55 | 16 | 10 | 9 | ... |
| 9 | 512 | 89 | 21 | 12 | 10 | ... |
| 10 | 1024 | 144 | 28 | 14 | 11 | ... |
| 11 | 2048 | 233 | 37 | 17 | 12 | ... |
| 12 | 4096 | 377 | 49 | 20 | 13 | ... |
| 13 | 8192 | 610 | 65 | 24 | 15 | ... |
| 14 | 16384 | 987 | 86 | 29 | 17 | ... |
| 15 | 32768 | 1597 | 114 | 34 | 19 | ... |

Note that $n_{r,1}$ are powers of 2, and $n_{r,2}$ are the Fibonacci numbers. Note also that if $k \geq r$,

$$n_{r,k} = r + 1$$

which means that there are only $r + 1$ *correct* Fibonacci tilings of length r . That is, these are the only tilings of length r without mistakes. Indeed this is consistent with the example we saw involving tilings of eight tiles, which yielded nine correct fragments.

From the recurrence relations it is clear that if we fix k , then $n_{r,k}$ will grow exponentially as r increases. But as noted, the growth in the number of correct Fibonacci tilings is just linear in r . This means that for fixed k and large r , the probability of making a mistake while constructing such a sequence becomes one. There is no way to avoid making mistakes.

4.5 Summary

In summary, we have seen that there is no local growth algorithm for the generation of Fibonacci tilings. In addition, attempting to avoid mistakes is an inherently non-local procedure.

Chapter 5

Non-locality of Penrose Tilings

5.1 Introduction

We have seen that Fibonacci tilings admit deceptions of all orders, and must grow in some kind of non-local way. This chapter will be dedicated to the examination of similar questions for Penrose tilings.

5.2 Local matching rules for Penrose tilings

Let's now turn our attention to the problem of attempting to build up a Penrose tiling of thick and thin rhombs one tile at a time. This is a more complicated scenario than the Fibonacci tilings, but we will soon see that it shares many similarities.

Beginning with some finite patch of tiles, there are three possible situations when attempting to place a tile along an unmatched edge of the patch. The first case is that the decision is forced: only one of the two types of tiles will fit (Figure 5.1). In these cases, only the thick or thin rhomb would be appropriate.

The second case is where neither tile will fit. This indicates that something has already gone wrong in the construction of the tiling. The situation in Figure 5.2 looks correct until closer examination reveals that the red tile is in fact a hole. The matching rules preclude the existence of a tile to fill this hole. Figure 5.3 shows a similar situation with a thick rhomb.

The last and most interesting case is when we have an apparent choice as to which tile to place.

In Figure 5.4, it seems that either tile would be an appropriate choice. This

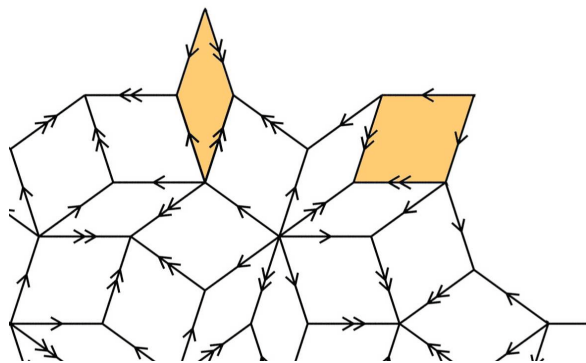


Figure 5.1: The yellow tiles are examples of two tiles that are forced.

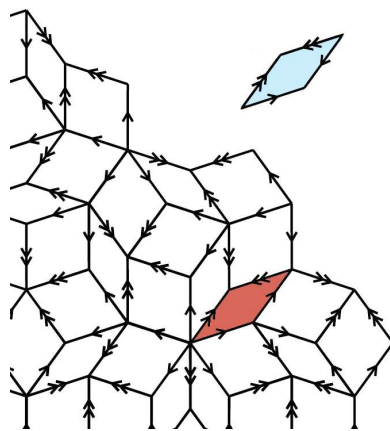


Figure 5.2: The area in red is a hole in the tiling that cannot be filled by any tile

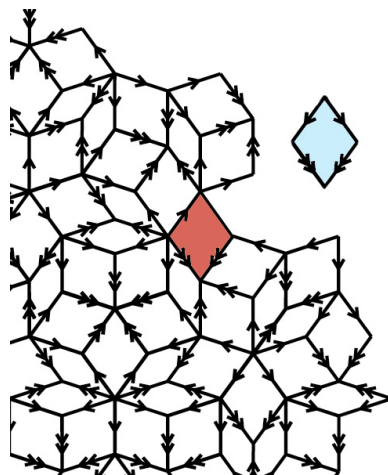


Figure 5.3: The red area is a gap in the tiling that cannot be filled with any tile

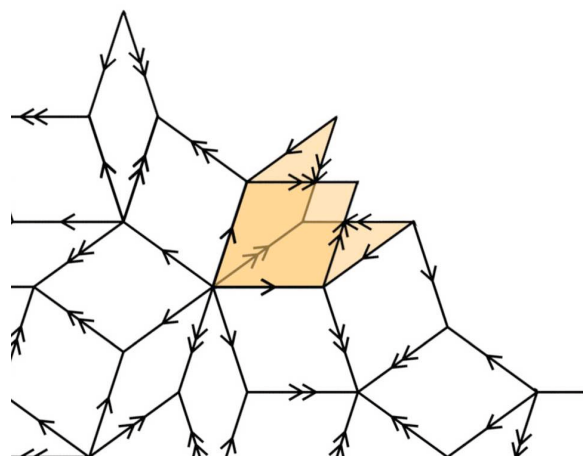


Figure 5.4: In this case, we have a choice about which tile to place: either tile appears to be appropriate

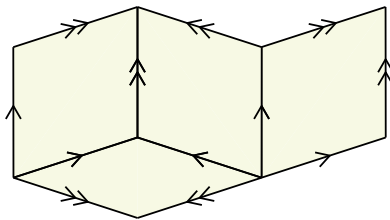


Figure 5.5: A growing patch of tiles: Suppose we wish to add a tile to the leftmost edge.

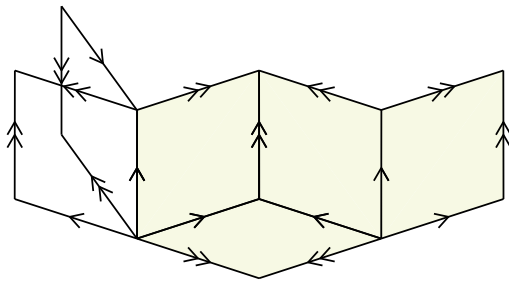


Figure 5.6: According to the matching rules, we can add either a thick or thin rhomb

case is not nearly as simple as it first appears, however. We will soon see that most of the time the appearance of choice is an illusion. That is, one of the choices will result in a patch of penrose tiles that is extensible, and the other will not. This problem is the central concern of the remainder of this chapter.

To begin, consider the arrangement of tiles shown in Figure 5.5. Suppose we wish to add a tile at the leftmost unmatched edge. According to the matching rules, we can add either a thick or thin rhomb (Figure 5.6). Suppose we choose the thick one, as shown in Figure 5.7. This choice immediately forces some surrounding tiles, shown in orange in Figure 5.8. However, at the far right there is a gap that cannot be filled by either tile. This is evidence that a

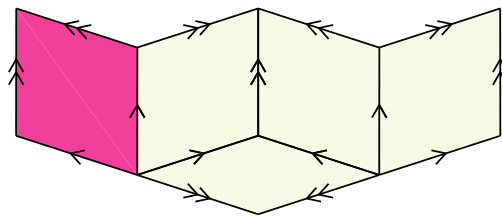


Figure 5.7: Suppose we add the thick rhomb

mistake has been made. Since all the tiles in orange are forced, it is evident that the pink tile is incorrect. Examining the entire patch of tiles makes it clear that we must place a thin rhomb along the left unmatched edge. To proceed, we must disassemble the patch and return to the original configuration of Figure 5.5. We now add the thin rhomb, and see that this produces more favorable results (Figure 5.9).

This simple example illustrates the problem with the local matching rules for Penrose tiles. Just because it is possible to place a tile locally, it does not guarantee that the tiling can continue to infinity.

Another way to view this problem is by using the composition rules. When two thick rhombs are placed together along an edge with a short arrow, there is always a specific way in which this arrangement is composed. It is easy to convince ourselves (by checking with Figure 3.29, for example) that in such a case, half of each of these rhombs will make up part of a new large rhomb, as shown in Figure 5.11. As a result, when two such matchings happen side by side as in Figure 5.7, we obtain the composed arrangement seen in Figure 5.10. It is not hard to see that this is an incorrect patch.

It is useful to develop some terminology to distinguish between placements that cause errors and those that do not.

For connected finite arrangements of tiles, the term **legal** will refer to a collection of tiles fitted together in accordance with the matching rules, but where an extension of the patch to infinity is not necessarily possible. In contrast, a **correct** arrangement of tiles is a subset of a legal tiling of the entire plane. In other words, all correct patches are also legal, but legal patches are

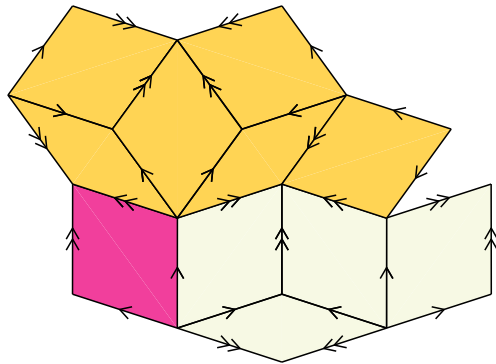


Figure 5.8: The choice of the thick rhomb forces the tiles shown in orange. At the far right there is a gap that cannot be filled by either tile. This is evidence that a mistake has been made.

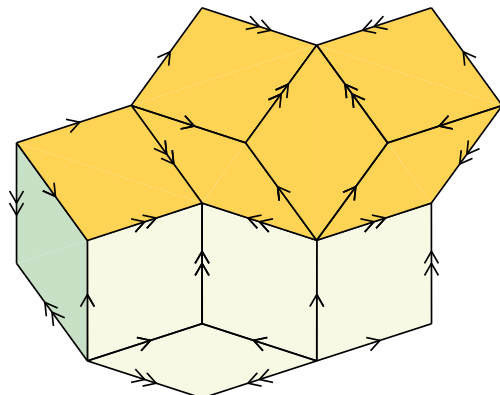


Figure 5.9: Adding a thin rhomb instead of the thick rhomb produces a patch of tiles without gaps.

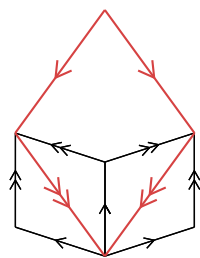


Figure 5.10: Two thick rhombs joined along a single arrow edge. These must compose to yield another thick rhomb, as shown in red.

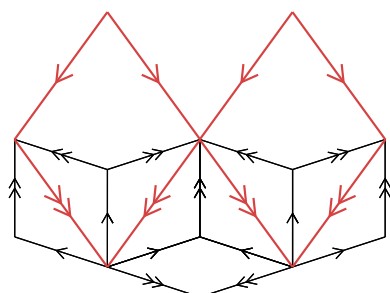


Figure 5.11: The patch of Figure 5.7, composed. The result is the incorrect arrangement, shown in red.

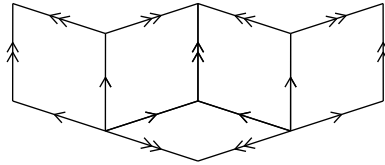


Figure 5.12: A simple mistake

not necessarily correct. Let us also define a **mistake** as the placement of a tile that will extend a correct tiling to a legal but incorrect tiling. [Pen89] In other words, the mistake will mean that the tiling will not extend to infinity. We will use **error** to mean the manifestation of a mistake in the tiling, such as a hole or an overlap. The curious thing about these mistakes is that the error in the tiling that results from the mistake is not necessarily local to the mistake. This will be the subject of Section 5.4.

In Figure 5.6, both choices are legal. However, we know that the five tile arrangement shown in Figure 5.12 is incorrect.

It would seem that now that we know to avoid this particular arrangement, we could easily construct tilings that would continue to infinity. We need only to make sure that the pictured arrangement does not occur anywhere in the growing patch of tiles. The problem is not so simple. Recall that all Penrose tilings of the plane (that is, infinite Penrose tilings) must accord with the composition and decomposition rules. This in turn means that the simple mistake pictured in Figure 5.12 must not appear *at any stage of the hierarchy*. In other words we need to avoid all of the arrangements in Figure 5.13

We can continue to decompose our original arrangement to obtain a version of this patch on any level of the hierarchy. This means that we need to avoid all of these arrangements when constructing tilings one tile at a time. This is a challenging task, and is made particularly challenging by the deceptive nature of the arrangements above. We have the following definition:

Definition 5.1 [DS95] A regular patch P of order r will be a **deception of order r** if every connected subpatch of P of cardinality less than r is a subset of some tiling of the plane but P is NOT a subset of any tiling of the plane.

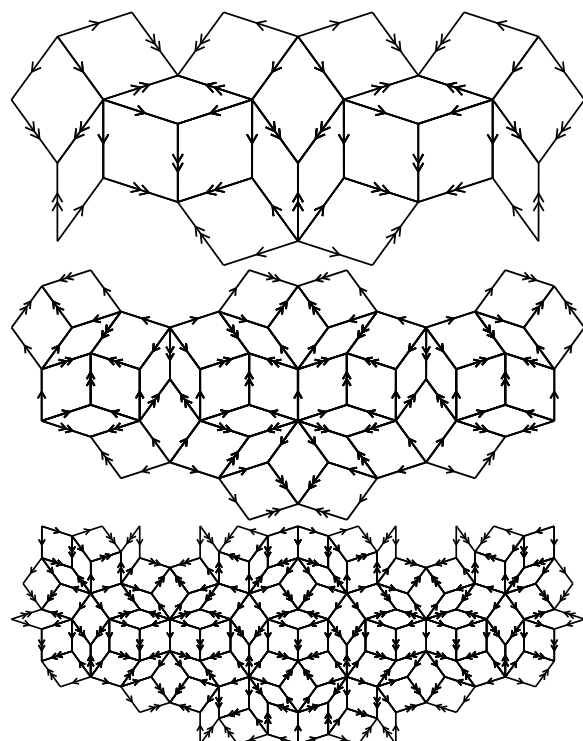


Figure 5.13: Decomposed versions of our five-tile mistake (Figure 5.12). We must avoid all of these configurations when building up a tiling of Penrose tiles. In addition, we can continue to decompose these arrangements indefinitely.

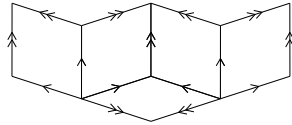


Figure 5.14: Example of a deception

Here a **patch** is a finite, non-overlapping set of tiles in \mathbb{R}^2 . It is called **regular** if it is homeomorphic to the closed unit disc. A regular patch is of **order r** if it covers some disc of radius r .

In short, a *deception* is an *incorrect* patch without holes for which we cannot decide by local inspection whether the patch is correct.

Theorem 5.2 [DS95] *The aperiodic protoset of Penrose rhombs admits deceptions of all orders.*

Proof. The simplest example of a deception is shown in Figure 5.14. We can decompose this deception using the decomposition rules to obtain deceptions of all orders. \square

Indeed because we can continue to decompose this simple deception indefinitely, there is *no limit* to how many tiles we need to examine in order to ensure that we do not make some version of our original mistake. That is, even an augmentation of the local matching rules to include the consideration of all tiles within the radius r would be insufficient to guarantee the creation of an arbitrarily large patch of a *correct* Penrose tiling.

Corollary 5.3 [Pen89] *When attempting to construct an infinite Penrose tiling of the plane according to local matching rules alone, there is NO LIMIT on the size of regions that must be examined around the tile being placed to ensure a correct tiling.*

In other words, the decision of which tile to place at an unmatched edge may require an analysis of an arbitrarily large area of the existing tiling. There is no upper bound on the size of this area, which follows from the fact that we can decompose the original mistake indefinitely, to obtain versions of the mistake at any level of the hierarchy.

Furthermore, we have the fact that:

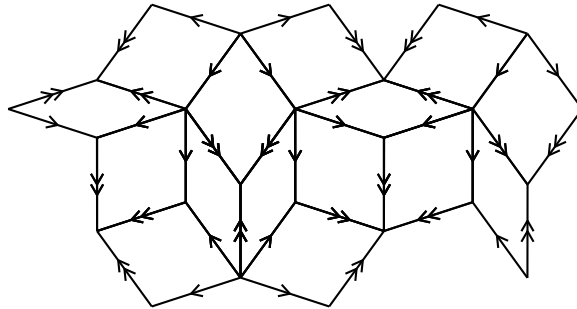


Figure 5.15: A growing patch of tiles. We need to determine what tile to place along the top left edge.

Corollary 5.4 [Pen89] *There is no local algorithm for the growth of Penrose tilings.*

In other words, no amount of local information is enough to guarantee that a given regular patch of Penrose tiles belongs to some tiling of the plane.

So how can we ensure that tiles we are placing are placed correctly?

5.3 An algorithm for correct placements

Indeed we have an algorithm for determining the correct placement. By definition, all Penrose tilings that continue to infinity must accord with the composition rules. Therefore, one way to guarantee the creation of an infinite tiling is by creating larger and larger versions of the tiles, made up of many rhombs of the original size. Begin by composing the existing tiles into larger tiles, and those tiles into larger tiles and so on, until we have the entire pattern that we started with contained within one large scale tile. Decomposing this large tile back down so that its constituent tiles are the size of our original tiles will answer the question of what tiles may be placed correctly. The easiest way to do this is to make use of the updown generation procedure.

Consider the patch of tiles shown in Figure 5.15. We need to decide what tile to place along the top left edge. In fact, this decision will dictate whether the patch is correct. Consider Figure 5.16. The placement of this top tile (the two options are shown in pink) will determine whether the patch is correct or merely legal. That is, if we choose to place a thick rhomb along this edge,

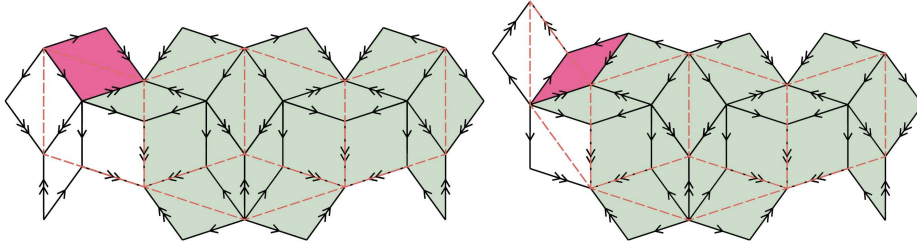


Figure 5.16: The two possibilities for placement of a tile along the top left edge (shown in pink). Note that the arrangement on the left corresponds to our original mistake, as indicated by the dashed red lines.

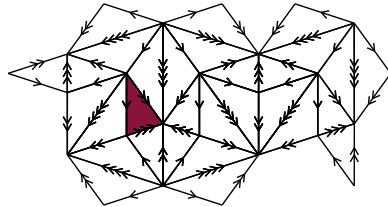


Figure 5.17: Divide the tiles into elementary triangles, and select a starting triangle, shown in red.

we will be creating a decomposed version our simple deception, the topmost image in Figure 5.13. In the following example, we will use the Updown procedure to determine what tile to place here.

Begin by subdividing the rhombs into elementary triangles and identify some starting triangle, as shown in red in Figure 5.17. Using the finite state automaton shown in Figure 3.30 we can create a map which will determine the red tile's position in the given patch of tiles. The red tile is of type t_R . We will use the following map:

$$\delta' \circ \gamma \circ \gamma' \circ \epsilon' \circ \epsilon' \circ \epsilon'$$

which will map the following

$$t_R \longrightarrow T_R \longrightarrow T_L \longrightarrow T_R \longrightarrow T_R \longrightarrow T_R \longrightarrow T_R$$

This process is shown in Figures 5.18 - 5.20.

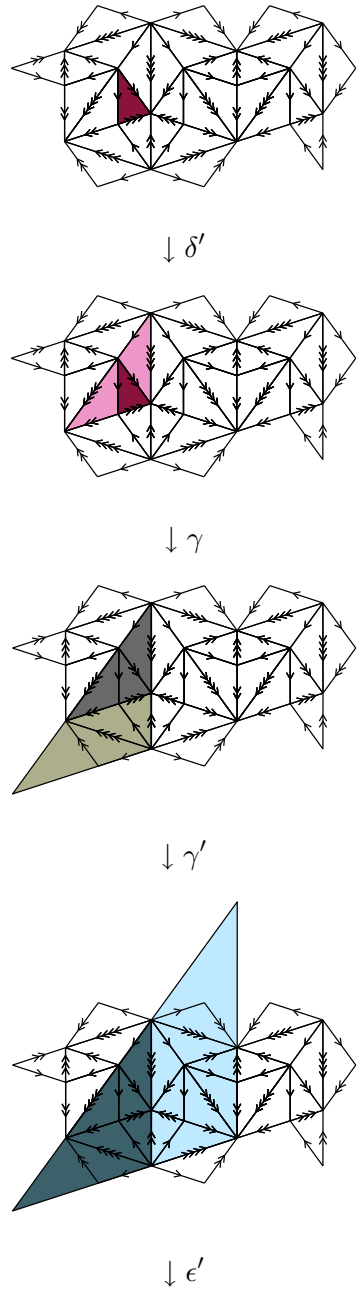


Figure 5.18: The Updown procedure used to determine correct placement. Pick a starting tile, and map it into increasingly larger tiles until the whole patch is contained within one large tile.

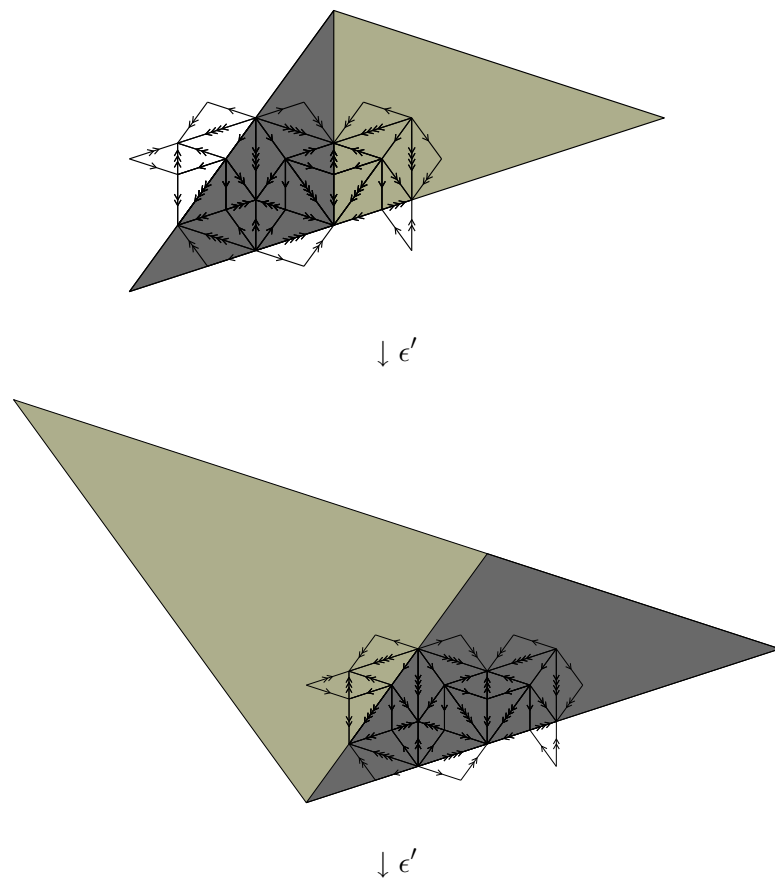


Figure 5.19: The Updown procedure used to determine correct placement, continued

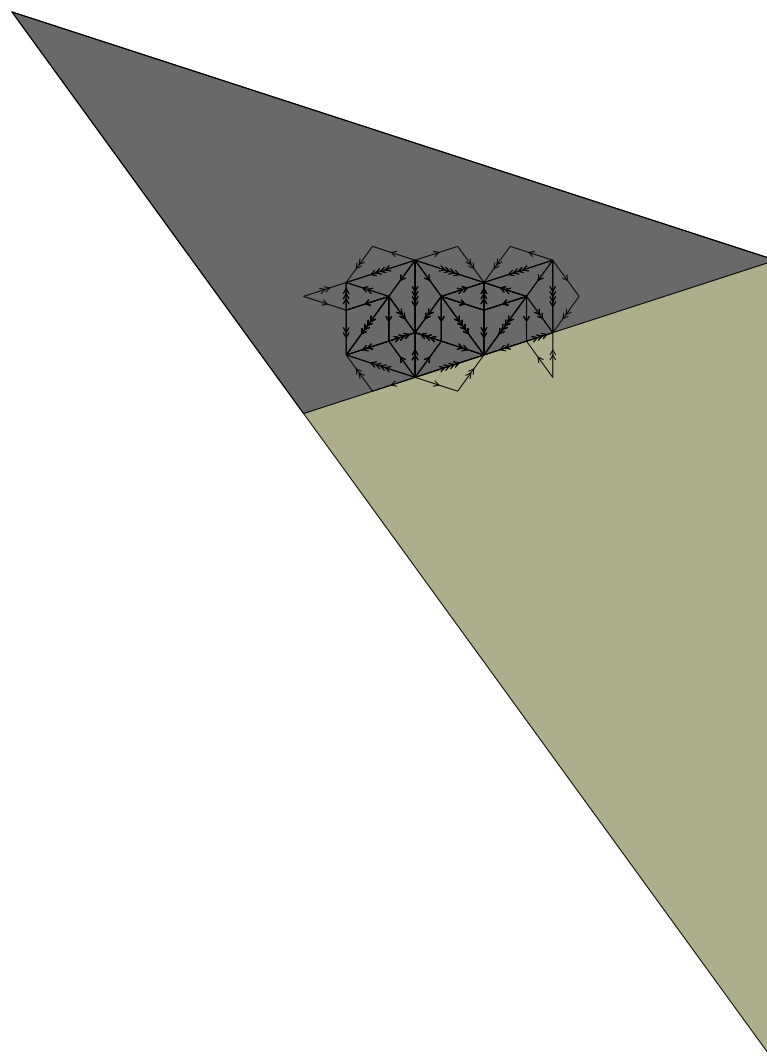


Figure 5.20: The Updown procedure used to determine correct placement, continued.

We stop when our whole patch of tiles is contained within one large tile, as shown. Now continuing with the ‘down’ part of the updown procedure, we decompose the large tile six times to obtain the correct tiling shown in Figure 5.21.

Associating the two elementary triangles making up each rhomb, we have the tessellation shown in Figure 5.22, which we know to be correct.

As we suspected, this algorithm has placed tiles along the left edge such that when composed, they will form a thin rhomb (Figure 5.23).

Note that there may be some choice about how the tiles are grouped together. This simply reflects the fact that there may be different paths through the FSA that lead to the same tiling, a consequence of Theorem 3.7. Of course we can pick different starting tiles. In addition, there may be different ways to include a small tile in a larger one.

This is always an algorithm for determining correct placement. However, even this method is flawed as the mistake can be repeated at each stage of the hierarchy. That is, while aiming to create large scale rhombs is a good strategy, the mistake can repeat itself at this larger scale. This in turn makes mistakes even harder to find. And of course, it is not a local algorithm.

To summarize so far, we have seen that Penrose tilings, like Fibonacci tilings, admit deceptions of all orders. In addition, legal patches of Penrose tiles may demonstrate interesting properties when they are not correct – overlapping tiles or unfillable gaps. The remainder of this chapter will be devoted to attempting to understand the relationship between errors, mistakes and deceptions, and the non-local character of these mistakes. We will soon see that the erroneous placement of a tile (a mistake) can cause gaps or overlaps (errors) at an arbitrarily large distance from the mistake.

5.4 Non-locality of Penrose tilings

Suppose again that we choose not to make use of the methods we know to generate Penrose tilings of the plane (Updown generation and the pentagrid method), and instead to begin adding tiles one at a time to some starting tile. Although we know that it *must* be possible to tile the plane this way by Theorem ??, the task is more difficult than one might at first suspect. Sooner or later in this process one will encounter a gap or hole in the tiling that cannot

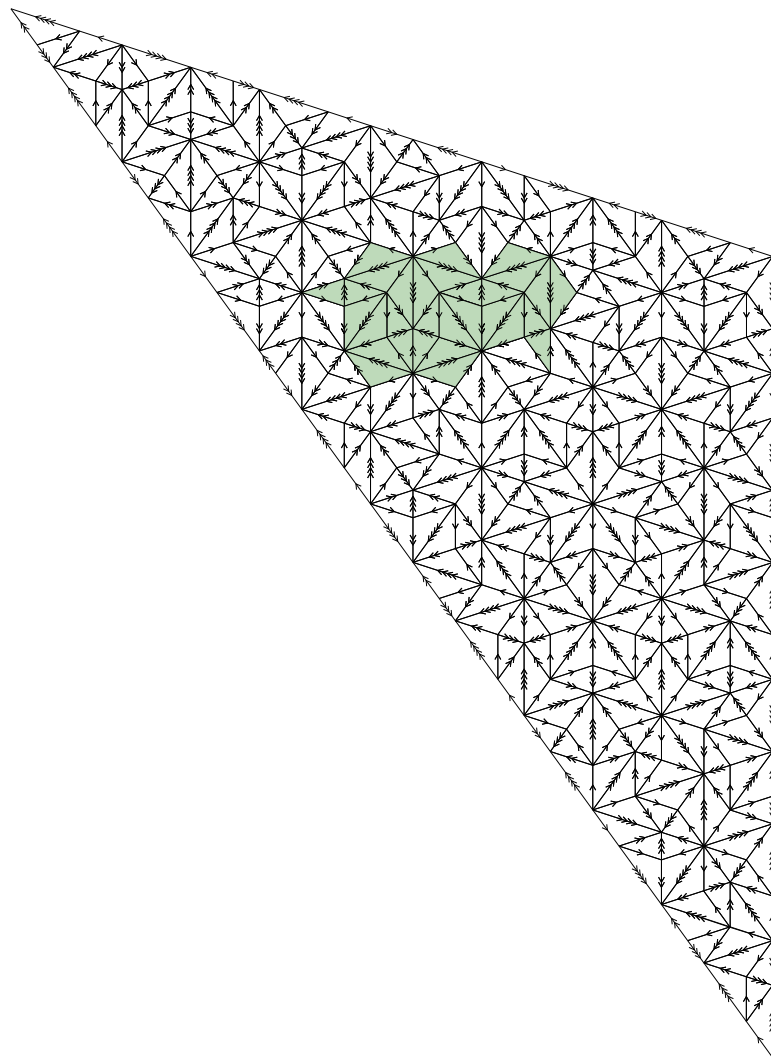


Figure 5.21: Decomposing the large tile six times to obtain this correct tiling of elementary triangles.

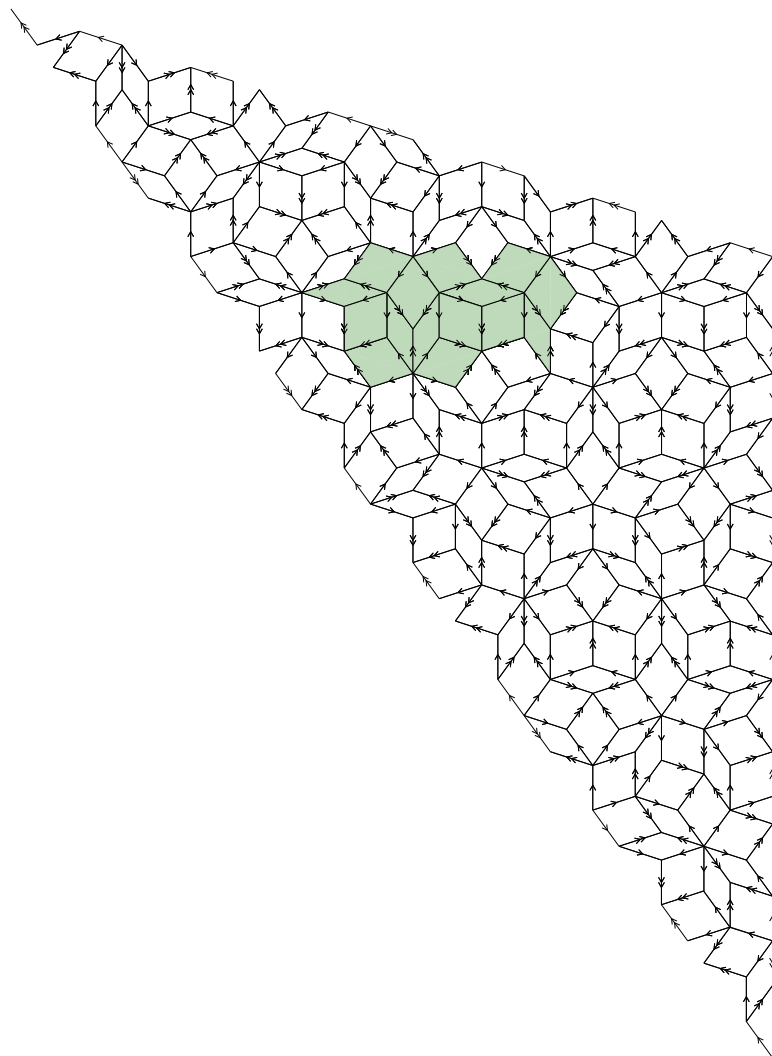


Figure 5.22: Associating the elementary triangles into rhombs.

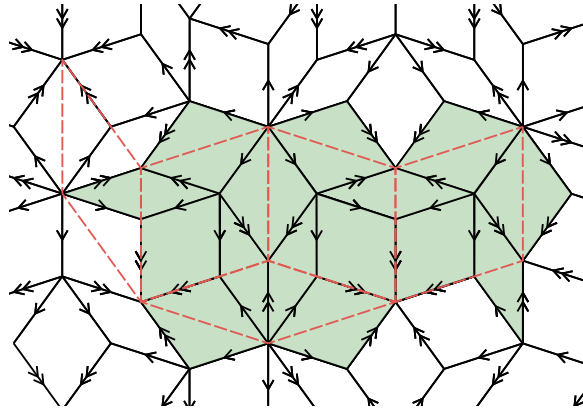


Figure 5.23: Our original tiling configuration is outlined in red. This algorithm placed a thin rhomb along the leftmost edge.

be filled. To proceed, we must disassemble part of the existing tiling, and rearrange it in an appropriate way. This is a well known fact about Penrose tiles [Gar77], and is particularly interesting problem in light of the fact that Penrose tiles are often used as models to represent the growth of quasicrystals. If quasicrystals are to be modeled on these tilings, then it would seem that there would be some way to grow the tilings in the most literal sense – by adding tiles one at a time.

Consider again our original configuration of Figure 5.5, and suppose we are adding tiles along the leftmost edge.

As we can see in Figure 5.24, the problem looks more complicated the further we decompose the rhombs. Now recall that we can legally add either a thick or thin rhomb to the unmatched left edge, although only the addition of the thin rhomb will result in a correct patch. In the Figure 5.25, we can see the differences between adding a thin or thick rhomb will make when the tiles are decomposed.

But now consider these possibilities overlapped (Figure 5.26). The orange tiles are shared by both possibilities.

The pattern formed by the orange tiles is quite remarkable. Suppose for a moment that we are again trying to grow a Penrose tiling by simply following the matching rules and that the rhombs are very small, as in the bottom sec-

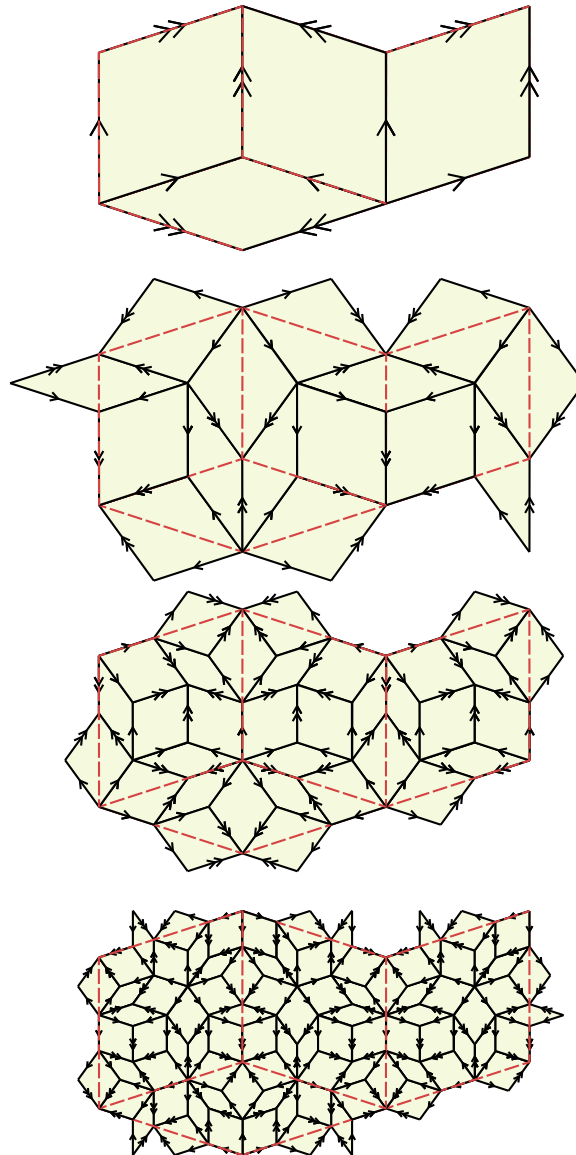


Figure 5.24: The original configuration of Figure 5.5, at various stages of decomposition. We know that we must add a thin rhomb to the leftmost edge of the top picture, and as a result we need to add tiles accordingly to the lower configurations. The problem becomes more difficult the further we decompose the patch.

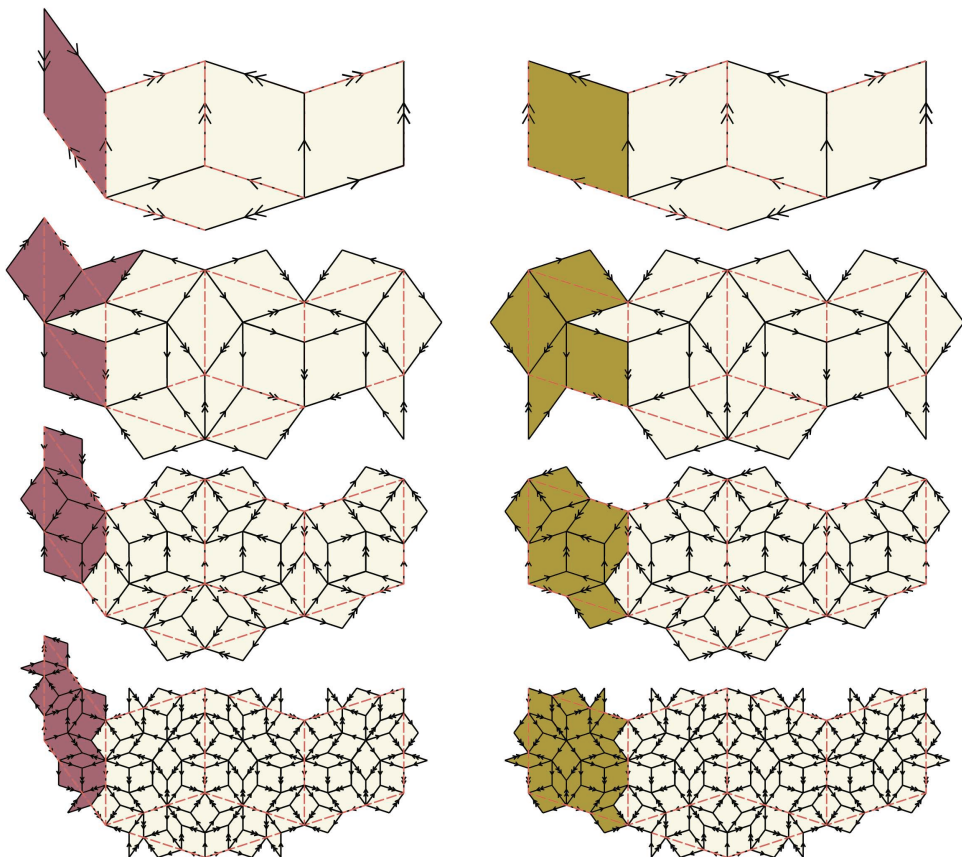


Figure 5.25: The differences between adding a thin or thick large scale rhomb at various stages of the decomposition process

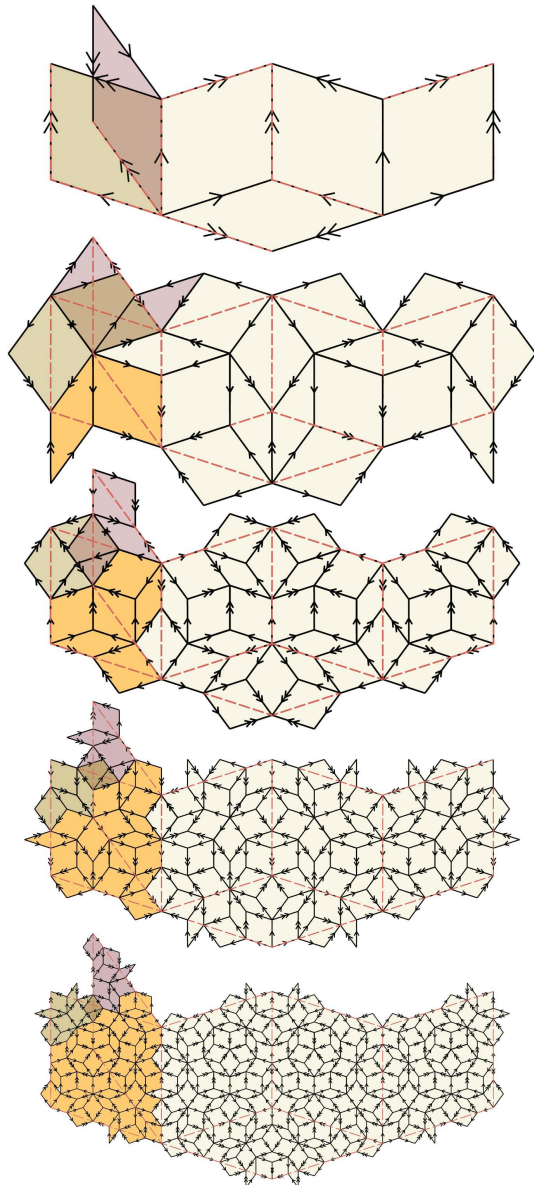


Figure 5.26: Adding a thin or thick rhomb: the scenarios overlapped. The orange tiles are shared by both possibilities. (Note that many of the orange tiles belong to the thick rhomb but not the thin one. In fact, it is easy to see that, due to the matching rules, the scenario involving with thin rhomb will still contain all of the orange tiles. That is, whether we add a thin or thick rhomb to the leftmost unmatched edge of the thin rhomb, we will obtain the pattern shown.)

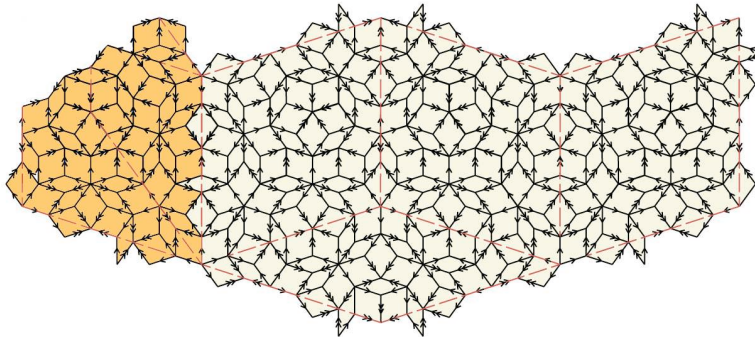


Figure 5.27: When adding tiles one by one, we may proceed unambiguously until this configuration is reached. Any tiles added along the top left diagonal will now determine whether we are growing a large scale thin rhomb or thick rhomb.

tion Figure 5.24. We know that to ensure a *correct* patch, we need to add small tiles in such a way that when composed they will constitute a large scale *thin* rhomb. The tiles in orange tell us that we may proceed unambiguously until we reach the configuration shown in Figure 5.27.

In other words, when we first begin adding tiles, there are no differences between the large thin rhomb and the large thick one. In fact, if the ratio of the sizes of the small tiles to the large ones is very large, we will have added an arbitrarily large number of tiles before the difference between the thin and thick rhombs become apparent.

Let us now turn to a slightly larger patch of tiles. Consider the two correct arrangements shown in Figure 5.28.

Overlapping the images, we see they only have a few tiles in common (Figure 5.29).

Decomposing the rhombs yields an interesting result. Contrary to what we might intuit about the decomposition of the above arrangements, the decomposed patches are strikingly similar, as we can see in Figure 5.30.

And colouring the tiles that are not the same for both decompositions yields the patterns seen in Figures 5.31 and 5.32.

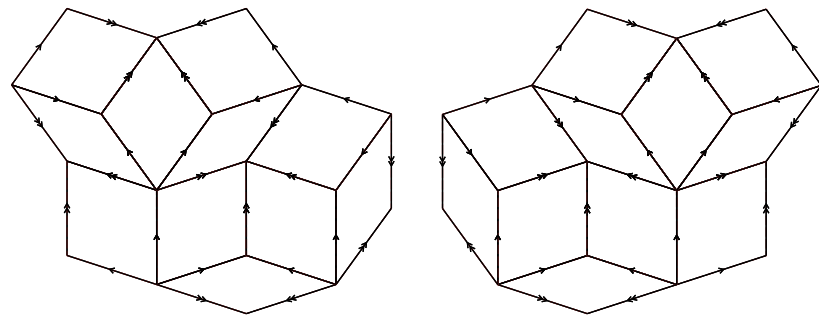


Figure 5.28: Two correct arrangements

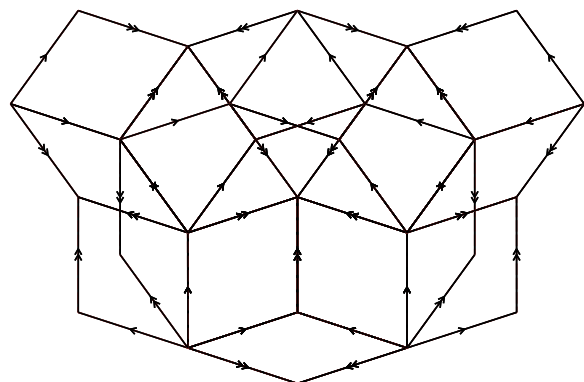


Figure 5.29: The configurations of Figure 5.28 overlapped. There are only a few tiles in common.

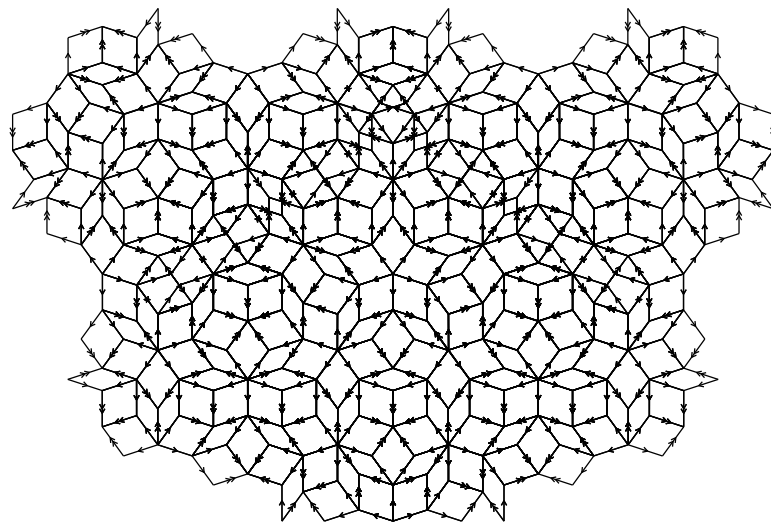


Figure 5.30: Decomposing the overlapped configurations reveals many shared tiles.

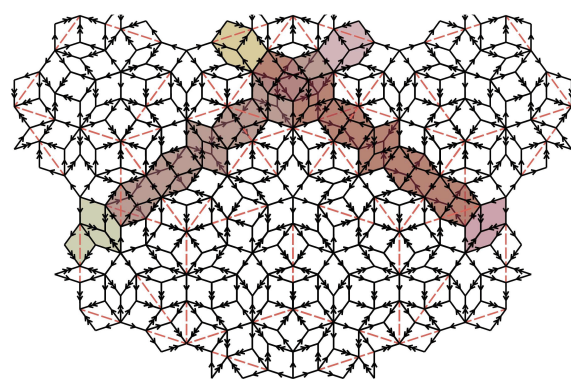


Figure 5.31: The tiles that differ in the two configurations of Figure 5.30 are coloured

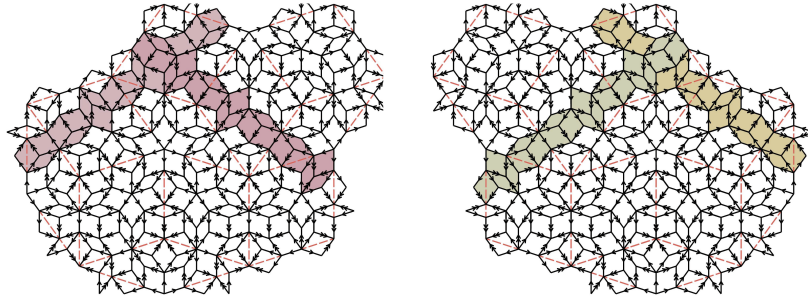


Figure 5.32: Separating the overlapped arrangements of Figure 5.31

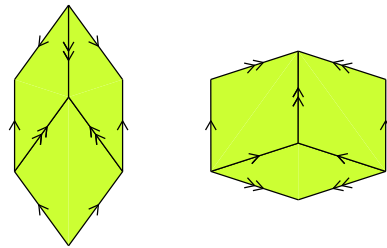


Figure 5.33: The thick and thin units that make up a worm

The differences between the two configurations manifest along **worms**, the coloured lines of tiles shown above.

5.4.1 Worms

Worms (or Conway Worms [GS87]) are the coloured ribbon-like patterns seen in Figures 5.31 and 5.32. They are built up of a sequence of short and long units (Figure 5.33), made up of three tiles each. The long unit is τ times as long as the short unit.

Decomposing a worm yields another worm with the opposite orientation and more intervals (Figure 5.34).

Despite the fact that the worms are not laterally symmetric, their horizontal boundaries are the reflections of one another across the central axis of the worm. In other words, the horizontal zigzag boundary on the top and bot-

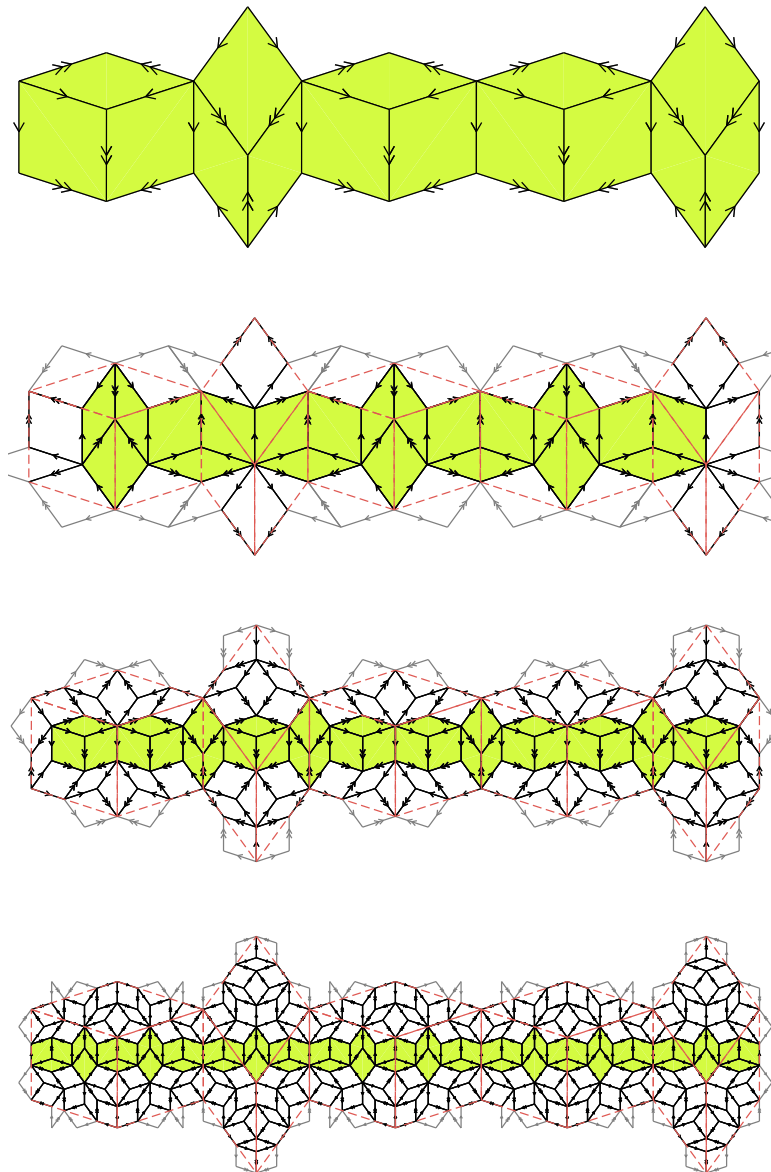


Figure 5.34: Decomposing a worm yields another worm with the opposite orientation and more intervals

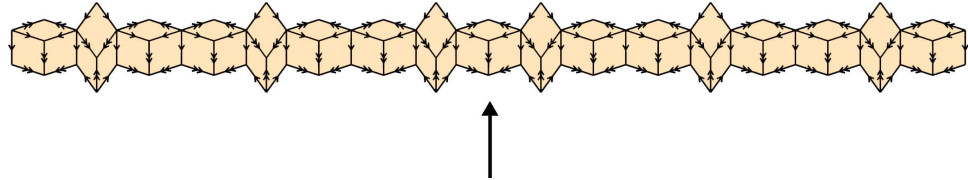


Figure 5.35: A worm oriented up

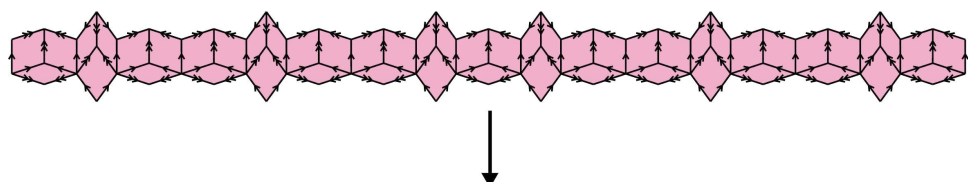


Figure 5.36: A downward oriented worm

tom of the worm is the same, including matching rules. [GS87] The worm in Figure 5.35 is oriented up, while the worm in Figure 5.36 is oriented down.

Overlapping the possibilities, we see that the horizontal boundary of the worm remains unchanged (Figure 5.37).

Worms meeting at an angle of 72° can intersect each other in two ways (Figure 5.38).

Decomposing these intersections, we obtain another intersection of the same type, with the orientations of the worms reversed (Figure 5.39).

Figure 5.40 shows an incompatible worm arrangement.

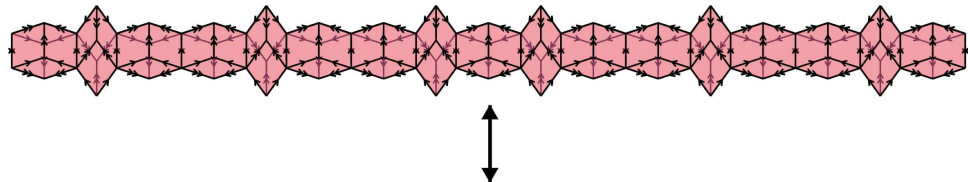


Figure 5.37: Overlapped worm orientations: the horizontal boundary remains unchanged.

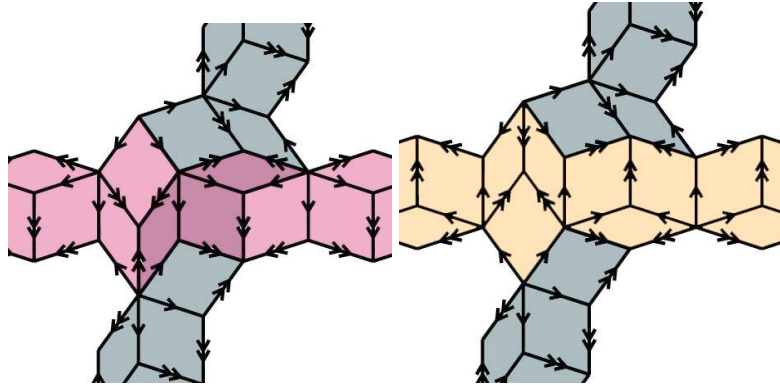


Figure 5.38: Worms intersecting in two ways. On the left, the intersecting worms share three common tiles that appear in both worms. On the right, one worm overlaps and interrupts the other worm.

This incompatible worm arrangement is the key to understanding mistakes and the resulting errors in Penrose tilings.

5.4.2 Mistakes

Now let us return for a moment to our previous example (Figure 5.41). Recall the following mistake (the placement of the pink tile) and the resulting error (the gap on the right that cannot be filled) :

Decomposing the tiles and identifying the worms, we can see that the error manifests itself in the incompatibility of the pink worms (Figure 5.42). That is, the two pink worms are of differing orientations. As a result, there is no tile that can be placed to join them. We can fix this by changing the right-most tile into a thin rhomb, as shown in Figure 5.43.

Note that the only thing we had to change was the orientation of the worm. That is, the only difference between the thin and thick rhomb is the orientation of the worm. The fact that not all of the worm orientations can intersect is what will cause mistakes to manifest themselves. As a result, errors will only emerge along the lines of the worm.

It is possible to associate with every rhomb a boundary of worms. Consider the thick rhomb. The three arrangements shown in Figure 5.44 are three

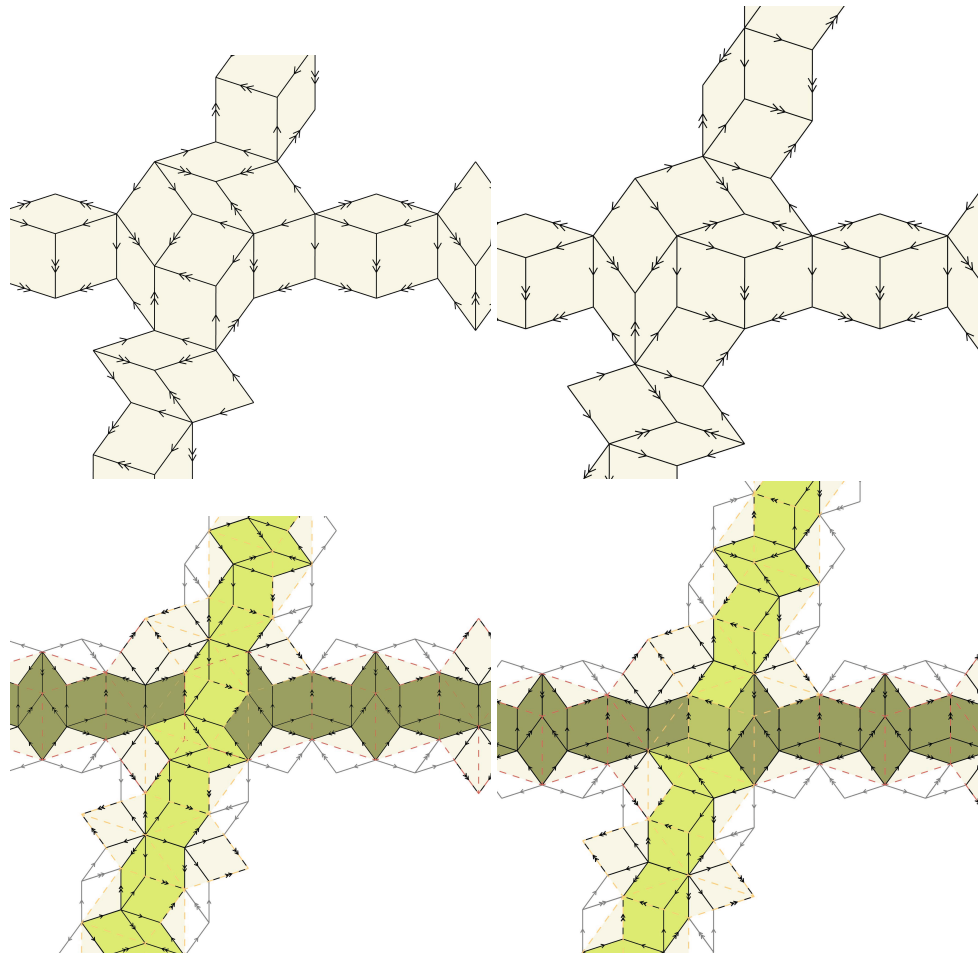


Figure 5.39: Decomposing worm intersections yeilds more intersections of the same type, with the orientation of the worms reversed.

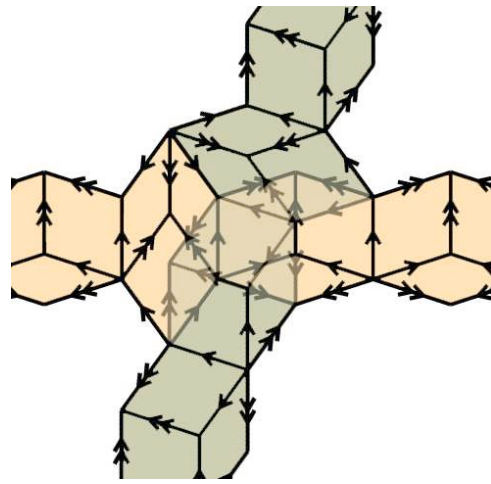


Figure 5.40: An incompatible worm arrangement

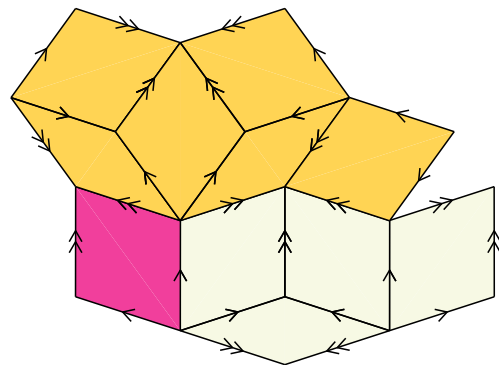


Figure 5.41: Our original mistake was the placement of the pink tile, and the unfillable gap is the resulting error.

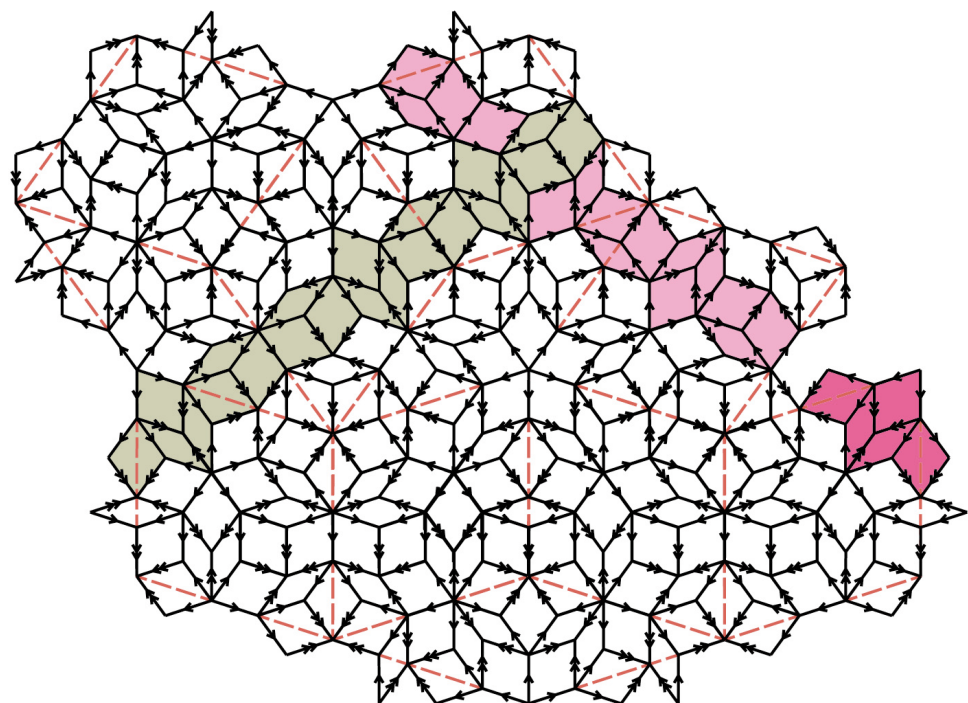


Figure 5.42: Decomposing the tiles and colouring the worms, we see that the error is actually the incompatibility of the two different worm orientations shown in pink.

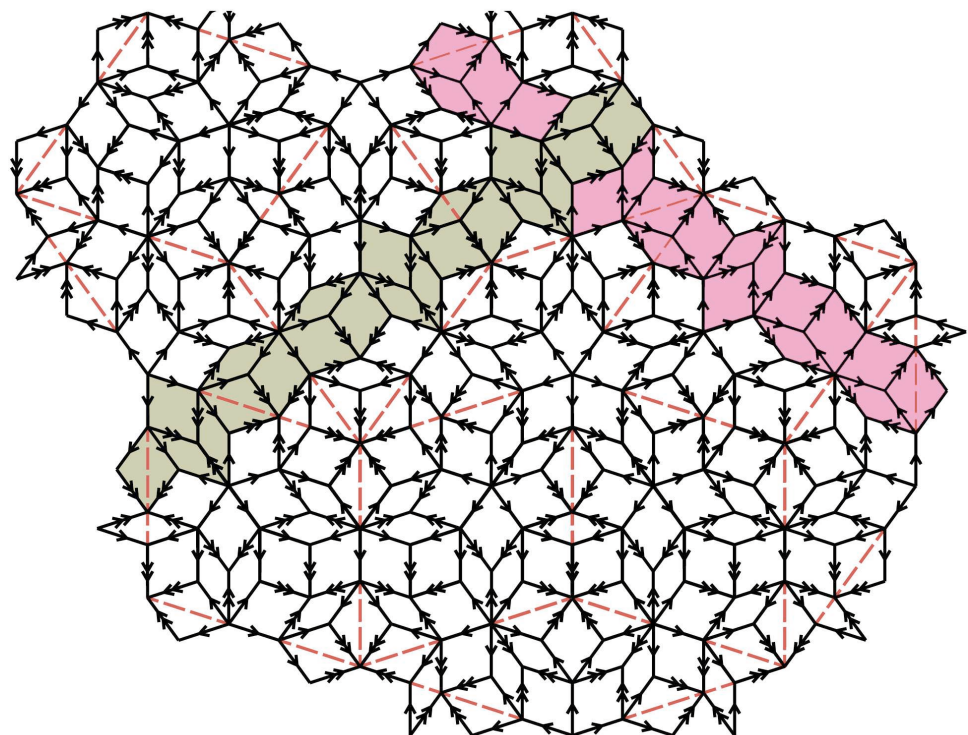


Figure 5.43: Changing the rightmost tile into a thin rhomb resolves the error of Figure 5.42. Note that this amounts to turning the worm orientations to match.

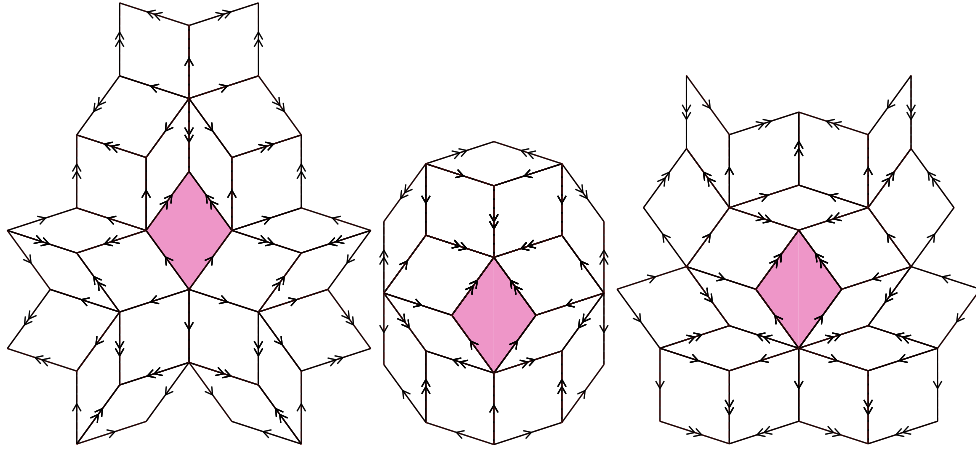


Figure 5.44: Three legal arrangements of tiles surrounding a thick rhomb

legal (and potentially correct) arrangements of tiles surrounding a central thick rhomb.

Overlapping these arrangements, we see that they share few common tiles (Figure 5.45). Decomposing the arrangements yeilds the three larger legal patches shown in Figure 5.46 Overlapping them produces the arrangement shown in Figure 5.47. We see clearly the emergence of a pattern of worms (Figure 5.48). Separating the three arrangements again, we can see that the only differences between the patches are the orientations of the worms (Figure 5.49). In other words, all three arrangements share all of the tiles shown in Figure 5.50. The only thing that differentiates the possibilities is the orientations of the worms. Now with four intersecting worms, each having two possible orientations, we have sixteen possible arrangements. We know, however, that one out of the four possible ways each pair of worms can intersect will not be correct (or even legal). Examining the cases, we find that only seven of these sixteen arrangements are legal. The other nine possibilities will have errors. The arrangements shown in Figures 5.51 and 5.52 are legal.

Composing these arrangements will yield seven different arrangements of tiles (three of which were used in the example above, and the other four are not shown). This is easy to see, once we notice that the central rhomb can be surrounded by four worms as shown In Figure 5.53. So we know that there

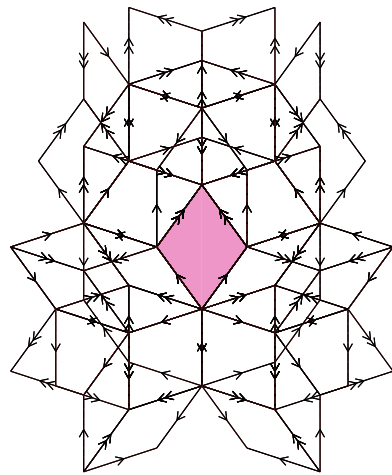


Figure 5.45: The patches of Figure 5.44 overlapped. The only shared tile is the central rhomb.

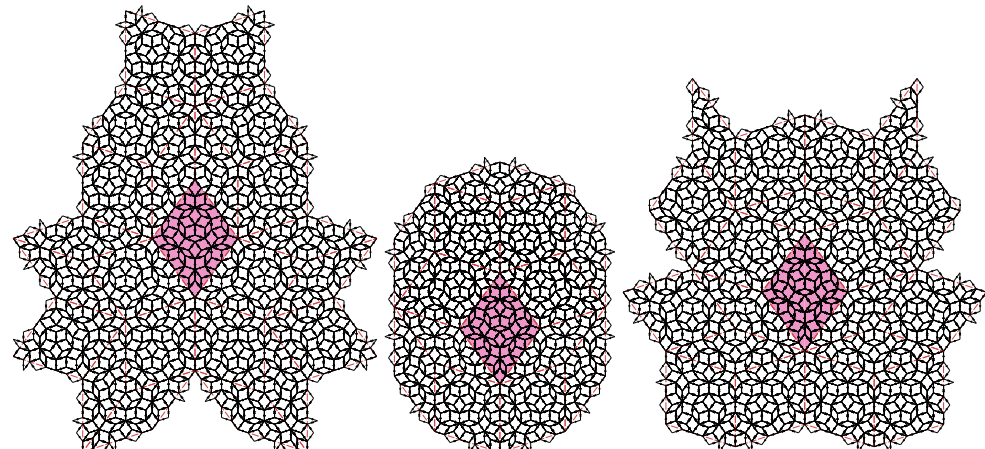


Figure 5.46: The arrangements of Figure 5.44 decomposed

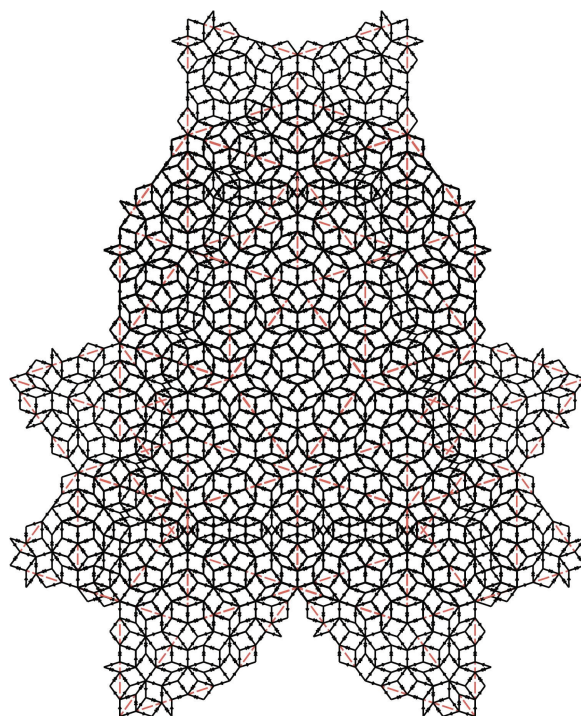


Figure 5.47: Overlapping the arrangements of Figure 5.46

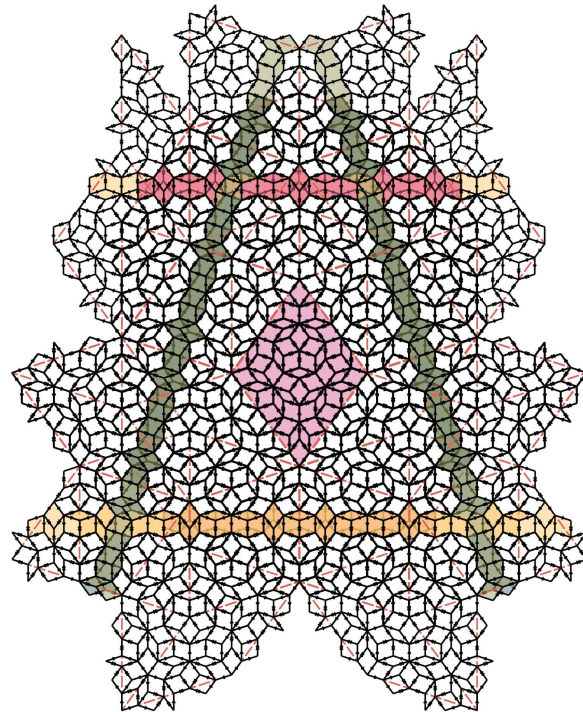


Figure 5.48: The patterns of worms in Figure 5.47

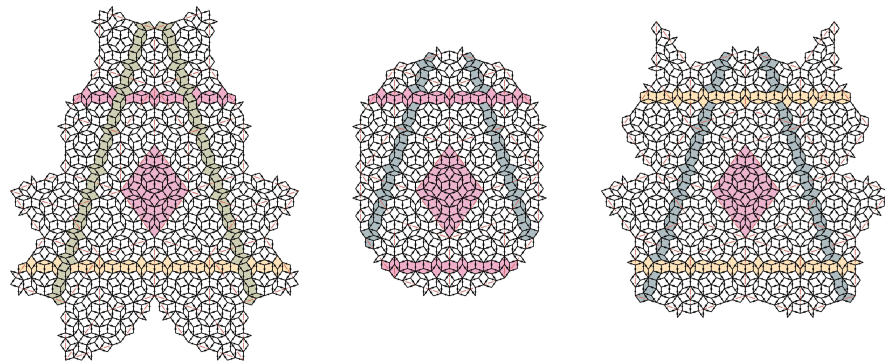


Figure 5.49: Separating the arrangements we see that the only differences between the patches are the orientations of the worms.

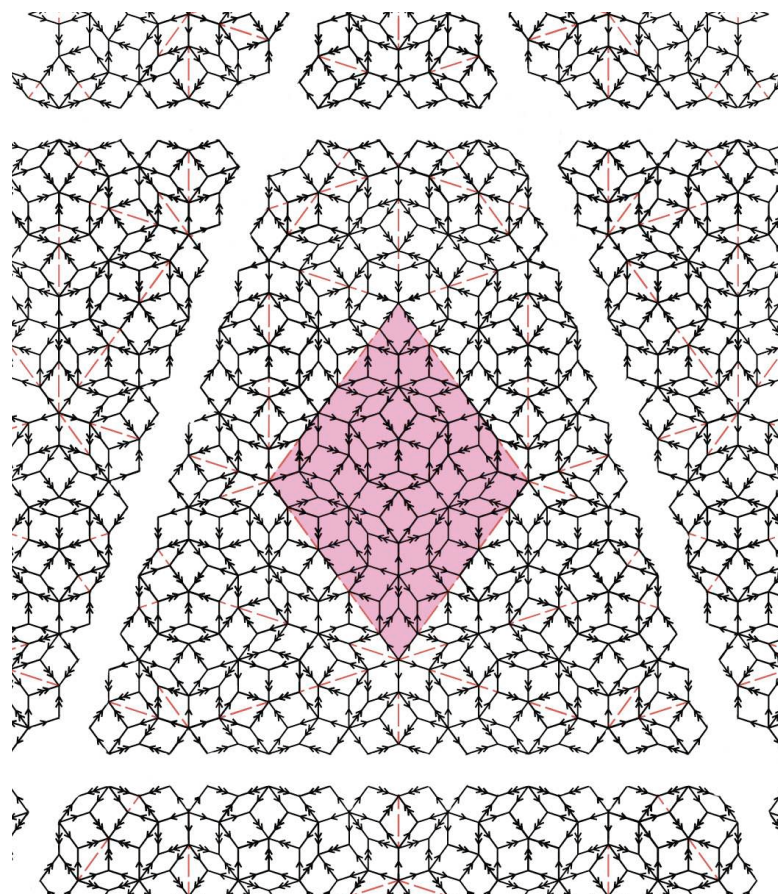


Figure 5.50: All three arrangements share all of the tiles in this diagram.

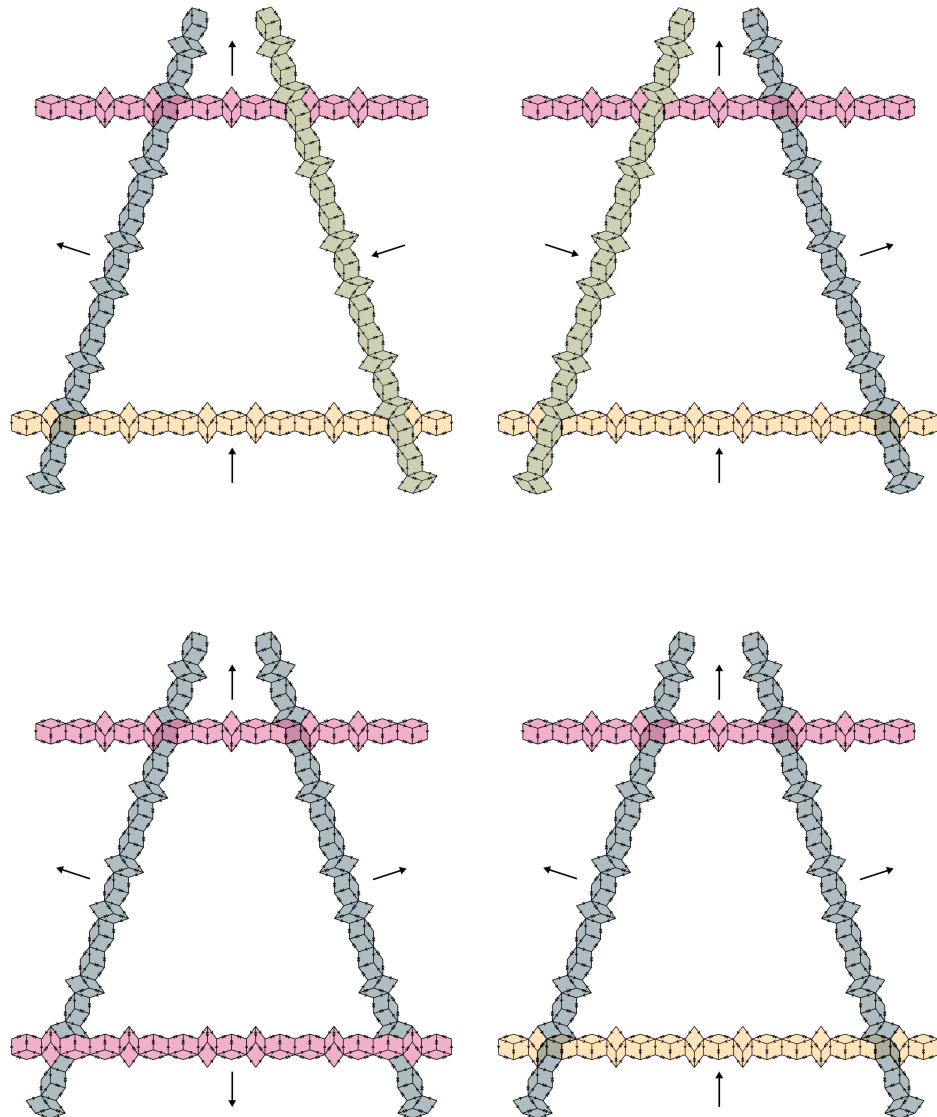


Figure 5.51: Four of the seven possible worm arrangements to fill the holes of Figure 5.50

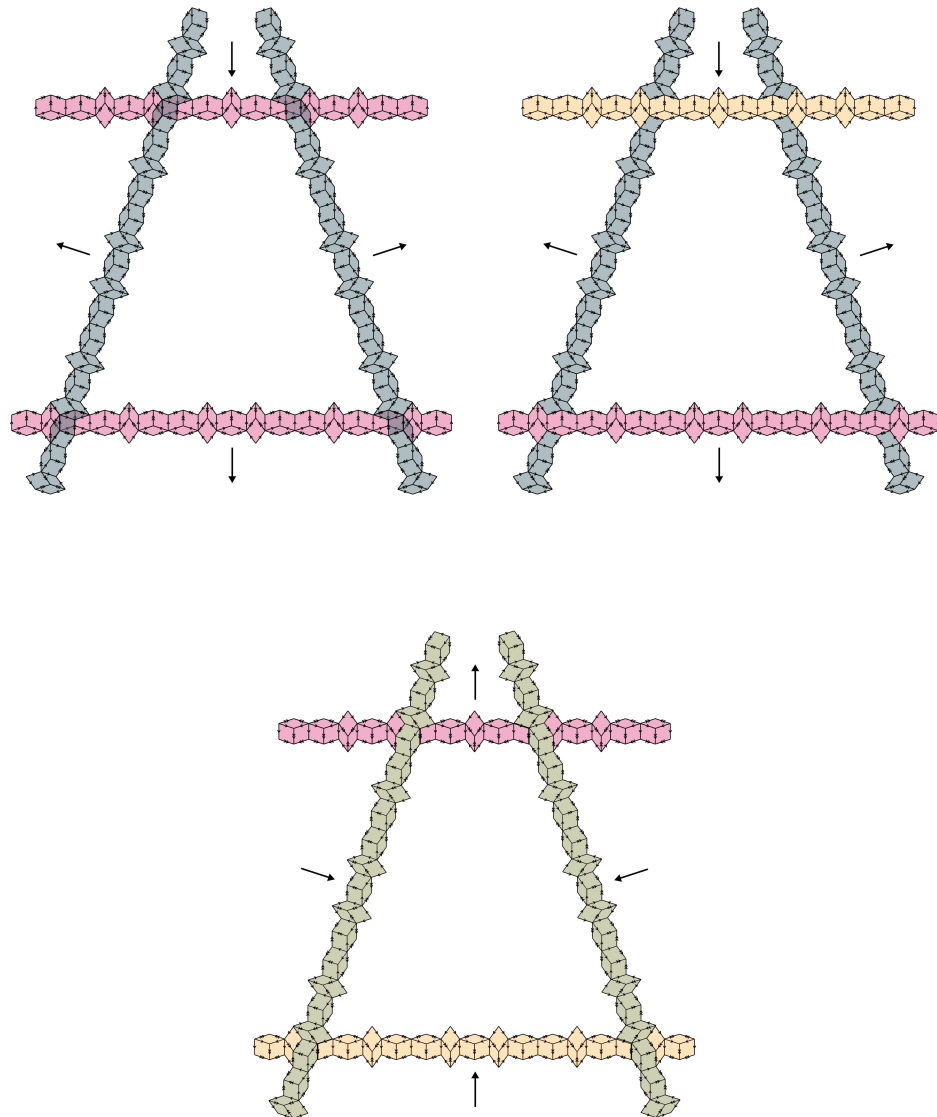


Figure 5.52: Three of the seven possible worm arrangements to fill the holes of Figure 5.50

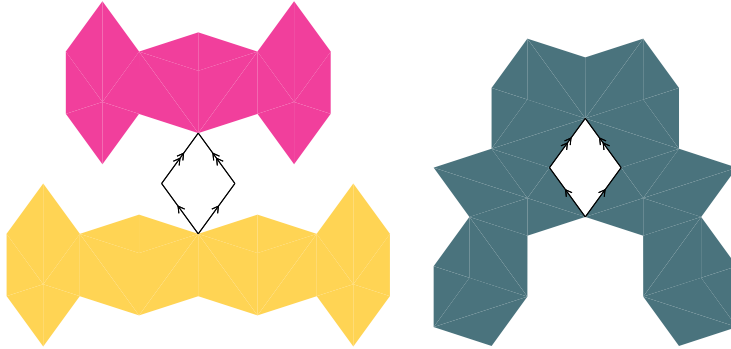


Figure 5.53: The thick rhomb can be surrounded by four worms

must be four worms in the coloured areas indicated in Figure 5.54 Note that what worm is on top will depend on the orientations. One possible arrangement is shown in Figure 5.55. We can decompose this to obtain the worm quadrilateral seen in Figure 5.56. Continuing to decompose this will give one of the seven correct worm arrangements shown previously. In fact we can continue to decompose these indefinitely to obtain larger and larger patches of tiles bounded by worms.

It is not hard to check that these seven arrangements are the only ways to *correctly* cover the quadrilateral shown in Figure 5.57 with tiles on the scale of the central tile. In this way every thick rhomb is bordered by four worms. Decomposing these arrangements yields increasingly large patches of tiles bounded by worms. The tiles inside the quadrilateral defined by the worms are **forced**. That is, in a correct tiling, the tiles inside the worm quadrilateral must be as shown.

This can also be seen in a slightly different way. Start with the thick rhomb, as shown in Figure 5.57. Decompose this (Figure 5.58) and add any forced tiles (shown in orange in Figure 5.59). Repeating this procedure (decomposing and adding forced tiles) on this arrangement yields a larger patch of tiles (Figures 5.60 and 5.61). As we continue this process, we will obtain a sequence of patches that are increasing in size, with their boundary approaching the quadrilateral shown in green.

Repeating this analysis with the thin rhomb, we find that the thin rhomb



Figure 5.54: There must be four worms in the coloured areas

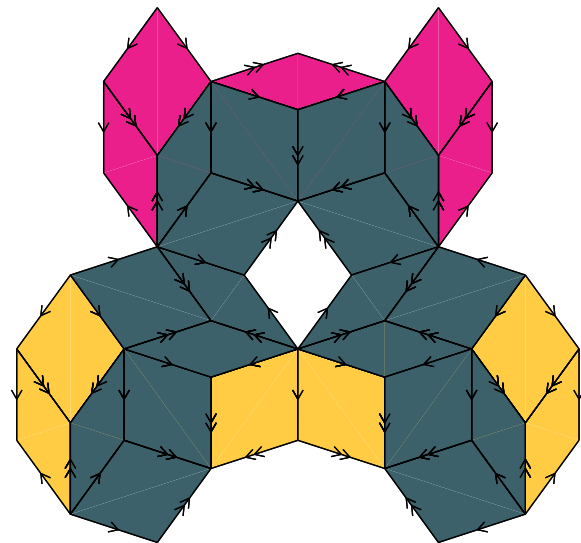


Figure 5.55: One possible arrangement of worms around a thick worm

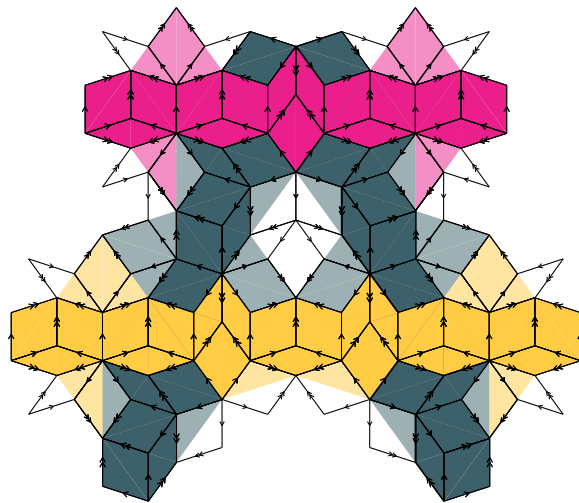


Figure 5.56: The worm quadrilateral obtained by decomposing Figure 5.55

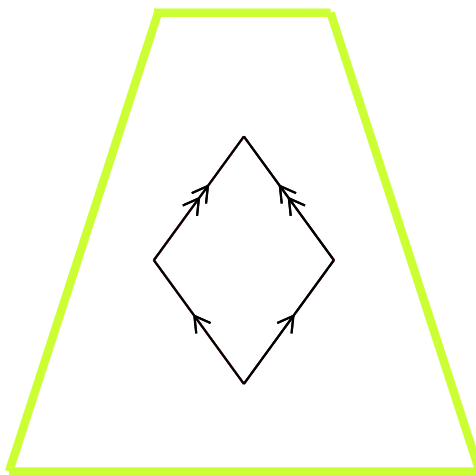


Figure 5.57: There are seven ways to correctly cover the quadrilateral above with tiles on the scale of the central rhomb.

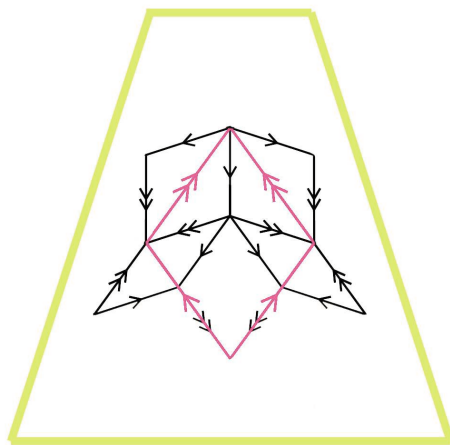


Figure 5.58: Decomposing the central rhomb

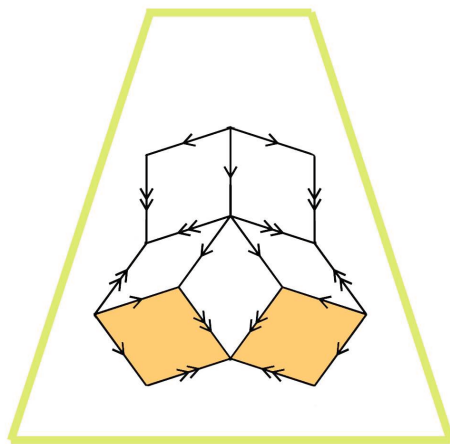


Figure 5.59: Adding forced tiles to the decomposed patch

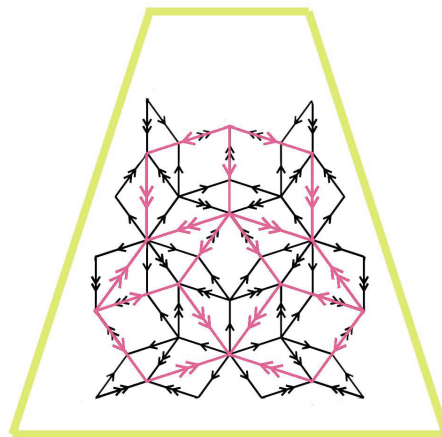


Figure 5.60: Decomposing the new patch

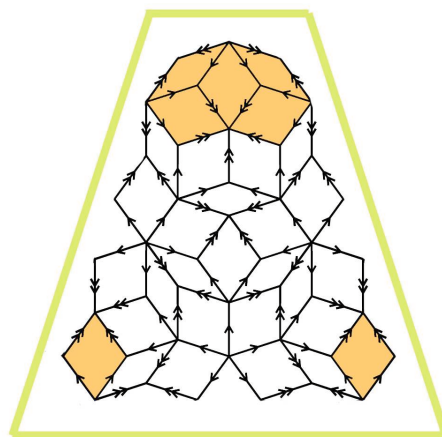


Figure 5.61: Adding forced tiles to the decomposed patch. Repeating this process will produce a patch of tiles whose boundary approaches the green quadrilateral.

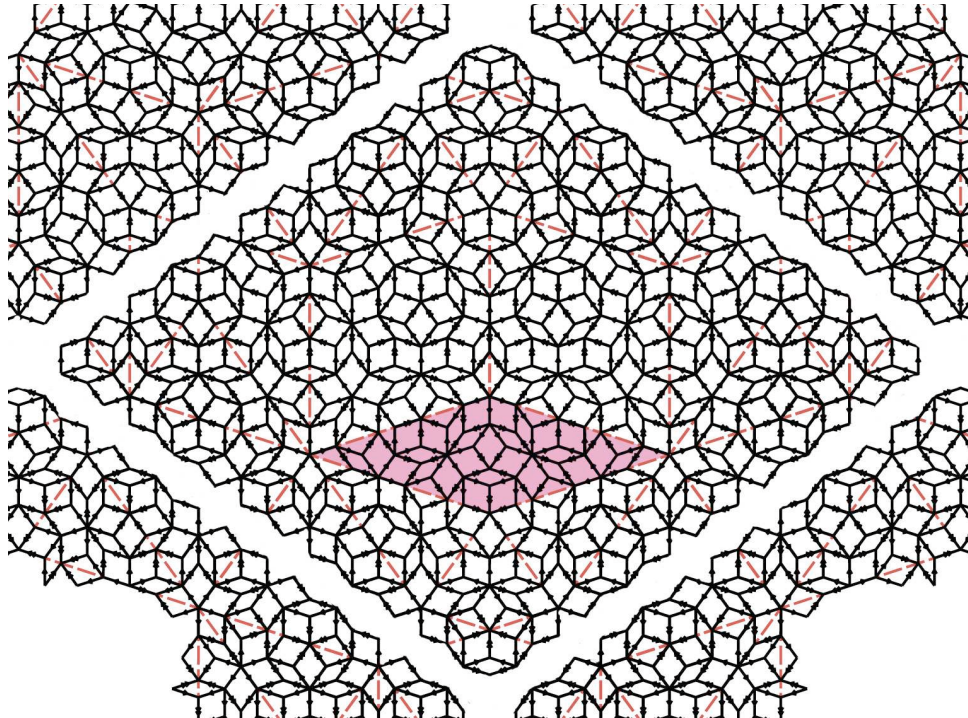


Figure 5.62: The quadrilateral surrounding a thin rhomb

is bordered by a different quadrilateral (Figure 5.62). Of the sixteen possible worm arrangements in this case, only five are without errors (Figure 5.63)

To summarize so far, we have seen that the only differences between various arrangements of tiles are the worm orientations. Now consider the arrangement shown in Figure 5.64. We need to fill in the blank space with a worm. But notice that a single tile, placed anywhere in the blank area will determine the orientation of the *entire* worm (Figures 5.65 5.66). This is precisely the reason that mistakes are so hard to avoid. Mistakes (the placements of tiles that will cause errors) occur because a single tile will determine the worm orientation. That is, a single tile placed in the path of a worm will determine the orientation of that worm. These placements may cause errors because worm interactions occur at an arbitrarily large distance from the determination of the worm orientation. In Figure 5.67, worms are indicated in red. Any single

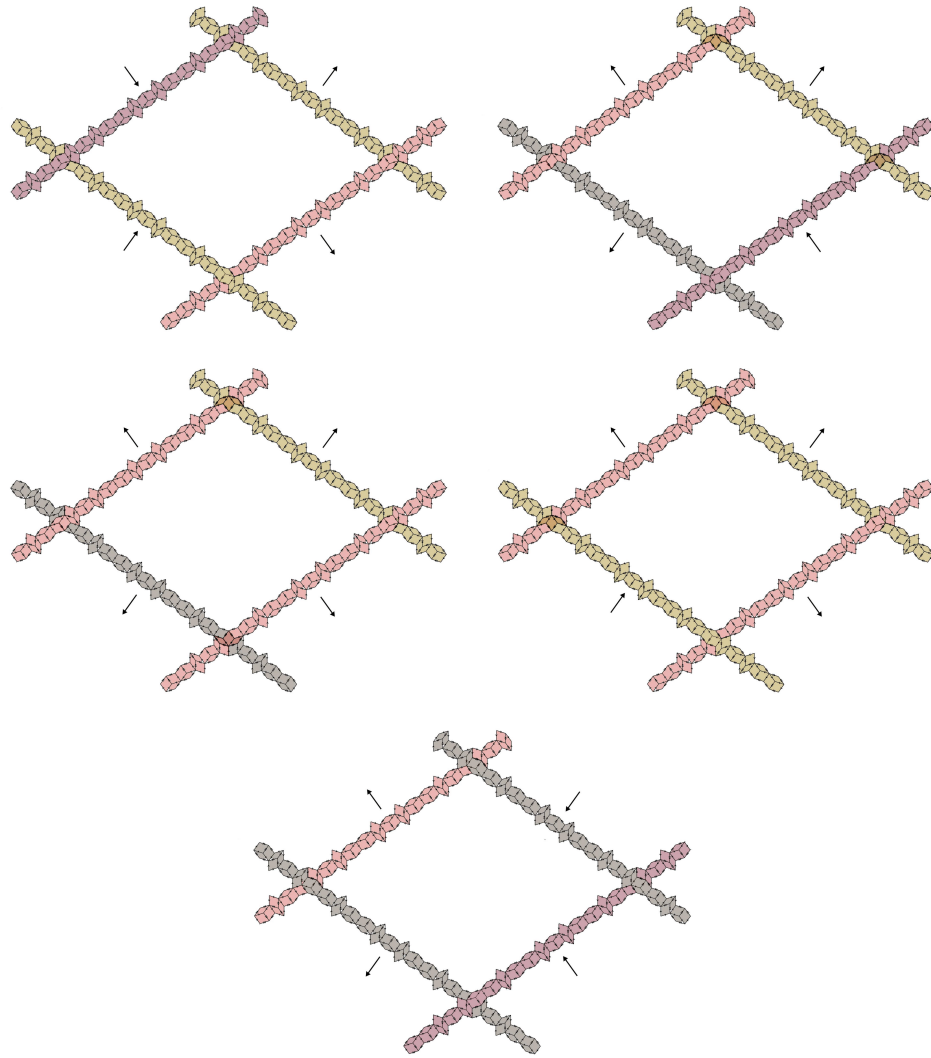


Figure 5.63: The five arrangements of worms that can surround a thin rhomb. The orientations will reverse as they are composed or decomposed.

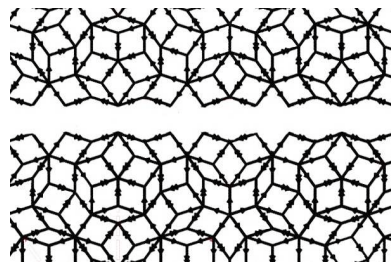


Figure 5.64: This blank space needs to be filled with a worm

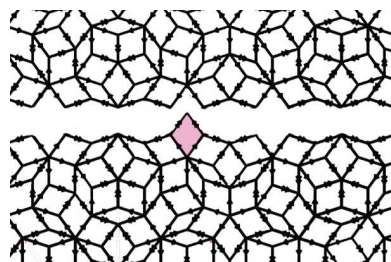


Figure 5.65: A single tile placed in the hole will determine the orientation of the worm

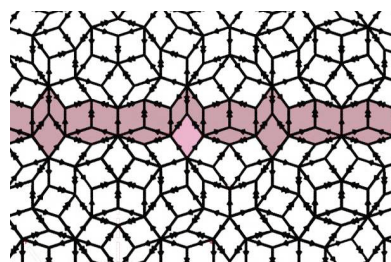


Figure 5.66: The worm orientation is determined by the first tile placed.

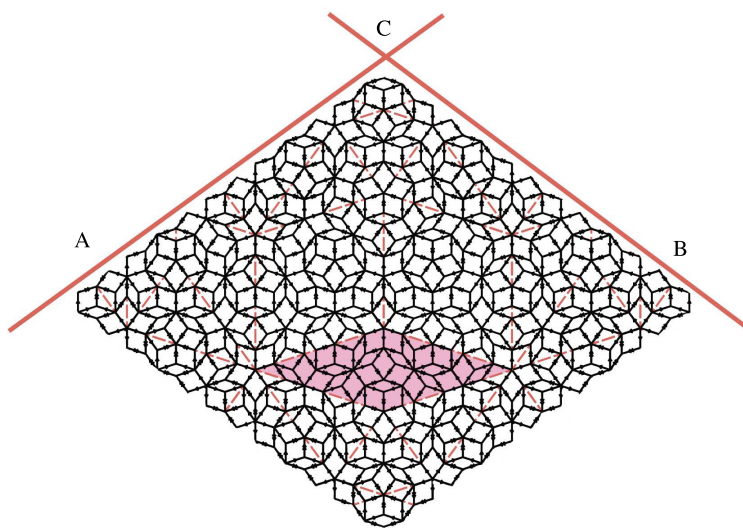


Figure 5.67: The quadrilateral of forced tiles surrounding a thin rhomb. Worms are indicated in red. A tile added at **A** may be incompatible with a tile placed at **B**. However, this incompatibility will only be evident at **C**

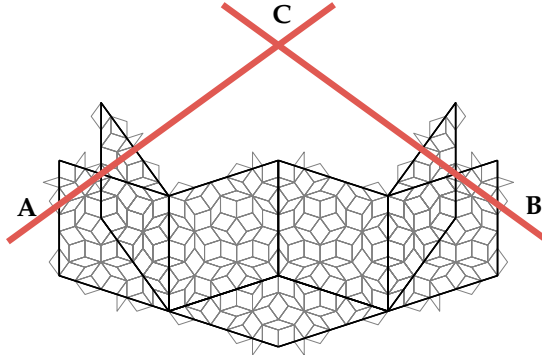


Figure 5.68: The difference between thin and thick rhombs is in the orientation of the worms. This is why our original mistake is indeed a mistake

tile added to any side of the worm quadrilateral will force the orientation of the entire worm. In the worst case scenario, a tile placed at **A** will be incompatible with a tile placed at **B**.

It is precisely this issue that is behind our familiar deception. As we have seen, the worm appears where the difference between thin and thick rhomb manifests, as seen in Figure 5.68. A tile placed at **A** (anywhere along the red line) will determine the orientation of the leftmost worm. Similarly, any tile placed along the line **B** will determine the orientation of the rightmost worm. These orientations have a one in four chance of being incompatible. The error will occur when both of the outermost tiles are thick rhombs. In this case, the error will occur at the point **C** (assuming that we are growing the tiling radially outward from the central tiles). The further we decompose the subtiles, the further away (in number of tiles) the error becomes from the site of the mistake.

In other words, when placing a tile at **A**, we need an awareness of what is happening at **B**, and how that will affect point **C**!

As we have seen, errors occur because worm orientations are incompatible. Mistakes occur because it may be the case that the tile being placed will determine the orientation of a worm that will be incompatible with an existing worm (that is, at least *one* tile of an existing worm). In other words, when adding a tile to an existing patch of Penrose tiles, we need information about

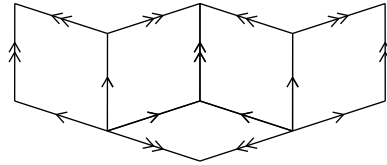


Figure 5.69: The simple mistake

tiles that are arbitrarily far away. As the number of tiles in our arrangement grows, the possibility of avoiding mistakes becomes vanishingly small. In this way, the growth of Penrose tiles is a **non-local** procedure.

5.4.3 Worms and Fibonacci Strings

One thing that is particularly amazing about the worms found in these tilings, is that they bear a striking resemblance to the Fibonacci tilings discussed in Chapter 2. The long unit is exactly τ times longer than the short one. We have the following:

Theorem 5.5 [Pen89] *For a correct tiling, the sequence of long and short units will be a Fibonacci string, as defined in section 2.3.2.*

Note that this simply means that a worm assembled according to a Fibonacci string will constitute a correct tiling. A random sequence of long and short worm units will create a patch of tiling that is merely legal. However, it is the orientation of the worm in relation to the worms that intersect it that will determine whether or not a tiling containing the correct worm will be correct.

The theorem itself is easy to prove, one simply needs to note that the matching rules correspond exactly with the hierarchical rules for generating Fibonacci Sequences, as discussed in Chapter 2.

In fact, the simple mistake that we now know so well (Figure 5.69), corresponds to the erroneous *LLL* in a Fibonacci sequence. That is, the mistake is simply three long units together (Figure 5.70).

Because worms play such a central role in creating a correct Penrose tiling, it would seem like a good strategy to develop the worms first, to create a kind of framework for the rest of the tiling. However, recall from Chapter 3

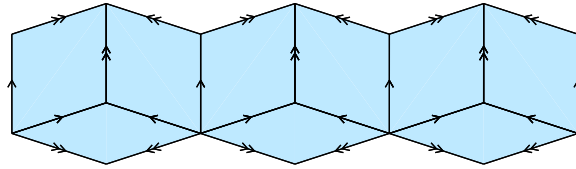


Figure 5.70: The simple mistake of Figure 5.69 corresponds to the erroneous LLL sequence in a Fibonacci tiling.

that Fibonacci tilings admit deceptions of all orders, and hence the growth of Fibonacci tilings is distinctly non-local. So attempting to solve this slightly simpler case will lead nowhere.

5.5 Summary

In summary, we have seen that the differences between correct arrangements of tiles manifest along worms. Inconsistencies in the tiling (overlaps, holes) occur when worm orientations are incompatible. Mistakes may occur because adding one tile may determine a worm orientation that is incompatible with one of the existing worms (even if the existing worm only has one tile). When adding tiles, one needs to be aware of tiles that are arbitrarily far away. In this way, the growth of a correct Penrose tiling is a non-local process.

Chapter 6

Conclusions

In conclusion, we have seen that the growth of Penrose tilings is a fundamentally non-local process. Although we have algorithms that we can use to generate these tilings, there is no local algorithm to create error-free tilings.

This is a particularly interesting statement in light of the fact that Penrose tiles are used to model quasicrystal structure. The relationship between Penrose tilings and quasicrystals is twofold. Firstly, the Penrose tilings were chosen as a model for quasicrystals because they share many structural properties, namely fivefold rotational symmetry with no translational symmetry. The second aspect is the use of Penrose tiles to attempt to understand the growth of the quasicrystals. This raises the important question: if we are to model quasicrystals on Penrose tilings, how does ‘nature’ know how to grow them, if the local growth of Penrose tilings is impossible?

Consider the patch in Figure 6.1, thinking about the tiles as units of a quasicrystal. When adding tiles to this patch, we may legally add either rhomb to

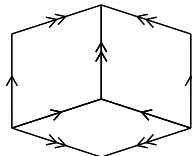


Figure 6.1: Attempting to grow a quasicrystal: we can add either rhomb to both sides of this figure, but the situation that involves adding two thick rhombs is incorrect. How does the mechanism governing the growth of a quasicrystal know this?

both sides of this patch. Three of the four possible combinations will be correct, and as we have seen, the situation involving two thick rhombs is a mistake. From the perspective of quasicrystals, the mechanism that determines how the crystal will grow must somehow keep track of what is happening at both of these sites. Indeed, using the decomposition argument, this mechanism must contend with the potential for incompatible tile placements at arbitrarily distant sites.

There have been some attempts to create algorithms using Penrose tiles that would somehow model Quasicrystal growth. In [OSDS88], George Onoda et. al. present an algorithm for growing defect-free Penrose tilings. This is done, in short, by growing forced patches of tiles and then adding tiles around the boundary of the patch in an ordered fashion. This algorithm, however, is not local in the sense intended by Penrose, and this is documented in [Jar89].

Since then, algorithms using Penrose tilings to model Quasicrystal growth have focused on growing defective tilings. See [OWD95] for an example of an algorithm that accepts some violation of the matching rules. In some ways these algorithms are more realistic, since the quasicrystals themselves often contain inconsistencies.

Penrose himself suggests that if we are to base our understanding of quasicrystal formation on these tilings, then we must face the fact that nature has some interesting non-local tricks up her sleeve.

Bibliography

- [Cas05] Bill Casselman, *Mathematical illustrations*, Cambridge University Press, Cambridge, 2005.
- [dB81] N. G. de Bruijn, *Algebraic theory of penrose's non-periodic tilings of the plane*, Proc. Konink. Ned Akad Wetensch. A **84** (1981), 39 – 53.
- [dB90] ———, *Updown generation of penrose patterns*, Indag. Mathem. N.S. **2** (1990), 201 – 220.
- [DS95] Steven Dworkin and Jiunn-I Shieh, *Deceptions in quasicrystal growth*, Commun. Math. Phys **168** (1995), 337 – 352.
- [Gar77] Martin Gardner, *Extraordinary nonperiodic tiling that enriches the theory of tiles*, Scientific American (1977), 110 – 121.
- [GS87] Branko Grunbaum and G. C. Shephard, *Tilings and patterns*, W. H. Freeman, New York, 1987.
- [Jar89] Marko V. Jarić, *Local growth of quasicrystals*, Physical Review Letters **62** (1989), no. 10, 1209.
- [OSDS88] George Y. Onoda, Paul J. Steinhardt, David P. DiVincenzo, and Joshua E. S. Socolar, *Growing perfect quasicrystals*, Physical Review Letters **60** (1988), no. 25, 2653 – 2657.
- [OWD95] G. van Ophuysen, M. Weber, and L. Danzer, *Strictly local growth of penrose patterns*, J. Phys. A: Math. Gen. **28** (1995), 281 – 290.
- [Pen89] Roger Penrose, *Tilings and quasicrystals: A non-local growth problem?*, Aperiodicity and Order (M. V. Jaríć, ed.), vol. 2, Academic, New York, 1989, pp. 53–80.
- [SBC84] I. Shechtman, D. Gratias Blech, and J. W. Cahn, *Metallic phase with long-range orientational order and no translational symmetry*, Physical Review Letters **53** (1984), no. 20, 1951 – 1953.
- [Sen95] Marjorie Senechal, *Quasicrystals and geometry*, Cambridge University Press, Cambridge, 1995.

Appendix A

Colophon

All of the illustrations in this document were created using the graphics programming language PostScript. The newly published book by Bill Casselman, *Mathematical Illustrations* [Cas05] was used as a reference for generating drawings using PostScript.

Some of the figures were cropped and made ready for press using Adobe Photoshop 7. Figures 3.7 and 3.11 were generated using the procedure for tilings from Pentagrids as developed by Jürgen Richter-Gebert and Kajo Miyazaki and reprinted in Senechal's book [Sen95].